MICROBIAL PROCESSES IN THE SUBARCTIC NORTHEAST PACIFIC: BACTERIAL STANDING STOCKS, RATE PROCESSES, AND CONTROLS

by

NELSON DANIEL SHERRY

B.S., The University of Oregon, 1991

M.S., The University of Oregon, 1995

A THESIS SUBMITTED IN PARTIAL FULFILMENT OF
THE REQUIREMENTS FOR THE DEGREE OF

DOCTOR OF PHILOSOPHY

in

THE FACULTY OF GRADUATE STUDIES

(Department of Earth and Ocean Sciences)

We accept this thesis as conforming

to the required standard

THE UNIVERSITY OF BRITISH COLUMBIA

June 2002

In presenting this thesis in partial fulfilment of the requirements for an advanced degree at the University of British Columbia, I agree that the Library shall make it freely available for reference and study. I further agree that permission for extensive copying of this thesis for scholarly purposes may be granted by the head of my department or by his or her representatives. It is understood that copying or publication of this thesis for financial gain shall not be allowed without my written permission.

Department of Earth and Ocean Sciences

The University of British Columbia
Vancouver, Canada

Date June 13, 2002

Abstract

During 11 cruises along the east/west line-*P* transect from slope waters at P4 (1200 m depth) to the open-ocean waters at Ocean Station Papa (OSP) (4250 m depth), heterotrophic bacterial abundance, productivity, and respiration rates were measured. While values from below the euphotic zone (~60 – 4200 m) are reported, detailed analysis is focused primarily on the euphotic zone. Within the euphotic zone, bacterial biomass in the winter was ~50% of the spring and summer values. Bacterial respiration rates in the summer increased >10-fold at P4 while showing much less change at the more oceanic stations. Bacterial productivity, measured as [^{3}H]-thymidine and [^{14}C]-leucine incorporation rates, was lowest in the winter with little spatial variability. Productivity increased 4 to 10-fold in spring at P4. Between 1995 and 1998, the average summer bacterial abundance along line-*P* decreased by ~50% while bacterial productivity decreased by ~ 90%.

Factors for converting the incorporation of radiolabeled substrate to bacterial productivity were determined empirically from grow-out dilution experiments. The empirical conversion factors for both thymidine and leucine were positively correlated to *in situ* cell abundance. A grow-out simulation model was developed and used to quantify the uncertainties associated with various conversion factor calculation methods leading to a more robust, non-linear cumulative method for calculating conversion factors.

Roughly 10% of the mixed-layer data showed extremely high bacterial productivity which was associated with physical features or fronts. Seasonal changes in bacterial abundance, productivity, and growth rate were driven predominantly by changes in the supply rate of phytoplankton derived dissolved organic carbon (DOC), and by changes in the dilution of surface water by deeper water (deepening of the mixed layer and/or changes in upwelling). Regional changes in bacterial abundance, productivity, and growth rate during the summer were driven predominantly by differences in the availability of limiting mineral nutrients and changes in the rates of loss processes. Experimental manipulations demonstrated that bacterial productivity was almost always limited by the availability of labile DOC. However, bacterial productivity in the late summer was further limited at P4 in 1996 by the availability of nitrogen, and at OSP in 1997 by the availability of iron.

Table of Contents

List of Tables

List of Figures

Acknowledgements

I am deeply indebted to my wife Lise Sherry, without whom I would not have begun this project, and without who's support, I would never have completed it. I thank Paul J. Harrison for his continued support, advice, and confidence in my efforts and ideas. I thank Phil Boyd for his guidance and encouragement throughout this project. I also thanks Curtis Suttle, F.J.R. (Max) Tayor and all of the faculty, staff and other students in the Oceanography group at UBC for their endless advice and support in everything from scientific questions, to logistical details. I thank Barry Sherr, David Kirchman, and Hugh Ducklow for their encouragement and advice in the early stages of my program and their feedback on manuscripts as I began to publish my results. A special thanks is also due to Frank Whitney, Hugh Maclean, officers and crew of the CCG vessel John P. Tully, and the technical staff from the Institute of Ocean Sciences for technical advice and assistance. Support for much of this work came from NSERC (Canada) via grant awards to the JGOFS-Canada program and from the University of British Columbia Graduate Fellowship award program.

Chapter 1

Introduction to Bacterial Processes in the Subarctic NE Pacific Ocean

1.1.0 Background

1.1.1 Importance of Bacteria

Free living heterotrophic prokaryotes (referred to herein as bacteria) in the marine environment play a multi-faceted biogeochemical role (Cho and Azam 1988). Bacteria break down organic material releasing excess macronutrients and micronutrients and thus stimulate phytoplankton growth (Berman *et al.* 1987). Conversely, they may, under nutrient limitation, compete with phytoplankton for nutrients (Kirchman 1994, Tortell *et al.* 1996), and thus contribute to the limitation of phytoplankton production. As secondary producers, bacteria consume dissolved organic material (DOM), originating from phytoplankton photosynthesis, and convert it to particulate organic material (POC) which sustains grazers within the microbial food web (Ducklow 1994). Furthermore, the magnitude of bacterial respiration (BR) is often a considerable proportion of the total community respiration (TR) (del Giorgio *et al.* 1997). Thus, bacteria may not only influence rates of primary production, but they also play a major role in the ocean carbon balance and thus the ability of the ocean to absorb or release atmospheric CO_2.

1.1.2 The Subarctic NE Pacific

The subarctic NE Pacific (Fig. 1.1) is of particular interest for understanding ocean biogeochemical processes. It is one of the three major high nitrate, low chlorophyll (HNLC) regions of the world ocean where phytoplankton production is limited by iron supply (Martin *et al.* 1989, Boyd *et al.* 1996). Tortell *et al.* (1996) provided evidence suggesting that heterotrophic bacteria may also be iron-limited in this region. Line-P, a transect from the coast (Juan de Fuca Strait) to Ocean Station Papa (OSP), provides a unique gradient in physical (Whitney *et al.* 1998), chemical (Whitney *et al.* 1998, Varela and Harrison 1999), and biological (LaRoche *et al.* 1996, Boyd *et al.* 1998; Boyd and Harrison 1999) parameters from slope waters to HNLC oceanic waters. This region has one of the world's longest running oceanic time series with

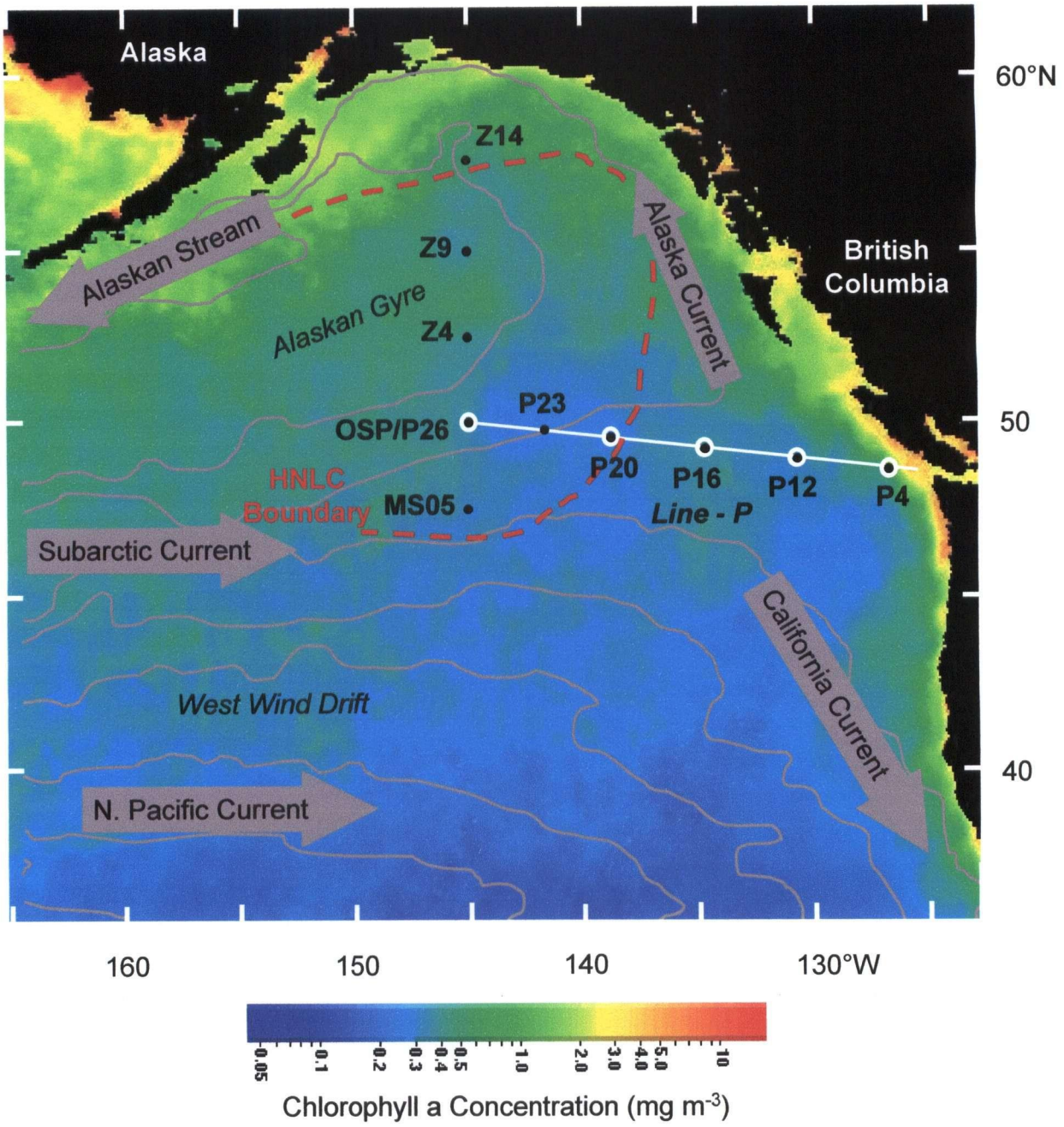

Figure 1.1 The subarctic NE Pacific showing the positions of the major hydrographic stations that were sampled during this study, overlaid on the SeaWiFS Level-3 standard mapped chlorophyll image for 1998. This image shows the position of the transition in chlorophyll concentration between the lower chlorophyll, oligotrophic subtropical gyre in the south and the higher chlorophyll, HNLC (high nitrate, low chlorophyll) subarctic region in the north, generally recognized as north of 42-45°N (Longhurst 1998). The chlorophyll image was provided by the SeaWiFS Project, NASA/Goddard Space Flight Center and ORBIMAGE. Gray contours are the 10 yr mean wind-forced circulation stream flow functions from Rienecker et al. (1996). The red dashed line is the approximate boundary of the subarctic NE Pacific HNLC region defined as the area where summer nitrate was consistently > 1 μM in 1998-2000 (Whitney and Welch, in press).

oceanographic measurements dating back to 1949 at OSP and extensive biological datasets including primary productivity (PP) dating back to 1956 (Tabata and Peart 1985).

The subarctic NE Pacific has been largely defined by measurements taken over the years at OSP. OSP (50°N, 145°W) is located along the SE edge of the Alaskan Gyre in the relatively slow (~ 7 km d^{-1}), eastward moving Subarctic Current (Bograd *et al.* 1999). The region is typified by a relatively shallow permanent halocline at 100-120 m that limits the maximum depth of winter mixing (Dodimead *et al.* 1963). The permanent halocline is overlain by a seasonal thermocline that typically begins to form in May/June, achieves a minimum of < 40 m in Aug/Sep, and is mixed down to ~ 100 m in Nov/Dec (Whitney and Freeland 1999). In association with the cyclonic circulation of the region, Ekman upwelling at OSP has been estimated to be ~ 30 m yr^{-1} (Gargett 1991).

Seasonally, there is a warming and freshening along line-P from winter to summer (Feb/Mar - Aug/Sep). The mixed layer temperature typically varies from 5 - 12°C at OSP and from 8 - 15°C at P4 (the shelf break, 48° 30'N, 126° 40'W). The mixed layer salinity typically varies from 32.7 - 32.5 at OSP and from 32.2 - 31.8 at P4 (Whitney and Freeland 1999). In association with the 1997/98 El Niño, there was warming in surface waters above the historical average by ~ 2°C all along line-P in Sep 97 and nearer the coast (P4 - P12) in Feb 1998 (Brown 1998).

With a few historical exceptions (see Wong *et al.* 1999), OSP is replete in macronutrients (nitrate, phosphate, and silicic acid) year round (Whitney *et al.* 1999). Chlorophyll is nearly constant year round at 0.2 - 0.4 mg m^{-3} and primary productivity roughly doubles in the spring and summer from a winter low of ~ 300 mg C m^{-2} d^{-1} (~ 3 winter to ~ 12 mg C m^{-3} d^{-1} in spring/summer assuming 100 m and 50 m euphotic zone depths respectively) (Boyd and Harrison *et al.* 1999). The biomass of both autotrophic and heterotrophic plankton is dominated by small cells, < 5 μm (Booth *et al.* 1993). Both primary productivity and total chlorophyll have been shown to increase with the addition of iron in summer (Boyd *et al.*, 1996), while Maldonado *et al.* (1999) demonstrated that phytoplankton productivity in the winter responded to a combined increase in iron and light, suggesting that phytoplankton were co-limited by these factors during the winter.

In contrast to OSP, there is greater seasonal and interannual variability closer to shore. During the Canadian JGOFS program (1992-97) Boyd and Harrison (1999) found that winter mixed layer chlorophyll at P4 ranged from 0.3 - 0.8 mg m^{-3} and typically increased from 2 - 5-fold in spring and summer. Winter mixed layer primary productivity at P4 ranged 5 - 20 mg C m^{-3} d^{-1} and increased as much as 10-fold in spring and/or summer depending on the year. In association with the seasonal phytoplankton blooms, nitrate is typically depleted in the mixed layer westward of P12 during the summer (Whitney and Freeland 1999).

1.1.3 Bacterial Standing Stocks and Productivity in the subarctic NE Pacific

Despite the extensive datasets and years of study within this region, the first research into heterotrophic bacterial processes in the subarctic NE Pacific took place at OSP in the late 1980s as part of the Subarctic Pacific Ecosystem Research (SuPER) program (Miller, 1993). Kirchman *et al.* (1993) found heterotrophic bacterial biomass (BB) to be similar to phytoplankton biomass while bacterial productivity (BP) accounted for only ~10% of primary productivity (PP) during the four SuPER cruises in spring and summer of 1987 and 1988. Kirchman (1990) and Kirchman *et al.* (1993) also found that both temperature and dissolved organic matter (DOM) supply limited the bacterial growth rate (Bμ). While the SuPER program included 3 week occupations of OSP, and observed changes on the scale of weeks during both the spring and summer of 1987/88, the study took place during only two years, did not include any winter observations and did not investigate respiration rates or the continental slope to open ocean gradients. Also in 1987, the Vertical Transport and Exchange (VERTEX) project (Martin *et al.*, 1989) visited OSP as part of their vertical particle flux program, but focused primarily on particle-associated bacterial activity. Doherty (1995) and Boyd *et al.* (1995a, b) addressed BB and BP both along line-P and at OSP in May and February of both 1993 and 1994, providing the first bacterial dataset across the slope to open ocean gradient of line-P and data during the winter at OSP. However, Doherty (1995) and Boyd *et al.* (1995a, b) did not attempt to address factors controlling bacterial biomass (BB) and bacterial productivity (BP), did not include data below the euphotic zone, and did not measure respiration.

1.1.4 Factors Controlling Open Ocean Bacterial Productivity

To further our understanding of what controls bacterial processes in the oceans, a number of studies have attempted to compare/correlate bacterial abundance and/or bacterial productivity (BP) against various other parameters including chlorophyll concentrations, dissolved organic carbon (DOC) concentration, PP, and temperature. Bird and Kalff (1984) found that bacterial abundance (B#) showed a strong positive correlation with chlorophyll concentration across both fresh and saltwater environments. Kaehler *et al.* (1997) found bacterial growth to be strongly dependent on DOC concentrations in the Southern Ocean, another HNLC region. From a broad review of aquatic literature, del Giorgio and Cole (1998) suggested that BP averages ~ 30% of net PP. They go on to suggest that bacterial growth rates as well as bacterial growth efficiency (BGE) also tend to increase with increased net PP and chlorophyll concentration. However, for any given time and location these general trends may not hold true because of either lag times in bacterial responses to, or other unexplained decoupling of bacterial processes from PP, the assumed primary source of bacterial substrate. In another broad literature review by Rivkin *et al.* (1996), there was only a weak ($R^2 = 0.058$) relationship between BP and temperature. The degree of coupling between PP and bacterial processes is not well understood in the subarctic NE Pacific and has not been addressed in the context of a eutrophic coastal to HNLC open-ocean gradient.

Another approach commonly used, and often presented in conjunction with correlation analysis, is experimental manipulation of incubations of natural bacterial populations. In the subarctic NE Pacific, Kirchman (1990) and Kirchman *et al.* (1993) found dissolved organic matter (DOM) amendments increased both bacterial abundance and bacterial productivity, while increases in temperature also increased productivity. During IronEx II, in the spring of 1995, Cochlan (2001) found that bacterial abundance and productivity increased 1.7 and 3-fold in conjunction with the 14-fold PP increase measured in an iron amended patch in a HNLC region of the equatorial Pacific. Church *et al.* (1999) found bacterial abundance and productivity in the HNLC Southern Ocean increased most dramatically with amendments of either glucose or dissolved free amino

acids. At 47 and 51°S, treatments with combined glucose and iron showed the highest growth rates. Ducklow *et al.* (1999) found little response in the Ross Sea to a range of treatments including temperature. An overview of perturbation experiments in the heterotrophic bacterial literature suggests that DOC/DOM limitation is widespread. However, unlike regressions across different regions, which show little temperature response (Rivkin *et al.* 1996), temperature increases often increase bacterial productivity in concurrent incubations from a given sample site. Though bacteria have been shown to respond to both DOC/DOM additions and temperature increases during some seasons, the interannual variability of response and the issue of iron limitation or co-limitation of bacterial productivity has not been resolved for the subarctic NE Pacific.

In order to tie together observations to aid in understanding potential nutrient and/or carbon flows between different parts of the food web and to test for internal consistency between data and mechanistic assumptions, Vézina and Savenkoff (1999) developed models for winter, spring, and summer at OSP from data collected as part of the Canadian JGOFS program including bacterial data presented herein. Balancing the winter model required a relaxation of constraints on bacterial growth efficiency from 25 to 10% and suggested that while food web structure was most sensitive to primary productivity in the winter, it was most sensitive to microbial processes in the summer. The models also suggested that the DOM source utilized by bacteria came mainly from grazers.

Ducklow (1994) reviewed several approaches to modeling of microbial processes including bacteria-nutrient interactions. The inverse models of Vézina and Savenkoff (1999) address the magnitude of influence that bacterial processes exert on the structure and resource distribution within the food webs of the subarctic NE Pacific, however they do not address the more specific mechanistic controls of bacterial processes and the magnitude of influence exerted by these controls. They also do not address differences along the coastal-to-offshore gradient found along line-P.

1.2.0 Overview of this thesis

This thesis extends the temporal and spatial scales of the previous studies. It provides measurements of bacterial stocks and processes taken during winter, spring, and summer over several years. It includes data along the coastal to off-shore gradient of line-P addressing the factors that control the magnitudes of carbon flow through heterotrophic bacteria as conditions vary seasonally, interannually, and spatially in the subarctic NE Pacific.

This thesis had three central goals:

1) to survey the seasonal and spatial trends in bacterial abundance, productivity, and respiration to quantify the magnitude and variability of carbon flow through bacteria in the subarctic NE Pacific,
2) to further quantify (model) the theoretical framework, and thus improve the interpretation of empirical conversion factor calculations commonly used in estimating bacterial productivity, and
3) to determine which changes in physical and biological processes drive the observed changes in bacterial properties (abundance and productivity), and to determine the relative influence of these different changes during different seasons in different regions.

These results will improve our ability to make robust predictions about what changes will occur in bacterial processes as other biological, chemical, and physical changes occur in the environment.

Chapter 2

Modeling Bacterial Growth in Dilution Cultures and an Assessment of the Methods used for Calculating Empirical Conversion Factors

2.1.0 Introduction

2.1.1 Background

Over the past two decades, the productivity of bacteria has been measured primarily using methods that infer bacterial productivity from the incorporation rate of a labeled substrate (Fuhrman and Azam 1980, 1982, Kirchman *et al.* 1985, Ducklow 2000 and references within). However, over these 20 years, there has not been a consensus regarding the most appropriate or accurate method for converting substrate incorporation rates into bacterial productivity. As we become more aware of the prominent role bacteria play in our biosphere (Pomeroy 1974, Azam 1983, Sherr and Sherr 2000, Williams 2000), the importance of accurately determining bacterial productivity becomes ever more apparent.

It is estimated that ~50% of the ocean's primary production is routed into the dissolved organic carbon (DOC) pool due to excretion, grazing, and viral lysis of phytoplankton cells (Nagata 2000 and references within). The majority of the labile DOC pool is processed by bacteria (Cherrier *et al.* 1996, Carlson and Ducklow 1996, Kahler *et al.* 1997, Williams 2000). For this reason, bacterial processes, including bacterial productivity, are central to understanding ocean biogeochemical fluxes.

Perhaps the most intuitively direct way of measuring bacterial productivity in natural populations is to eliminate or substantially reduce loss processes by filtration or dilution and then count bacterial cell abundance as it increases (Fuhrman and Azam 1980, Landry and Hasset 1982, Kirchman *et al.* 1982). However, filtration/dilution incubations have been unreliable for estimating *in situ* bacterial productivity because they alter growth conditions by eliminating grazing, altering the grazing-associated nutrient feedbacks, and reducing competition for potentially limiting resources (see discussion below).

The use of [^{3}H-methyl]-thymidine (TdR) incorporation rates as a quantitative estimator for DNA production, and thus bacterial division rates, was introduced by Fuhrman and Azam (1980, 1982). This technique provided a sensitive method for measuring bacterial productivity while minimizing experimental manipulation and thus reducing experimental artifacts. TdR incorporation as a proxy for bacterial productivity was supported by filtration/dilution incubations, demonstrating that the increase in TdR incorporation over time was proportional to the increase in bacterial cell abundance (Fuhrman and Azam 1980, 1982; Kirchman *et al.* 1982). TdR as a macromolecule precursor works well because it is readily taken up by a wide variety of bacteria (Furman and Azam 1980, Moriarty 1985). During short incubations TdR is taken up almost exclusively by bacteria, and when it is present in high enough concentrations cellular synthetic pathways are generally shut down, so dilution of the labeled substrate by cellular synthesis is minimized or eliminated (Moriarty 1985).

The use of [^{3}H]-leucine (Leu) incorporation rate as an estimator of bacterial productivity was introduced by Kirchman *et al.* (1985). Similar to TdR incorporation into DNA, Leu incorporation into proteins during short incubations is proportional to bacterial biomass production (Kirchman *et al.* 1985, 1986, Simon and Azam 1989). Leu exhibits little dilution and is metabolically routed almost exclusively into protein. The incorporation rate of Leu is also about 10-fold higher than the incorporation rate of TdR, making Leu incorporation a more sensitive method. However, Leu incorporation follows biomass more directly than cell division rates, occasionally confounding reconciliation between TdR and Leu bacterial productivity measurements (Ducklow 2000).

Although positive or negative responses to experimental manipulations can be identified based on comparisons between label incorporation rates (v_p) alone, converting v_p to bacterial productivity requires the use of a conversion factor (F) to estimate the amount of cells or biomass produced per unit of label incorporated. Conversion factors can be determined theoretically from estimates of the DNA content (protein content for Leu), of the cells and the thymine content in DNA (leucine content in protein for Leu) if a reasonable estimate of naturally occurring substrate relative to the addition of labeled substrate (dilution) can be quantified. A theoretical conversion factor of $0.2 - 1.3 \times 10^{18}$ cells produced per mole of TdR incorporated was initially proposed by Fuhrman and

Azam (1980). Further studies suggest ~$1 - 4 \times 10^{18}$ cells produced per mole of TdR incorporated is probably a better general estimate after accounting for isotope dilution (Fuhrman and Azam 1982, see Table 3.4). Variability in the environment (isotope dilution) and unknown variability in the non-DNA-specific incorporation of TdR, or in the case of Leu, variability in protein per cell suggests that a simple theoretical approach (instead of an empirical one) is unlikely to provide a single robust conversion factor for a broad range of environmental conditions (Kirchman *et al.* 1982, Rivkin *et al.* 1996, Ducklow 2000).

To address these issues of uncertainty in the conversion factors, Kirchman *et al.* (1982) introduced the practice of empirically deriving conversion factors based on filtration/dilution incubations (also referred to herein as grow-out experiments). The idea behind grow-out experiments is to eliminate bacterial loss processes and then measure the increase in bacterial abundance (N) along with the incorporation rate of the label (v_p) (i.e., TdR and/or Leu). The label incorporation rate can then be compared to the rate of cell increase measured during the grow-out experiment. The key assumption is that even if the filtration/dilution incubation perturbs the system, the bacterial production rate relative to the label incorporation rate will still be representative of the *in situ* community and be reasonably constant over the length of the grow-out experiment (see Kirchman and Ducklow 1997).

2.1.2 Conversion Factor Calculation Methods

Four different methods for calculating conversion factors are reviewed below. They are analyzed in greater detail later in the discussion using various permutations of a grow-out simulation model to address the strengths and failings of these different methods.

The Derivative Method – Kirchman *et al.* (1982) proposed deriving F empirically by assuming simple logarithmic growth during grow-out experiments. The intrinsic growth rate of the population was estimated from the slope of either the natural logarithm of cell abundance over time (semi-log plot of N) or the natural logarithm of label incorporation rate over time (semi-log plot of v_p) and by using the $N(0)$ and $v_p(0)$ measured at the

beginning of the incubation (see discussion below). This method of calculating F was termed the derivative method.

If there was a dormant or slow-growing fraction of cells in the population (N_d), they could be accounted for by fitting the cell abundance growth curve to a non-linear equation (see discussion below). Then the growth rate (μ) for the active fraction of the population (N_a) and an estimate of $N_a(0)$ could be calculated (Kirchman *et al.* 1982)). However, this non-linear approach to account for N_d has not been widely used, probably because of the increased uncertainty associated with fitting non-linear equations to sparse and/or noisy data.

The Modified Derivative Method – This method is an improvement to the derivative method and calculates $N(0)$ and $v_p(0)$ from the y-intercepts of the semi-log plots of N and v_p (Ducklow *et al.* 1992). Since the modified derivative method uses a linear fit to several data points, it reduces the sampling error issue intrinsic in the derivative method which uses a single t_0 data point. But the modified derivative method is still based on the assumptions that μ does not change significantly during the grow-out experiment, and that there is not a significant portion of the population that is dormant or slow-growing.

The Integrative Method – To avoid the assumption of simple exponential growth, Riemann *et al.* (1987) used a method later termed the integrative method by Ducklow *et al.* (1992). The integrative method makes the simplifying assumption that, regardless of growth rate, increases in cell abundance over time are proportional to the amount of label taken up over the same time. F is determined by dividing the increase in cell number by the integrated label incorporation rate. F is accurate so long as the number of cells produced per mole of label incorporation remains constant, and so long as an appropriate method of integration is used.

The Cumulative Method – Like the original derivative method, the original integrative method uses only the end points of the growth curve and is thus prone to bias from sampling error. An improvement on the integrative method, termed the cumulative method (Bjornsen and Kuparinen 1991), uses logic similar to the integrative method, but

fits a line to the cell abundance, $N(t)$ plotted against the label incorporation rate integrated from the beginning of the experiment to t. The slope of the line is F. The cumulative method has the advantage of using all the data points from a growth curve and weights the result toward earlier time points, because each subsequent value is calculated as the current time point plus the cumulated values of all earlier time points. The weighting reduces the error associated with any changes in F that may occur during a grow-out experiment, but the weighting will not fully correct such error.

All of these methods for calculating empirical conversion factors make certain assumptions which are not fully supported in all grow-out experiments. Understanding the mechanisms that can cause grow-out experiments to deviate from the assumptions and expectations of the models used to interpret them, is critical to improving the accuracy of conversion factor estimates.

2.2.0 Model Description

Changes in bacterial growth characteristics during grow-out experiments may be placed in one of two categories for this discussion: 1) quantitatively predictable changes as modeled below, and 2) changes that are not quantitatively predictable (e.g., the onset of grazing or shifts in community structure). Recognizing predictable patterns allows for the inclusion of data that might otherwise appear erroneous and/or the removal of seemingly anomalous data with more confidence, and thus improving the reliability of conversion factor estimates.

The grow-out model presented here was developed for three reasons:

1) to provide insight into some of the non-linear grow-out patterns that have eluded or confounded interpretation,
2) to clarify the conditions under which each of the various conversion factor calculation methods fails, and
3) to clarify which data are best included in, or excluded from empirical conversion factor calculations.

The grow-out simulation model output includes cell abundance (N) and label incorporation rates (v_p) for a series of time points during a theoretical grow-out

experiment. Thus, the grow-out simulation model output is the mathematical idealization of that which is measured during typical bacterial productivity assessments. The input variables are manipulated to demonstrate how changes in various unmeasured parameters can affect the measured variables.

Although many of the published grow-out data seem to fit models based on the assumption of simple exponential growth, at least early in the incubations, many do not. In this grow-out simulation model, the factors assumed to drive non-linearity in the semi-log plots of N and v_p are: 1) the presence of a dormant or slow-growing fraction (N_d) (i.e., cells growing slowly enough, relative to the active fraction, that they do not contribute significantly to the incorporation of substrate during these experiments), 2) a change in growth rate (μ) over time, 3) a change in the conversion factor (F) over time, and 4) combinations of the above factors.

A series of input variables that defined the growth conditions of the theoretical grow-out experiment were fed into the grow-out simulation model and "observations" of cell abundance (N) and label incorporation rate (v_p) were returned. Model parameters were as follows:

2.2.1 Input Variables

- t' – the length of each time step. The grow-out simulation model returns data for 11 equally spaced time points from $t_0 - t_{10}$.
- r_0 – the intrinsic growth rate (μ) (in units of time^{-1}) of the actively growing fraction of the population at t_0
- r' – the change in μ with each time step
- f_0 – the conversion factor (F) (in units of biomass or cells mol^{-1} of substrate) at t_0
- f' – the change in F with each time step
- $N_a(0)$ – the abundance of actively growing cells (in units of biomass or cells volume^{-1}) at t_0
- N_d – the abundance of dormant or slow growing cells (in units of biomass or cells volume^{-1})

2.2.2 Definitions and Assumptions

1. Growth rate (μ) can change over time, but only in a linear fashion.

$$\mu(t) = r_0 + r't \qquad (1)$$

2. The conversion factor (F) can change, but only linearly with time

$$F(t) = f_0 + f't \qquad (2)$$

3. Cell abundance (N) can be described as the combination of two cell populations, one that is active or fast-growing (N_a) and one that is dormant or slow growing (N_d)

$$N(t) = N_d + N_a(t) \qquad (3)$$

4. Isotope incorporation rate (v_p) (in units of mol volume^{-1} time^{-1}) is the product of N_a and the cell specific incorporation rate for active or fast growing cells (v_c).

$$v_p = N_a v_c \qquad (4)$$

5. The conversion factor (F) is the number of new cells (or biomass) produced (μN_a) per unit of label incorporated (v_p).

$$F = \mu N_a / v_p \qquad (5)$$

2.2.3 Derived Variables

- N_a – the abundance of active or fast-growing cells. At any time, N_a is the result of the exponential increase of N_a from the previous time point (t–1) while accounting for the effects of any change in μ that may have occurred over the time interval t–1 to t.

$$N_a(t) = N_{a(t-1)} \times \exp[(\mu_t + \mu_{t-1}/2) \times (\Delta t)] \qquad (6)$$

- N – the total cell abundance (see Equation 3).

- v_p – the isotope incorporation rate based on Equation 5 above.

$$v_p(t) = N_a(t) \times \mu(t)/F(t) \qquad (7)$$

where μ and F are model input values, and $N_a(t)$ is calculated as stated above.

2.3.0 Model Output

2.3.1 Patterns in Model Output

The following discussion draws on the grow-out simulation model output presented in Fig. 2.1 representing six different permutations of the model using input as presented in Table 2.1. The different patterns produced by this grow-out simulation model suggest specific mechanisms that may underlie similar patterns in actual grow-out experiments. There are three patterns commonly seen in actual grow-out experiments that do not fit the assumptions of simple exponential growth, but are explained by the grow-out simulation model: 1) different slopes for the semi-log plots of cell abundance and the label incorporation rate over time, 2) non-linearity of either or both semi-log plots of cell abundance and the label incorporation rate over time, and 3) initial decreases in label incorporation (Ducklow and Hill 1985.

Probably, the most widely discussed of these anomalies are the inconsistencies in slope between increasing cell abundance with time and increasing label incorporation rates with time, which are identical during simple logarithmic growth (Fig. 2.1 A and G). This difference in slope is typically a faster rate of increase for label incorporation than for cell abundance. This grow-out simulation model suggests three mechanisms that can lead to this type of pattern: 1) the presence of an inactive or slow-growing fraction of the population (Fig. 2.1 B and H), 2) an increase in the intrinsic growth rate (Fig. 2.1 C and I), and 3) a decrease in F, the number of cells produced per mole of label incorporated (Fig. 2.1 F and L).

Figure 2.1. Model output showing bacterial growth curves for cell abundance (N), label incorporation rate (v_p) and specific incorporation rate (v_p/N) under conditions when a portion of the bacterial population is dormant or slow growing ($+N_d$), when growth rate changes ($\pm \mu$) over time, and when the conversion factor changes ($\pm F$) over time. The slope (m) and coefficient of multiple determination (R^2) are shown for each linear regression. Input values used in these model runs are presented in Table 2.1.

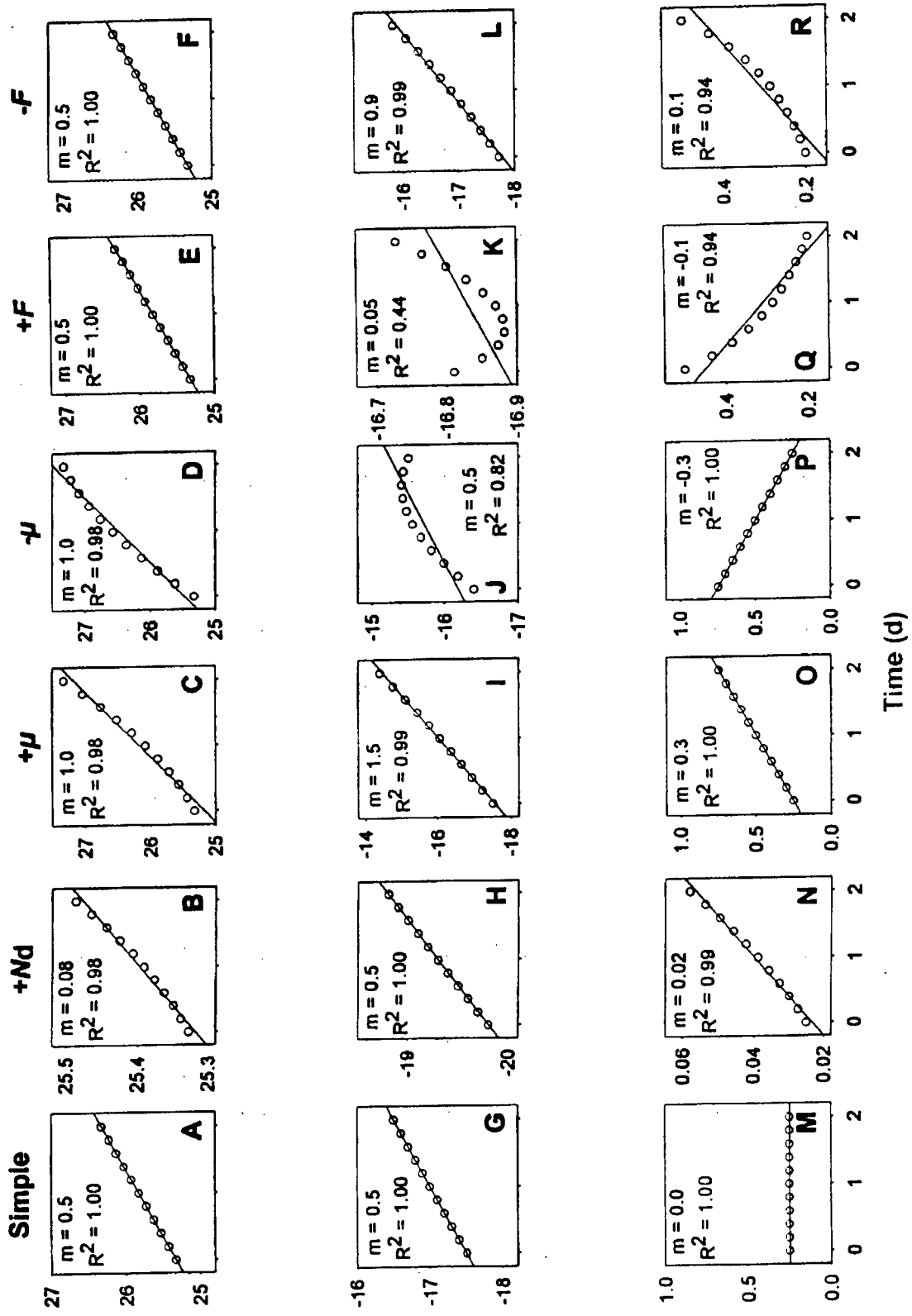
Simple
+Nd
+μ
-μ
+F
-F
log$_e$ N (cells m^{-3})
log$_e$ Vp (mol label m^{-3} d^{-1})
Vp/N (amol label cell^{-1} d^{-1})
Time (d)
A m = 0.5 R^2 = 1.00
B m = 0.08 R^2 = 0.98
C m = 1.0 R^2 = 0.98
D m = 1.0 R^2 = 0.98
E m = 0.5 R^2 = 1.00
F m = 0.5 R^2 = 1.00
G m = 0.5 R^2 = 1.00
H m = 0.5 R^2 = 1.00
I m = 1.5 R^2 = 0.99
J m = 0.5 R^2 = 0.82
K m = 0.05 R^2 = 0.44
L m = 0.9 R^2 = 0.99
M m = 0.0 R^2 = 1.00
N m = 0.02 R^2 = 0.99
O m = 0.3 R^2 = 1.00
P m = -0.3 R^2 = 1.00
Q m = -0.1 R^2 = 0.94
R m = 0.1 R^2 = 0.94

Table 2.1 Grow-out simulation model input parameters used to generate the sample output in Fig. 2.1: growth rate (μ), conversion factor (F), abundance of dormant or inactive cells (N_d), and abundance of actively growing cells (N_a). Model perturbations were all variations on simple logarithmic growth (Simple), with the addition of an inactive fraction ($+N_d$), increasing ($+\mu$) and decreasing ($-\mu$) growth rates, and increasing ($+F$) and decreasing ($-F$) conversion factors. The model was run for 10 time steps over two time units presumed to be days (i.e., each time step was 0.2 d).

Model Perturbation	μ (d^{-1})	F (10^{18} cells mol^{-1})	N_d (10^9 cells)	$N_a(0)$ (10^9 cells)
Simple	0.5	2.0	0	100
$+N_d$	0.5	2.0	90	10
$+\mu$	0.5 - 1.5	2.0	0	100
$-\mu$	1.5 - 0.5	2.0	0	100
$+F$	0.5	1.0 - 2.5	0	100
$-F$	0.5	1.0 - 2.5	0	100

In the presence of an inactive fraction, growth of the active fraction is still a simple exponential curve leading to a linear semi-log plot of the label incorporation rate (Fig. 2.1 H). But, the apparent growth rate based on total cell abundance is proportionately smaller since only a fraction of the population is contributing to growth. The slope (m) of N vs. t is much less than the slope (m) of v_p vs. t (Fig. 2.1 B and H). The curve of the semi-log plot of cell abundance is concave compared to a linear fit because the proportion of active cells is increasing with time and thus giving the appearance of an increase in growth rate with time (cf. Ducklow 2000). In this case the slope of the semi-log plot of the label incorporation rate, and not cell abundance, is the actual growth rate of the active fraction of the population.

When the intrinsic growth rate increases during the grow-out experiment, there is a disproportional increase in the rate of label incorporation relative to the rate of increase in cell abundance, because in addition to more cells taking up the label, as the growth rate increases, each cell takes up the label faster (2.1 I). An increase in the growth rate leads to a semi-log plot of cell abundance that is concave relative to a linear fit (similar to the case with an inactive fraction) and the slope of the plot gives an average growth rate for the experiment, not the growth rate at t_0 needed for the calculation of F using one of the derivative methods (Fig. 2.1 C).

If the conversion factor F decreases during the incubation (fewer cells produced per unit of label) then the incorporation of the substrate (label) must increase with time to maintain the same growth rate. Thus the slope of the semi-log plot of the label incorporation rate increases with time becoming proportionately steeper than the semi-log plot of cell abundance and very slightly concave (Fig. 2.1 L). In this case, the slope of the semi-log plot of abundance, not the slope of the semi-log plot of the label incorporation rate represents the true growth rate of the population (2.1 F).

Without exceptionally precise data, it is difficult or impossible to differentiate between the presence of an inactive fraction and an increase in growth rate, especially since both may be acting together. However, it may be possible to discern a decreasing conversion factor because the plot of label incorporation per cell (v_p/N) over time changes as $1/F$ and is thus concave compared to the nearly linear increase in v_p/N associated with either an inactive fraction or increasing growth rate (Fig. 2.1 R).

There are two cases where the rate of increase in cell abundance is faster than the rate of increase in label incorporation (slope of ln $N(t)$ > slope of ln $v_p(t)$). Not surprisingly, they occur when μ decreases and when F increases. A decrease in the growth rate produces a decrease in the slope (convex) for the semi-log plots of both cell abundance and label incorporation rate (Fig. 2.1 D, J). A decreasing growth rate is the only permutation of the grow-out simulation model that produces a convex semi-log plot of cell abundance.

Unlike a decrease in growth rate, an increase in F does not affect the linearity of the semi-log plot of cell abundance (2.1 E), but produces a concave semi-log plot of label incorporation rate (2.1 K). Surprisingly, when the conversion factor increases linearly (as in the grow-out simulation model) there is often an initial decrease in label incorporation (Fig. 2.1 K).

2.3.2 Assessment of Different Conversion Factor Calculations Using Model Output

Model output was used to assess the ability of the various conversion factor calculation methods to accurately predict F. Calculations of F were made: 1) directly from the grow-out simulation model output, 2) from output with a random ± 10% error added to each output value, and 3) from the grow-out simulation model output reduced to 3 time points (beginning, middle, and end of the grow-out) with the ±10% error included (Table 2.2). All methods performed well under simple exponential growth where no inactive or slow-growing cells were present. All the methods discussed above failed to provide an accurate estimate (better than ± 60% of the actual value) of $F(0)$ under at least one of the perturbations.

Generally (the exception being in the presence of N_d), all the methods performed better on model data if points from later time steps in the "incubations" were removed and thus only the few data points closest to the t_0 value were used. This increased accuracy would not necessarily be observed with the noisier data from real experiments where more data points can decrease the uncertainty associated with sampling error. However, this does suggest that under many circumstances, there is justification for using data from as short a time-frame as possible from the starting time when calculating F (see discussion below of Kirchman and Hoch 1988).

Table 2.2 Accuracy and robustness of the seven conversion factor (F) calculation methods for calculating F at t_0. Methods were tested on model output generated from known values of F. The model output was generated either from simple logarithmic growth or from simple logarithmic growth perturbed by the presence of 1) a dormant or inactive fraction of the population ($+N_d$), 2) an increasing or decreasing growth rate ($\pm \mu$), or 3) an increasing or decreasing conversion factor ($\pm F$). See Table 2.1 for specific input values used. The accuracy value is the known F divided by the calculated F for each of the six model purtibation. For model runs where ± 10% random error was included, 10 replicate runs were used to calculated the mean F (used in the comparison) and the coefficient of variation (CV).

Model Perturbation	Derivative 1[A] Accuracy	CV	Derivative 2[B] Accuracy	CV	Non-linear Derivative[C] Accuracy	CV	Modified Derivative Accuracy	CV	Integrative Accuracy	CV	Cumulative Accuracy	CV	Non-linear Cumulative Accuracy	CV
Calculated on 11 point model output														
Simple	1.0		1.0		1.0		1.0		1.0		1.0		1.0	
$+N_d$	10.0		1.6		1.0		1.6		1.0		1.0		1.0	
$+\mu$	3.1		2.0		1.6		1.8		1.0		1.0		1.0	
$-\mu$	0.3		0.7		0.6		0.6		1.0		1.0		1.0	
$+F$	0.1		1.1		1.0		1.2		2.0		1.8		0.9	
$-F$	1.6		0.9		1.0		0.9		0.5		0.6		0.9	
Calculated on 11 point model output that included ± 10% random sampling error														
Simple	1.0	0.05	1.0	0.11	0.9	0.13	1.0	0.06	1.0	0.08	1.0	0.04	1.0	0.17
$+N_d$	9.7	0.12	1.3	0.33	1.5	0.51	1.5	0.08	1.0	0.08	1.0	0.48	1.3	0.62
$+\mu$	13.1	0.51	3.9	0.11	1.7	0.41	2.8	0.21	0.9	0.11	1.0	0.14	1.1	0.18
$-\mu$	-0.7	0.10	0.6	0.09	0.6	0.08	0.5	0.08	0.9	0.11	1.0	0.10	1.0	0.23
$+F$	-0.1	0.29	1.0	0.09	0.9	0.14	1.1	0.04	2.0	0.08	1.8	0.07	1.1	0.26
$-F$	2.1	0.06	1.0	0.09	0.9	0.13	1.1	0.07	0.5	0.08	0.6	0.09	0.9	0.12
Calculated on 3 point model output that included ± 10% random sampling error														
Simple	1.0	0.09			NA	NA	1.0	0.10	1.0	0.10	1.0	0.14	NA	NA
$+N_d$	10.0	0.17			NA	NA	1.6	0.15	1.0	0.10	1.0	0.14	NA	NA
$+\mu$	7.1	0.75			NA	NA	1.9	0.67	1.0	0.43	0.9	0.67	NA	NA
$-\mu$	0.8	0.04			NA	NA	0.9	0.06	1.0	0.07	1.0	0.09	NA	NA
$+F$	0.6	0.04			NA	NA	1.0	0.07	1.2	0.10	1.3	0.13	NA	NA
$-F$	1.2	0.15			NA	NA	1.0	0.13	0.9	0.10	0.9	0.14	NA	NA

[A]Derivative 1 used the slope of the semi-log plot of cell abundance as μ.

[B]Derivative 2 used the slope of the semi-log plot of the label uptake rate as μ.

[C]Non-linear derivative used a non-linear fit (Equation 9) to determine μ and N_a.

NA, The non-linear equations use three unknowns and are thus not appropriate for fitting a curve to two or three data points.

Derivative methods – The two derivative methods attempt to predict F from the following relationship:

$$F(0) = \mu N_a(0)/v_p(0) \qquad (8)$$

However, in practice (unless non-linear fitting is used, see below) the derivative methods actually use the total cell abundance (N) instead of the abundance of active or fast-growing cells (N_a), because N_a is not easily quantified. They assume a constant μ over the time for the grow-out experiment and calculate μ from the slope of either the semi-log plot of cell abundance ($ln\ N(t)$) or the semi-log plot of label incorporation rate ($ln\ v_p(t)$). In determining the parameters for the above equation, $v_p(0)$ can be measured, but N_a and μ must be inferred by fitting equations that assume there is no change in μ, and there is no inactive fraction (N_d). If these assumptions are met, the derivative models provide an accurate estimate of $F(0)$.

Neither of the derivative methods accounts for the difference between the active fraction of the population (N_a) and the total population (N) when N_d is present. If the slope of the semi-log plot of label incorporation rate ($ln\ v_p(t)$) is used to determine the growth rate (μ), then the growth rate of the active fraction of the population is obtained, because only the active cells take up the label. But, when calculating F, if μ of the active fraction is used in conjunction with total cell abundance instead of the active cell abundance (i.e. $F = \mu(N/v_p)$, instead of $F = \mu(N_a/v_p)$), then the estimate of F is systematically overestimated by $N(0)/N_a(0)$ which can easily be a factor of 10 (Table 2.2).

If the semi-log plot of cell abundance is used to determine growth rate, the derivative methods become more accurate, because the errors confound instead of exaggerate each other. Using μ calculated from the change in cell abundance in the presence of an inactive fraction can significantly underestimate the μ of the active fraction. But, this error is offset when total cell abundance (N) instead of the active fraction (N_a) is used in Equation 8. These errors still lead to a systematic overestimate of F, but less of an overestimate than if the slope of the semi-log plot of label incorporation rate were used to determine μ.

Kirchman *et al.* (1982) suggested the use of a non-linear fit (Equation 9) to more accurately determine μ in the presence of "dormant" or non-dividing cells.

$$N(t) = N_d + N_a(0)e^{\mu t} \qquad (9)$$

However, the application of this formulation to real systems is limited, because the addition of the third variable (N_d) in the growth equation substantially reduces the confidence/reliability of the fit especially when sampling error is present (see Table 2.2).

If the growth rate (μ) is changing over time, then instead of $\mu(0)$, the calculated μ will be closer to the average μ over the whole length of the grow-out experiment. This results in the derivative methods overestimating $F(0)$ when μ increases and underestimating $F(0)$ when μ decreases over time.

The derivative methods are the only previously published methods that provided an accurate estimate of $F(0)$ when F changed over time. However, they did so only when the semi-log plot of N was used to calculate μ and when there was no N_d present and no associated change in μ.

Integrative methods – The integrative methods (including the cumulative method) are based on comparing the increase in cell abundance to the label incorporation rate integrated over the same time. The original integrative (Rieman *et al.* 1987) method uses the following equation to calculate F:

$$F = \frac{N(t_{max}) - N(0)}{\int_0^{t_{max}} v_p \, dt} \qquad (10)$$

and thus, it is sensitive to the data point chosen to represent the end of the grow-out experiment, $N(t_{max})$. It is also sensitive to the any error associated with the measurement of $N(0)$. The cumulative method (Bjornsen and Kuparinen 1991) uses essentially the same relationships shown in Equation 10, but plots x and y for each time point (t_i) sampled and uses the slope of the regression of y on x as F.

$$x = \int_0^{t_i} v_p dt \qquad (11)$$

$y = N(t_i)$, or alternatively (12)

$y = N(t_i) - N(t_0)$ for each t. (13)

An orthogonal (Type 2) linear regression is appropriate since the slope of y on x is used to describe the relationship between the two variables x and y (each associated with an error term) and not used to predict a dependent y from an independent x. The relationship of x to y in Equation 13 suggests that when x = 0, y = 0. Therefore, when using Equation 13, the regression may be forced through the origin to improve the accuracy of the *F* estimate.

The integrative methods seem the most robust since they provide for an accurate estimate of *F* both in the presence of an inactive or slow-growing fraction N_d, and in the presence of a changing growth rate μ (Table 2.2). However, because the basic assumption of the integrative methods is that *F* is constant with time, these methods fail to predict *F*(0) in model simulations where *F* is variable. Instead of estimating *F*(0), these methods estimate *F* closer to the average for the whole grow-out incubation. When *F* changes, the integrative methods predict *F*(0) most accurately from data points that lie closest to t_0 suggesting a trade-off between better predictive power in the presence of sampling errors (i.e. having more data points) and improving the accuracy if the error is small.

One approach to improving the accuracy of the cumulative method under conditions of changing *F* is to relax the assumption of a constant *F* and fit the following polynomial equation to the x and y variables used in the cumulative regression (Equations 11-13).

$$y = ax + bx^2 \qquad (14)$$

where a is an estimate of f_0 as defined in Equation 2 and b is the rate of change in F relative to the label incorporation (functionally similar to f' in Equation 2). The regression should again be forced through the origin if Equation 13 is used to calculate y. This method can substantially improve the accuracy of the cumulative method under changing F, but it also increases the uncertainty of the estimate when the data are noisy (Table 2.2).

Not surprisingly, the integrative methods are quite sensitive to the method of integration used. For instance, a linear interpolation between adjacent time points in the grow-out model underestimated F by 30%, whereas a logarithmic interpolation provided an accurate estimate of the correct F in all cases except where F changed with time.

Since the grow-out simulation model uses exponential growth equations to produce its output, it is expected that an exponential integration will fit the data better than a linear one. Under field conditions, if the assumption of underlying exponential growth is not valid during a grow-out experiment, then the advantage of exponential integration does not hold. Nevertheless, the substantial difference between linear and exponential integration still serves to illustrate the potential error associated with the choice of the integration method used.

2.3.3 Conversion Factors From Real Data

Several issues associated with predictable non-steady-state growth were addressed above. However, in real grow-out experiments confidence in the calculated conversion factors may be further undermined by less predictable variability due to the following: 1) changes in data later in the incubation that do not match the initial trends, 2) initial time points being anomolously high or low relative to the remainder of the growth curves, or 3) differences between experimental and *in situ* cell-specific label incorporation rates (v_p/N). However, with an improved understanding of what causes the observed patterns, anomalous data, particularly near the end of an experiment, can be included or excluded from the calculations of F with greater confidence.

To enhance the discussion on problem data, three grow-out experiments previously discussed in the literature will be highlighted (Fig. 2.2). The data presented are approximations made from the original published plots.

Figure 2.2. Growth curves from historical bacterial grow-out experiments showing cell abundance (N), label incorporation rate (v_p), cell specific incorporation rate (v_p/N), and cumulative cell abundance vs. cumulative label incorporation as used for determining conversion factors. Also shown are slopes at t_0, based on a least squares best fit quadratic (m_0) or linear (m) equation, the y-intercepts (y_0), and the coefficients of multiple determination (R^2). Filled circles indicate data excluded from the analysis. Great Sippewissett Marsh and Ice House Pond data are from Kirchman *et al.* (1982). Warm-core ring data are from Ducklow and Hill (1985).

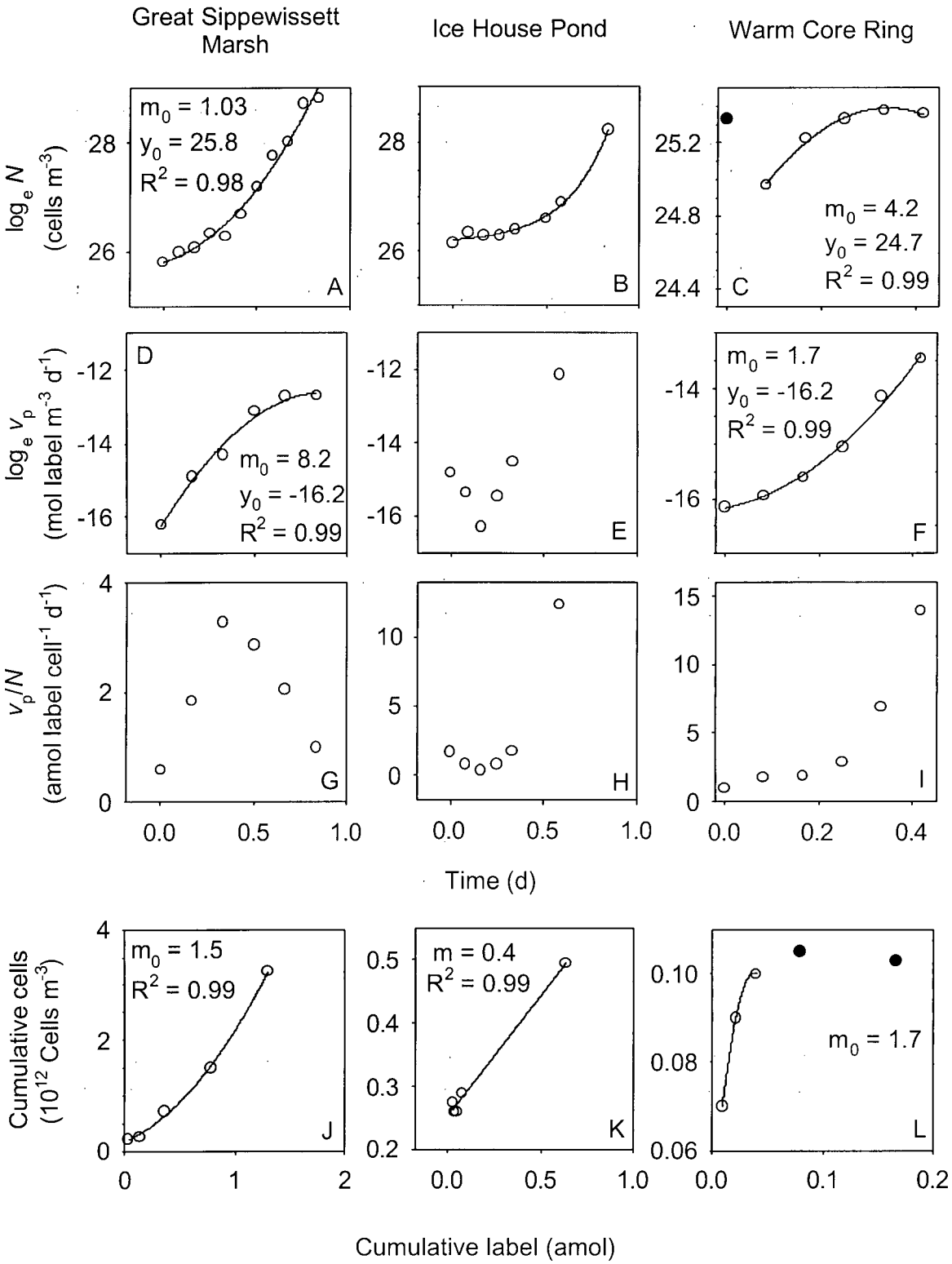
Great Sippewissett Marsh
Ice House Pond
Warm Core Ring
log$_e$ N (cells m^{-3})
m$_0$ = 1.03
y$_0$ = 25.8
R^2 = 0.98
A
B
m$_0$ = 4.2
y$_0$ = 24.7
R^2 = 0.99
C
log$_e$ v$_p$ (mol label m^{-3} d^{-1})
D
m$_0$ = 8.2
y$_0$ = -16.2
R^2 = 0.99
E
m$_0$ = 1.7
y$_0$ = -16.2
R^2 = 0.99
F
v$_p$/N (amol label cell^{-1} d^{-1})
G
H
I
Time (d)
Cumulative cells (10^{12} Cells m^{-3})
m$_0$ = 1.5
R^2 = 0.99
J
m = 0.4
R^2 = 0.99
K
m$_0$ = 1.7
L
Cumulative label (amol)

Kirchman *et al.* (1982, see their Fig. 1) presented data from Great Sippewissett salt marsh showing typical examples of non-linear semi-log plots for bacterial abundance and label incorporation rates. Kirchman *et al.* (1982, see their Fig. 4a) presented data from Ice House Pond in August where label incorporation decreased during the first four hours of the incubation. Ducklow and Hill (1985) presented data from warm core rings in the N Atlantic where cell abundance decreased initially and then increased only slightly while label incorporation increased continuously. The following discussion is a reinterpretation of these observations within the context of this grow-out simulation model. Although the following interpretations are not necessarily the only explanations for the patterns observed in these grow-out data, they do suggest a more comprehensive alternative explanation.

Great Sippewisset Marsh – Kirchman *et al.* (1982) present data from two replicate grow-out experiments from Great Sippewissett Marsh. The *A* replicate showed a distinctly convex semi-log plot of [^{3}H]-thymidine incorporation, while the *B* replicate showed a distinctly concave semi-log plot of bacterial abundance. These data appear to show distinct trends that are not linear on a semi-log plot and v_p/N is not linear with respect to time. Since the grow-out simulation analysis suggested the same basic interpretation for both replicates, the data from both replicates were averaged together for this discussion (Fig. 2.2). The original interpretation of these data suggested that the semi-log plots of both bacterial abundance and label incorporation were fairly linear and the slopes were similar, and therefore 1) the slopes probably presented a realistic growth rate for the population, 2) most of the population was actively growing, 3) growth rate was constant, and 4) the "specific incorporation" (assumed to mean cell specific incorporation of label, v_c) was constant. The presence of an inactive or slow-growing subpopulation of cells and a change in specific incorporation were also discussed, based on the concave semi-log plot of bacterial abundance and the convex semi-log plot of label incorporation.

This grow-out simulation model takes these inferences a step further and alters the overall conclusions. The convex semi-log plot of label incorporation rate is indicative of a decreasing growth rate, not a constant one (Figs. 2.1 J, 2.2 D). The concave semi-log bacterial abundance plot is indicative of an inactive fraction as suggested in the initial

analysis (Figs. 2.1A, 2.2 A). A decreasing growth rate counteracts the concave pattern caused by an inactive fraction on the bacterial abundance curve, thus straightening the semi-log plot and presenting the appearance of simple logarithmic growth. A decreasing growth rate also disproportionately reduces the slope of the semi-log plot of the label incorporation rate bringing it closer over time to the slope of the cell abundance plot, again presenting the appearance of simple logarithmic growth. The co-occurrence of an inactive fraction and a decreasing growth rate is further supported by the increase and then decrease in v_p/N (found in both replicates) which is only explained by the grow-out simulation model if both growth rate and the inactive fraction interact in this way (Figs. 2.2 A, 2.3 A, Table 2.3). Complicating the interpretation, the conversion factor increases with time when calculated by the non-linear cumulative method (Fig. 2.2 J). The change in conversion factor does not change the overall patterns in this case, but does require a higher initial growth rate and a faster associated decrease in growth rate to balance the changing conversion factor (Table 2.3). Accepting that μ was decreasing and F was increasing during this grow-out experiment, the relationship expressed in Equation 15 between μ, F, and the cell specific incorporation rate for active cells (v_c)

$$v_c = \mu/F \text{ (derived from Equations 4 and 5)} \qquad (15)$$

suggests that v_c was decreasing, contrary to the original interpretation. The differences between the replicates are likely due to the subtle differences in the ratios of the active to the inactive fractions, the rate at which the growth rates were decreasing, and the rate of change of the conversion factor.

According to this reinterpretation, the growth rate at t_0 required to balance the grow-out simulation model was about twice that estimated from the slopes of the semi-log plots (~10 d^{-1} instead of ~5 d^{-1}) (Table 2.3). The inactive fraction was also 2-fold higher than the original estimate based on Equation 9 alone, because Equation 9 does not account for the decreasing growth rate. The conversion factor (F_0) was ~ 1×10^{18} cells mol^{-1}, roughly a factor of 4 lower than originally reported (Kirchman *et al.* 1982), because the derivative method used in the original paper overestimates the conversion factor when a population contains dormant or slow-growing cells.

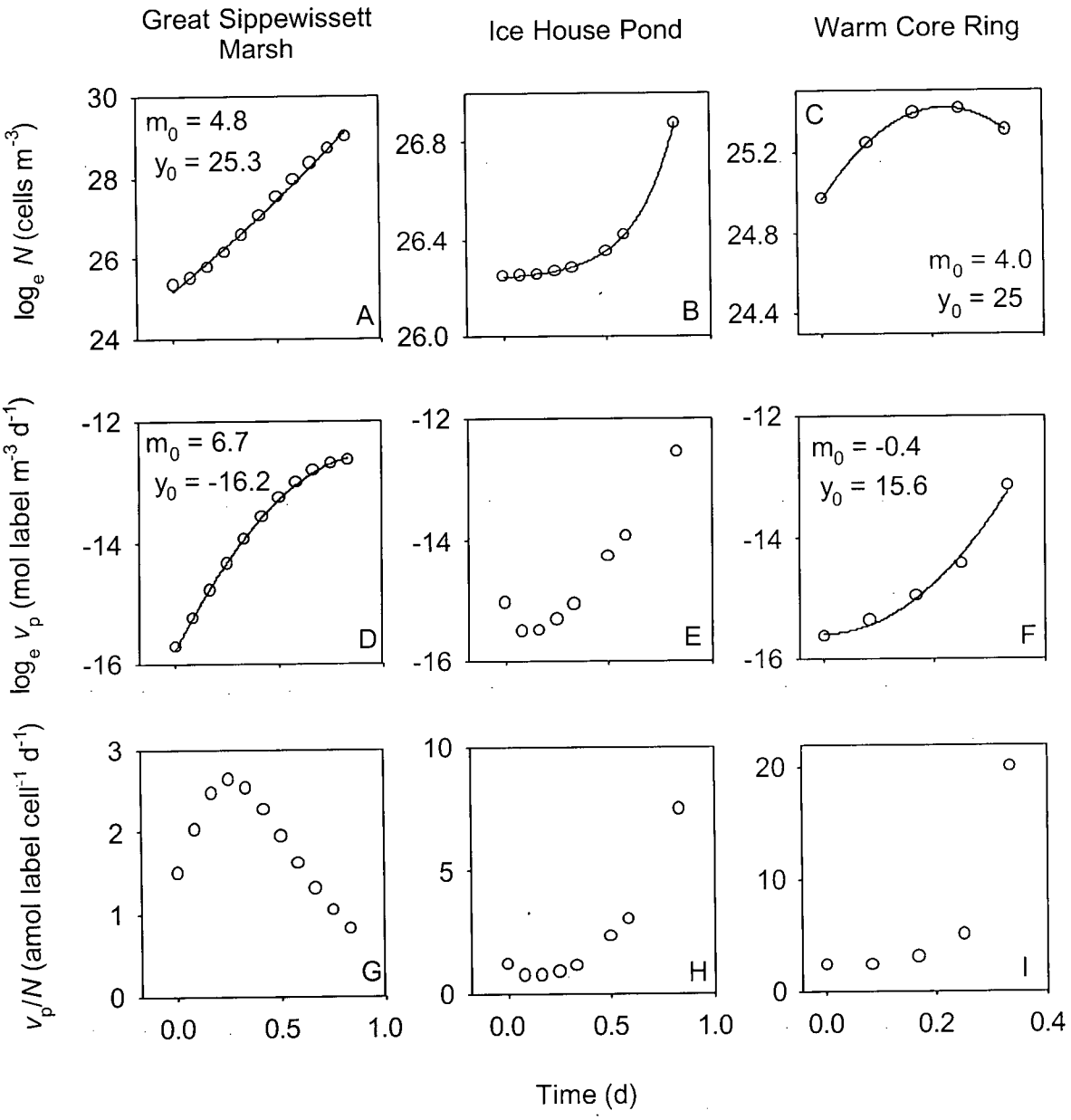

Figure 2.3. Model output showing the recreation of historical growth curves accomplished by adjusting the model input parameters to reproduce the general shape and magnitude of the historical data presented in Fig. 2.2. Also shown are slopes at t_0, based on a least squares best fit quadratic equation (m_0) and the y-intercepts (y_0). Deviations from a simple logarithmic growth model were generated by the addition of inactive cells ($+N_d$), decreasing the growth rate ($-\mu$), and/or changing the conversion factor ($\pm F$) over the course of the modeled incubation (see Table 2.3).

Table 2.3 Model input parameters used to generate output replicating published grow-out experiments as in Figure 2.3: growth rate (μ, d^{-1}), conversion factor (F, 10^{18} cells mol^{-1}), abundance of dormant or inactive cells (N_d, 10^9 cells m^{-3}), abundance of actively growing cells (N_a, 10^9 cells m^{-3}), and loss rate (L, d^{-1}).

Study	Length (d)	μ	F	N_d	$N_a(0)$	L
[a]Great Sippewissit Marsh	0.83	10 - 3.3	1 - 4	85	15	-
[a]Ice House Pond	0.83	6	0.03 - 0.38	250	1.5	-
[b]Warm-core Ring	0.42	4 - 1.5	1.7 - 0.01	0	70	0 - 5

[a]Kirchman *et al*. 1982

[b]Ducklow and Hill 1985

Ice House Pond – Kirchman *et al.* (1982) present another puzzle with data from Ice House Pond where label incorporation actually decreased during the first four hours while cell abundance increased. The authors suggest that such a decrease is evidence of a change in specific activity that may be linked to label dilution. This interpretation is consistent with an increasing F that is required for the grow-out model to replicate this grow-out experiment. Kirchman *et al.* (1982) then estimate what they considered to be an anomolously high conversion factor based only on the more linear data from later in the incubation, after the 4 h sample. But, the grow-out model suggests that the declining label incorporation rate need not be treated as incongruent with the later data. The initial decline followed by a nearly linear increase can also be explained by a linearly increasing conversion factor (Figs. 2.1 K, 2.2 E, 2.3 E). The general patterns in these data are explained by an increasing conversion factor in combination with a substantial inactive fraction. Using all the data with the cumulative method provides a more typical estimate for the conversion factor ($\sim 4 \times 10^{17}$ instead of $6 - 30 \times 10^{19}$ cells mol^{-1}).

North Atlantic Warm Core Ring – Ducklow and Hill (1985) present data from a warm core ring in the N Atlantic where cell abundance decreased initially and then increased only slightly while label incorporation increased continuously (Fig 2.2 C, F). This case is presented as an example of the apparent decoupling between the rate of label incorporation and the rate of increase of bacterial abundance.

The initial decrease in cell abundance is not directly addressed by this grow-out model. It seems unlikely that the decrease in abundance was caused by a substantial loss of actively growing cells since there was not an associated decrease in the label incorporation rate. In fact, the grow-out simulation model balances nicely when the initial cell abundance value is left out of the analysis. This pattern of initial cell loss is not uncommon and may be associated with adhesion of senescent or slow-growing cells to the walls of the incubation container. For the purpose of illustrating the grow-out simulation model's explanation of decoupling, these data will be discussed assuming that the first cell abundance point is an outlier and growth parameters are calculated from the second time point onward.

The grow-out simulation model suggests that when conversion factors decrease over time, decoupling between cell abundance and label incorporation rate may be observed, in association with a concave semi-log plot of label incorporation rate. These patterns are seen in these data (Fig 2.2 C and F). In this instance, the best estimator of the growth rate is the slope of the semi-log plot of the cell abundance near t_0, not the label incorporation rate, since a changing conversion factor substantially alters the slope of the label incorporation rate. Following the initial decrease, there is an increase in cell abundance. If the assumptions of the grow-out model are accepted, then the semi-log plot can be fit to a second order polynomial instead of a straight line giving more accurate estimates of $\mu(0)$ and $v_p(0)$ (Fig 2.2 C, F). Using these values with the derivative equation should provide the most accurate $F(0)$ (2.3×10^{18} cells mol^{-1}) since there is no evidence of an inactive fraction (aside from the first datum that was removed for this analysis) and thus $N \approx N_a$. The changing conversion factor can also be calculated at t_0 using the non-linear cumulative method (1.7×10^{18} cells mol^{-1}). Although the grow-out model can qualitatively match the patterns of decoupling observed in this grow-out experiment, the addition of an increasing loss term (to mimic the onset of grazing) was required to quantitatively reproduce these data. According to this analysis, the growth rate at t_0 was ~ 0.17 h^{-1} instead of the 0.28 h^{-1} that the authors calculated and rejected as being too high. However, even 0.17 h^{-1} is too high if loss processes and a decreasing growth rate are not included in the analysis.

The grow-out simulation model suggests that in all three of the above previously published examples, the conversion factor (F) changed over time. In two of the three examples, an inactive or slow-growing fraction of the population (N_d) was evident. In two of the examples, there was a change in growth rate (μ) over time. No single previously published method for calculating conversion factors adequately addresses all of these variations. However, the non-linear cumulative method introduced here appears to be a fairly robust solution when more than three time points are available.

Changes in the trend of the later time points are indicative of a shift in growth parameters due to a change in nutrient status, a change in species composition, initiation of grazing, increased viral mediated loss, or other physiological or ecological factors. All the methods for calculating conversion factors depend on either steady-state growth or

linear changes in properties over time. Accordingly, any shift in growth parameters not accounted for by the calculations will reduce the accuracy of the result. Therefore, when the earlier data from the grow-out experiments fit the assumptions of the calculations reasonably well, F is most accurately determined by using only the earliest data in the calculations. The problem is that the choice of time after which data should be excluded is often arbitrary. However, the practice of removing data from later in the time-course of a grow-out experiment is supported by this analysis.

In some cases, anomolously high conversion factors were observed during the first few hours of grow-out experiments (Kirchman and Hoch 1988). It was suggested that an initially high level of label dilution could explain the observations and that the later time points were most appropriate for use in estimating *in situ* conditions. This grow-out model does not address possible mechanisms for changing conversion factors, but these data do highlight the need to compare the label incorporation per cell of *in situ* samples to the early time-points in filtration/dilution incubations. Without such a comparison, it is difficult to differentiate between anomalous conditions due to the filtration/dilution treatment, or anomalous but real conditions *in situ*.

In general, with more insight into the potential mechanisms underlying the patterns observed in the grow-out data, seemingly anomalous data, particularly near the end of an experiment, can be included or excluded from conversion factor calculations with confidence.

2.4.0 Conclusions

The grow-out simulation model presented herein suggests that the apparent anomalies in, and decoupling of, cell growth/division and label incorporation rates often seen in real data can be explained by one or a combination of changes in growth rate, changes in conversion factor, or the presence of inactive or slow growing cells in the population. This grow-out simulation model suggests that a reasonable conversion factor (F) may still be calculated from some previously uninterpretable data sets. Understanding the sources of patterns lends confidence to either the inclusion or exclusion of more data from later time points. Insightful inclusion or exclusion of more

data will improve the confidence in, and accuracy of, the conversion factor calculations being made. Finally, the integrative methods, when used with an appropriate integration algorithm provide the most robust calculations of F under the various permutations so long as F is constant. When F changes with time, the cumulative method using a polynomial fit instead of a linear fit may be the best choice for determining empirical conversion factors.

Chapter 3

Seasonal and Interannual Trends in Heterotrophic Bacterial Processes Between 1995 and 1999 in the Subarctic NE Pacific Ocean

3.1.0 Introduction

Bacteria are estimated to constitute > 50% of the total biomass of the ocean (Wilhelm and Suttle 1999). They consume a large portion of primary production (2 - 130%) (Williams 2000 and references within) and mineralize most of the dissolved organic carbon (DOC) that they consume back into CO_2 through respiration (del Giorgio and Cole 2000 and references within). At present, one of the central issues associated with ocean biological processes is their role in the global carbon cycle. Before useful models addressing the role of biological processes on carbon cycling are developed, a basic understanding of the variability in the factors controlling biological standing stocks and rate processes must be established.

In part to address carbon budget issues, work has been carried out estimating bacterial abundance and productivity around the world (Ducklow 1999, Ducklow 2000 and references within). However, most of these studies lack respiration measurements which are needed to estimate bacterial growth efficiency, bacterial carbon demand, and ultimately balance the ocean carbon budget and determine CO_2 mineralization rates (Cole and Pace, 1995; Jahnke and Craven, 1995; del Giorgio *et al.*, 1997; Williams 1998). Also, few studies have had the opportunity to address seasonal and interannual changes in abundance and productivity either in the open ocean or along a coastal to open ocean transect especially in high-nitrate, low-chlorophyll (HNLC) regions where primary productivity has been shown to be limited by the availability of Fe (Martin *et al.* 1989, Boyd *et al.* 1996, Coale *et al.* 1996).

In association with the SuPER program which visited Ocean Station Papa (OSP) in 1987 and 1988, Kirchman *et al.* (1993) found a 2 – 5-fold increase in both bacterial biomass (BB) and bacterial productivity (BP) in spring and summer 1988 and consistently low growth rates (< 0.1 d^{-1}). Boyd *et al.* (1995a, b) and Doherty (1995)

measured BB and BP in the euphotic zone along line-*P* providing the first shelf-break to HNLC open-ocean transect, including both the winter and spring of 1993 and 1994.

Sherry *et al.* (1999) extended this historical data over two more years adding both deep sampling and respiration measurements. Data reported by Sherry *et al.* (1999) are included as the first two of the four years of observations presented herein.

This chapter addresses uncertainties in the methods associated with determining the conversion factors used in estimating bacterial productivity from the incorporation rates of labeled macromolecule precursors. It presents bacterial productivity and biomass estimates for winter, spring, and summer over 4 years along a 1420 km long transect (line-*P*) from the continental slope to the open ocean HNLC waters off the coast of British Columbia, Canada. This, in conjunction with Sherry *et al.* (1999) is the first study to address changes in bacterial properties both within the surface mixed layer and through the depth of the water column over these three seasons and during multiple years. This is also the first study to measure both bacterial and whole-community respiration in the subarctic NE Pacific, measurements critical to understanding carbon flow in the ocean.

3.2.0 Methods

3.2.1 Data Collection and Sample Processing

Samples were collected during 11 cruises over a 4 year period along the line-*P* transect (Fig. 1.1). Sampling took place in late winter, spring, and late summer between summer 95 and winter 99 (Table 3.1). Sampling was carried out, weather permitting, at all five of the CJGOFS line-*P* stations (P4, P12, P16, P20, and OSP) on each cruise.

Bacterial productivity and biomass – Euphotic zone sampling for bacterial abundance and bacterial productivity (BP) was done using acid-cleaned 10 L GoFlo bottles mounted on a Kevlar line. Deeper sampling was done from 10 L Niskin bottles mounted on a 24 bottle CTD/rosette. The GoFlo bottles were cleaned before each cruise with a 10% HCl acid soak for > 24 h. Niskin bottles were not maintained under trace-metal clean

Table 3.1
Dates of cruises, depth (m) of the euphotic zone as defined by 1% of surface irradiance, and depth (m) of the mixed layer (shown in parentheses) determined subjectively as the shallowest abrupt change with depth in either temperature or salinity. Euphotic zone depths for Sep 95 – Jun 97 were previously presented in Sherry et al. (1999). ND signifies missing data.

Season	Cruise Dates	Year	Euphtoic Zone (Mixed Layer) depth in meters				
			OSP	P20	P16	P12	P4
Summer	22-Aug - 13-Sep	1995	35 (20)	30 (10)	35 (16)	30 (12)	25 (15)
	12-Aug - 6-Sep	1996	40 (25)	35 (20)	40 (20)	40 (17)	30 (7)
	25-Aug - 17-Sep	1997	75 (18)	50 (15)	56 (17)	40 (11)	55 (8)
	24-Aug - 20-Sep	1998	55 (40)	60 (32)	55 (22)	45 (18)	33 (20)
Winter	20-Feb - 8-Mar	1996	80 (95)	80 (95)	80 (120)	50 (40)	40 (70)
	10-Feb - 28-Feb	1997	60 (105)	ND	60 (80)	60 (55)	45 (55)
	16-Feb - 6-Mar	1998	50 (85)	80 (80)	60 (80)	ND (75)	40 (65)
	8-Feb - 28-Feb	1999	75 (115)	75 (94)	60 (92)	ND (95)	40 (11)
Spring	7-May - 30-May	1996	60 (9)	35 (60)	40 (63)	60 (28)	35 (8)
	2-Jun - 26-Jun	1997	70 (20)	70 (25)	65 (23)	75 (20)	35 (6)
	1-Jun - 26-Jun	1998	50 (20)	58 (21)	52 (23)	40 (15)	33 (22)

conditions and the closure springs were well aged latex tubing or Teflon coated steel springs. Euphotic zone sampling was done following an early morning light meter cast used to select 6 sampling depths corresponding to 100, 55, 20, 10, 3.5, and 1% of surface irradiance (PAR) from summer 95 through spring 97 and was reduced to four depths corresponding to 100, 50, 10, and 1% from summer 97 through winter 99. Deep samples were collected at various times of the day from summer 95 through spring 97. The 6 deep sampling depths for each station were based on logarithmically increasing depth increments between the shallowest (1% light depth) and the deepest sample (~ 10 m above the seabed).

Duplicate slides for the determination of bacterial abundance were made within 2 h of water sampling by filtering 5 to 20 ml of a DAPI-stained sample onto black 0.2 μm pore size 25 mm diameter polycarbonate track-etched Poretics filters (Turley, 1993). At least 300 cells were counted in a minimum of 10 fields. Bacterial abundance was converted to BB (see discussion) using the conversion factor of 10 fg C $cell^{-1}$ (Fukuda *et al.* 1998).

BP estimates were based on either [^{3}H]-thymidine (Bell 1993) or dual-labeled [^{3}H]-thymidine/[^{14}C]-leucine (Chin-Leo and Kirchman, 1988) incorporation in 30 ml of sample during a 4 h incubation in the dark. Samples were incubated in 30 ml, acid cleaned, amber, low-density polyethylene bottles. Incubations were maintained at ±2 °C of ambient sea-surface temperature in a dark deckboard incubator with a continuous flow of surface seawater. Converting [^{3}H]-thymidine (TdR) and [^{14}C]-leucine (Leu) incorporation rates into productivity of cells was done empirically using the dilution method as described by Kirchman and Ducklow (1993). The isotope conversion factors used were 3.5×10^{18} cells mol^{-1} for TdR and 0.106×10^{18} cells mol^{-1} for Leu (see determination of conversion factors below). Final cell productivity was calculated as the average of the TdR and Leu cell productivity values. Conversion of the final cell productivity into mg C m^{-3} d^{-1} was done based on 10 fg C $cell^{-1}$ (Fukudo *et al.* 1998) (see discussion). No attempt was made to correct estimates of bacterial productivity to account for the difference between the ambient temperature below the mixed layer and the mixed layer temperature at which all samples were incubated. Therefore the reported

BP estimates may be overestimates of the *in situ* conditions for stations where the euphotic zone was deeper than the mixed layer depth (Table 3.1).

Respiration – Sampling for water column respiration rates was carried out in summer 96, winter 97, and spring 97 only. Water from 10 L Niskin bottles, mounted on a 24 bottle CTD/rosette was drawn either directly into 125 ml oxygen flasks for whole water samples or gravity fed directly from the Niskin bottles through a 1 μm nominal pore size capsule filter (Gelman PN 12023) into the same type of oxygen flasks for the < 1 μm size fraction. It was assumed that the majority of respiration in the < 1 μm fraction was attributable to heterotrophic bacteria (see discussion in Williams, 1981a, b). Triplicate samples for both total community respiration (TR, whole water samples) and bacterial respiration (BR, < 1 μm size-fraction) were drawn for both t_0 controls and incubation bottles giving a total of 12 bottles per depth. Incubations were for 24 h during all cruises except spring 97 during which they were 48 h. Oxygen consumption was estimated from the difference in total oxygen between the t_0 controls and the incubated samples as measured using an automated microwinkler titration (after Furuya and Harada, 1995). The conversion of oxygen consumption in ml O_2 to respiration in μg C was based on the assumption of a 0.8 respiratory quotient (RQ) (Johnson *et al.*, 1981).

Respiration values reported herein were calculated from data that were passed through a data filter which removed "bad" data points according to the following rules: 1) incubated bottles containing more O_2 than the associated t_0 bottle were removed; and 2) size-fractionated incubated samples with less O_2 than the matched whole water incubated sample were removed. The data filter removed 15% of the samples from the respiration dataset.

3.2.2 Calculations

Mean values reported throughout this paper for euphotic zone measurements were calculated by integrating over the six light depths and dividing by the depth of the euphotic zone (depth of 1% of surface irradiance). Thus, these data must be multiplied by the depth of the euphotic zone (Table 3.1) to be directly compared to values of integrated primary productivity (m^{-2}) often reported in other studies.

Other definitions used throughout include:

Bacterial growth rate (Bμ) = BP/BB

Bacterial turnover time (TT) = BB/BP = 1/(Bμ)

Bacterial growth efficiency (BGE) = BP/(BP+BR)

Bacterial carbon demand (BCD) = BP+BR.

Calculations of BCD for stations P16 and OSP in winter 97 (when data were not collected) were based on the assumption that the measure of bacterial processes was nearly invariant along line-*P* in the winter (Fig. 3.1). Therefore the values for BCD at P16 and OSP during winter 97 were calculated from the BP using BCD = BP(1/BGE) using a BGE of 10% which was the average BGE for P4 and P12, where respiration was measured.

Determination of Conversion Factors – Filtration/dilution incubations, also referred to as grow-out experiments, were carried out intermittently during all three sampling seasons to determine the conversion factors for the calculation of cell production from label incorporation rates (TdR and/or Leu) (Table 3.2). Dilutions were 100 mL of sample diluted into 900 mL of water previously filtered through a 0.2 μm capsule filter (Gelman PN12117). Grow-out experiments were run in either duplicate or triplicate parallel incubations over 2 to 5 days with sampling for both bacterial abundance and label incorporation rates done every 12 to 24 h and processed in the same manner as described above for *in situ* measurements. Incubations were done in 1 L polycarbonate bottles incubated at 50% ambient light and ± 1°C of ambient surface temperature (except 300 and 1500 m depths which were incubated in the dark at 9°C).

Conversion factor (*F*) calculations were done for each filtration/dilution incubation time series, the results of which were averaged across replicates (Table 3.2). The cumulative method (Bjørnsen and Kuparinen 1991) was used as the default calculation method. After plotting cell increase against the integrated label incorporation (plots used for the calculation of *F* using the cumulative method), the data were examined for linearity.

If the first few points were linear and then deviated from linearity with time, the later points were removed from the calculations. If all the points were non-linear, but showed a constantly increasing (or decreasing) trend, they were fit to the following equation:

$$y = ax + bx^2$$

where a is an estimate of F at t_0 and b is the rate of change in F relative to the label incorporation.

3.3.0 Results

3.3.1 Empirical Conversion Factors

Euphotic zone conversion factors (F) ranged from $1.6 - 7.1 \times 10^{18}$ cells mol^{-1} for TdR and $4.7 - 23.0 \times 10^{16}$ cells mol^{-1} for Leu (Table 3.2). With three noted exceptions, the plots of cell increase against integrated label incorporation (plots used to calculate F with the cumulative method) were linear suggesting little if any change in F at least during the first 48 h of the grow-out experiments. The three exceptions to the linearity of F were also the three grow-out incubations where the label/cell at t_0 was the furthest from *in situ* values suggesting that these filtration/dilution incubations were substantially different from the *in situ* conditions raising the question of whether any F calculated from such data should be considered valid (Table 3.2). The same non-linear characteristics were present in both TdR and Leu F calculations.

The label incorporation rates per cell at the start of the grow-out experiments varied substantially about the *in situ* values. The per cell Leu incorporation rates following the dilution at the start of the grow-out experiments averaged 2-fold higher than *in situ* ($p < 0.01$) (Table 3.2) suggesting a regular shift-up in Leu incorporation (maybe more protein per cell and/or bigger cells) associated with the filtration, dilution, and incubation of the grow-out experiments. The increase in cell volume (and thus Leu/cell) that is a common artifact of grow-out experiments (Bjørnsen and Kuparinen 1991, Ducklow *et al.* 1992) supports the calibration of F for Leu in terms of measured biomass instead of cell abundance. Under these circumstances, calculating the F for Leu in terms of cell abundance alone would lead to a regular underestimate of Leu-based BP.

During both spring and summer (but not winter) Leu-based BP estimates in this study were consistently lower than TdR based BP estimates (cf. Fig. 3.2) even though the conversion factors for both labels were calculated from the same samples in the same way.

The mean F for the mixed layer was 3.5×10^{18} for TdR and 10.6×10^{16} for Leu. In spring 97, there was a distinctive trend with F (in the mixed layer) decreasing in the off-shore direction for both TdR and Leu (Table 3.2). The lowest values for F in the euphotic zone were those below the mixed layer. Other than spring 97, sampling was insufficient to determine with confidence whether there were any persistent spatial, seasonal or interannual trends in F.

3.3.2 Bacterial Biomass

The depth-averaged euphotic zone bacterial biomass ranged from 3.4 to 25 mg C m^{-3} over this study (at P16 in winter 99, and P20 in summer 95 respectively) (Figs. 3.1 and 3.2). Winter BB was low and relatively constant (~ 5 mg C m^{-3}) all along line-*P*, showing little variability either interannually or within the euphotic zone. In contrast, spring and summer BB averaged 2 to 3-fold higher (7 – 17 mg C m^{-3}) and showed much greater interannual and within euphotic zone variability. There were no consistent trends in magnitude or interannual variability along line-*P*, although relative to P4, OSP showed lower variability within the euphotic zone. Summer BB at OSP was lower during 1997 and 1998 than during the previous two years.

In general, BB decreased exponentially between the bottom of the euphotic zone and 1000 m (Fig. 3.3). In contrast to the other seasons, the spring BB peak observed at P4 in the euphotic zone, continued down the whole water column. However, the summer estimates of BB at P4, although intermediate in the euphotic zone, were the lowest below the euphotic zone. Below 100 m depth at OSP there was only a small difference in BB between seasons (Fig. 3.3), indicating a minimal seasonal response below the mixed layer, in contrast to the stronger seasonality above. Samples from near the sea bed (4000 and 4200 m) typically showed a slight increase in BB relative to shallower samples.

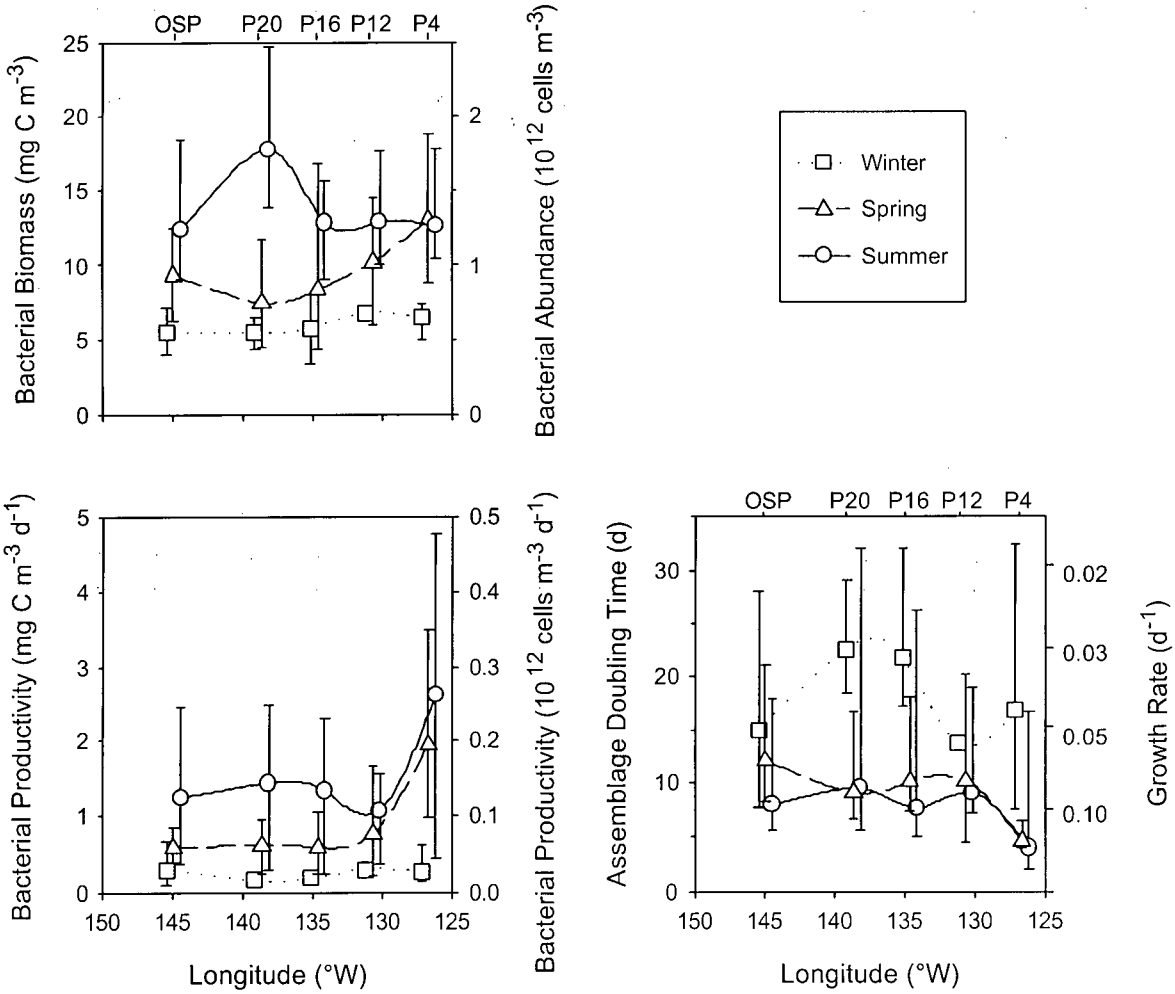

Figure 3.1. Bacterial biomass, bacterial productivity, and bacterial growth rate along line-P during winter (···□··), spring (– –△– –), and summer (—○—). Data represent the mean seasonal euphotic zone values calculated by stepwise integration of euphotic zone measurements divided by the depth of the euphotic zone. Data collected from between Sep 1995 and Feb 1999 (see Fig. 3.2). Error bars represent the interannual range. The longitude for summer and winter values are offset slightly for clarity.

Table 3.2

Conversion factors (F_{TdR}, F_{Leu}) for the determination of bacterial production from [^{3}H]-thymidine and [^{14}C]-leucine uptake rates as determined by linear and non-linear cumulative methods (see text). Also shown are the in situ cell abundance and the ratio between the initial label uptake rate during filtration/dilution incubations and the in situ uptake rate from the same locations (t_0:in situ ratio).

Cruise	Station	Depth (m)	F_{TdR} (10^{18} cells mol^{-1}) ±SE (n)	F_{Leu} (10^{16} cells mol^{-1}) ±SE (n)	t_0:*in-situ* ratio TdR	Leu	*In situ* cell Abundance (10^{12} cells m^{-3})	Calculation Method
Spring 97								
	P4	10	7.1 ±1.9 (2)	23.0 ±6.4 (2)	0.07	0.32	2.39	Non-linear Cummulative (increasing)
	P4	50	2.4 ±0.7 (2)	6.4 ±1.9 (2)	1.88	0.94	1.70	Cummulative
	P4	300	3.1 ±0.3 (2)	4.1 ±0.1 (2)	0.34	1.25	0.43	Cummulative
	P12	10	5.0 ±0.3 (2)	11.4 ±1.9 (2)	0.90	2.00	1.23	Cummulative
	P16	10	5.0 ±0.4 (2)	16.7 ±1.1 (2)	0.75	1.52	1.77	Cummulative
	P20	10	2.2 ±0.1 (2)	7.1 ±0.1 (2)	0.85	2.58	1.13	Cummulative
	P26	5	2.4 ±1.0 (2)	7.2 ±3.0 (2)	1.84	3.72	1.02	Cummulative
	P26	45	1.6 ±0.3 (2)	4.7 ±0.9 (2)	1.28	2.23	1.08	Cummulative
	P26	1500	0.8 ±0.4 (2)	2.4 ±0.8 (2)	2.30	4.09	0.08	Cummulative
Summer 97								
	P4	10	2.7 ±0.6 (3)		2.42		1.40	Cummulative
	P26	10	4.5 ±1.4 (3)		4.68		1.12	Non-linear Cummulative (decreasing)
Winter 98								
	P26	10	4.0 ±2.3 (3)	7.5 ±4.0 (3)	7.40	6.24	0.55	Non-linear Cummulative (decreasing)

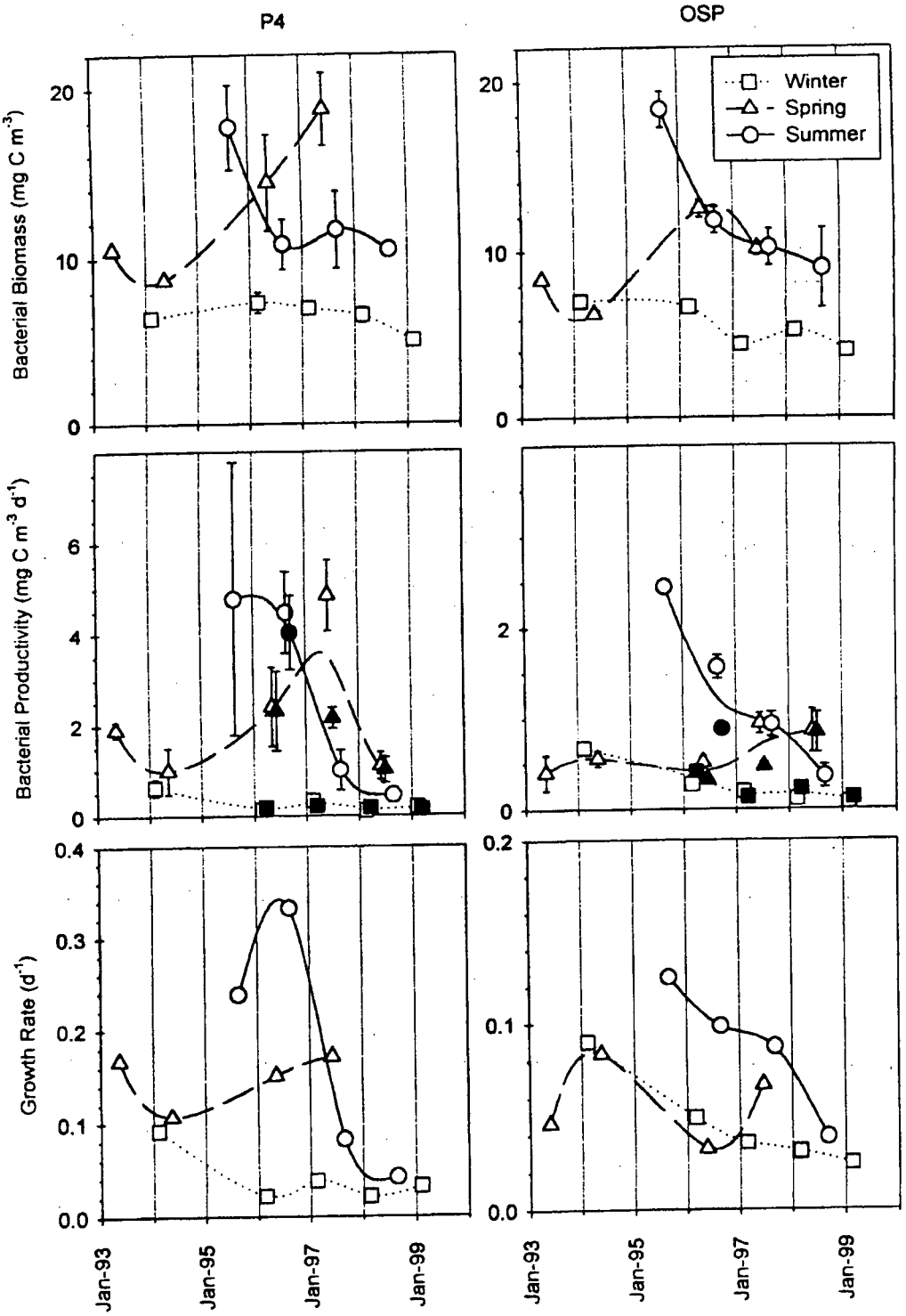

Figure 3.2. Bacterial biomass, bacterial productivity, and bacterial growth rates along line-P during winter (···□···), spring (– –△– –), and summer (—○—). For bacterial productivity, filled symbols indicate rates based on Leu uptake, while open symbols indicate rates based on TdR uptake. Values for spring 1993 and 1994 are from Doherty (1995). Values for winter 1994 are from Boyd et al. (1995a, b). Data represent the mean euphotic zone values calculated by stepwise integration and divided by the depth of the euphotic zone. Error bars represent range of values measured in the euphotic zone.

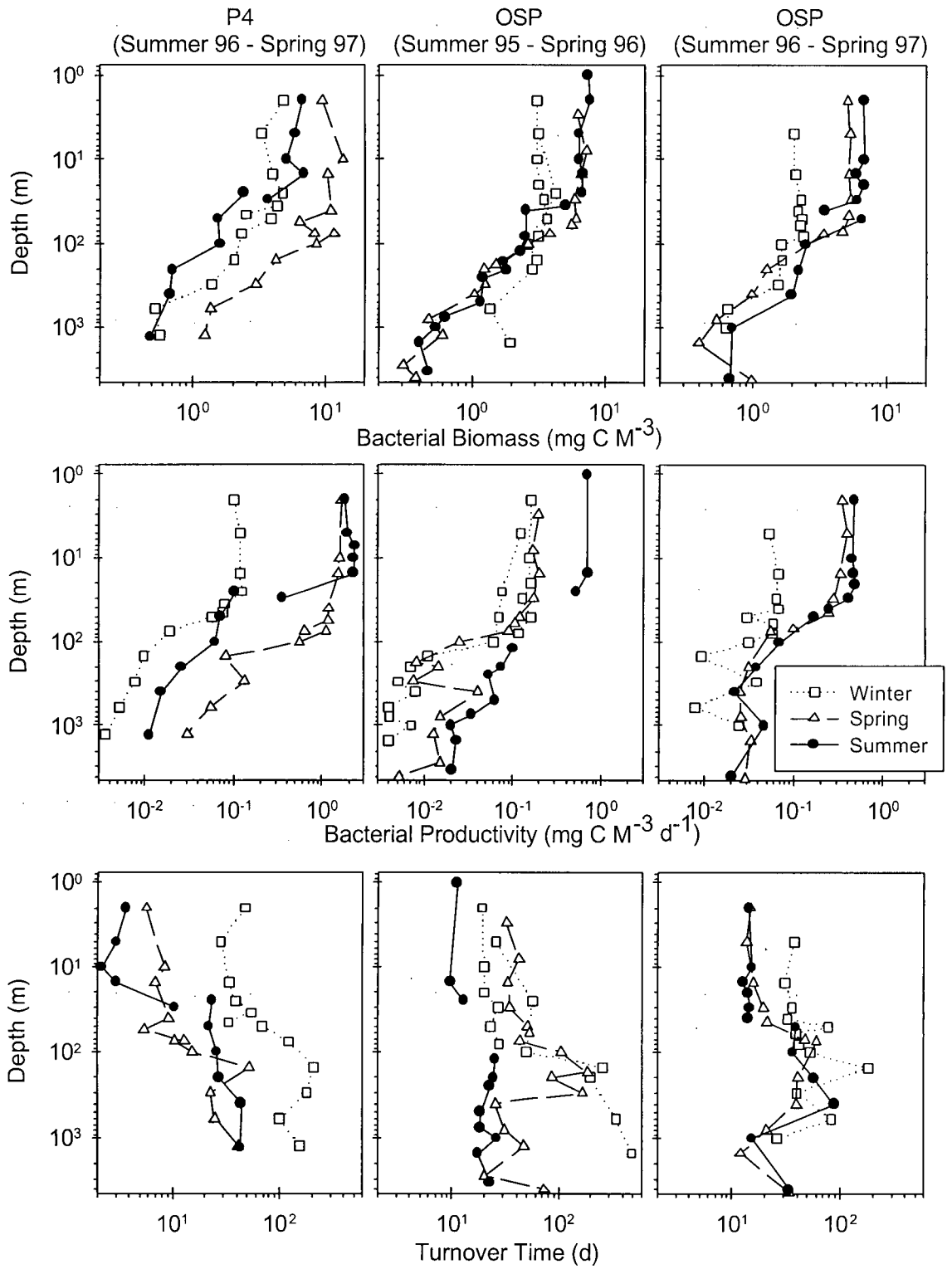

Figure 3.3. Vertical depth profiles of bacterial biomass, bacterial productivity, and bacterial turnover times at stations P4 and OSP during winter (···□··), spring (– –△– –), and summer (—●—). Line breaks between data points indicate different casts (separate sampling periods).

3.3.3 Bacterial Productivity

The depth-averaged euphotic zone bacterial productivity ranged from 0.01 to 4.3 mg C m^{-3} d^{-1} over this study (at OSP in winter 99 and P4 in summer 96 respectively; Fig. 3.2) Winter BP was low and constant all along line-*P* (~ 0.2 mg C m^{-3} d^{-1}) and showed little interannual or within euphotic zone variability (Figs. 3.1 and 3.2). West of P4 during the spring and summer, BP averaged 3 and 5-fold higher than winter (0.7 – 1.0 mg C m^{-3} d^{-1}) and showed much greater variability. At P4, BP was 2 – 3-fold higher (~2.5 and ~3.0 mg C m^{-3} d^{-1}) and more variable than the more oceanic stations (Figs. 3.1 and 3.2). At P4, summer BP decreased almost 10-fold between 1996 and 1997, while it decreased ~ 5-fold at OSP between 1996 and 1998 (Fig. 3.2).

At P4 the >10-fold increase in BP from winter to spring was accompanied by only a 2-fold BB increase, indicating that changes in BB were strongly influenced by changes in loss processes (top-down control) and to a lesser extent by changes in BP. If changes in BB were controlled strictly by production rates (bottom-up control), then higher BP would be accompanied by higher BB which was only partially true for the shift from winter to spring.

The 1996 summer peak in upper ocean BP at P4 decreased by > 10-fold between the bottom of the mixed layer (0-20 m) and the bottom of the euphotic zone (~30 m) giving rise to deep summer BP closer to winter values than to spring (Fig. 3.3). Spring BP below the mixed layer was high relative to other seasons showing a similar pattern to spring BB. At OSP, BP was nearly constant with depth in the mixed layer during all seasons, then decreased immediately below it, regardless of euphotic zone depth (Fig. 3.3). Unlike BB, there was substantial variability in BP below 100 m during most cruises indicating a patchiness in BP that was not apparent in the BB profiles.

3.3.4 Euphotic Zone Growth Rates and Turnover Times

The depth-averaged euphotic zone bacterial growth rate (Bμ) ranged from 0.02 to 0.4 d^{-1} (turnover time from 46 to 2.5 d, at P4 in winter 98 and in summer 96 respectively; Fig 3.2). Winter turnover time was on average about twice as long (~ 30 d) as spring and summer (~ 15 d) (Fig. 3.1). Summer growth rates showed the greatest interannual

variability. In association with the increased BP during spring and summer, the average growth rate was higher at P4 than the more oceanic stations (Figs. 3.1 and 3.2). Summer growth rates decreased by ~ 10-fold at P4 between 1996 and 1998 and decreased ~ 3 fold at OSP between 1995 and 1998. Winter growth rates decreased at OSP by ~ 2-fold between 1996 and 1999 (Fig. 3.2). Overall, P4 showed a much greater range in growth rates than OSP.

Population turnover times increased (i.e. growth rates decreased) inconsistently with depth in association with decreasing BB and BP (Fig. 3.3). Turnover rates ranged from ~ 2 to ~ 500 days from the highly productive summer surface waters at P4 to the deep winter values at OSP respectively. Below 100 m, turnover rates typically ranged between 10 and 200 days. The lack of a consistent increase in turnover time with depth below the euphotic zone suggests that changes in BP are primarily associated with changes in BB, not changes in bacterial growth rate.

3.3.5 Respiration

BR accounted for ~10 to 80% of the TR (Table 3.3, Fig. 3.4). Euphotic zone respiration rates (both TR and BR) during summer 97 at P4 were > 10-fold higher than any other season or any of the three most oceanic stations. BR and TR were indistinguishable from each other during the spring at OSP and during the winter at P4 (no winter OSP data were collected). Thus at OSP, BR accounted for the majority of the TR in spring while only ~ 25% in the summer (Table 3.3).

The summer bacterial carbon demand (BCD) at P4 was ~ 20-fold higher than during winter and spring (Fig. 3.5). However, P4 bacterial growth efficiency (BGE) showed a strikingly different picture with summer and winter being comparable at ~ 5% and spring being ~ 10-fold higher. Since BP was low relative to BR, BCD was dominated by the respiration signal. BCD at OSP was highest in the spring (Fig. 3.5). High BR and low BP in the spring at OSP resulted in a low BGE of ~ 5% increasing to ~ 20% during the summer. Respiration (Fig. 3.4) and BCD (Fig. 3.5) were much higher at P4 in the summer compared with the rest of line-*P*. Spring and summer showed opposite trends in BGE. Spring BGE was high closer to the shelf break (P4) and decreased offshore, whereas summer BGE was low near the shelf break and increased offshore (Fig. 3.5).

Table 3.3
Bacterial respiration as a percentage of total (community) respiration.

	Bacterial Respiration as % of total				
Season	OSP	P20	P16	P12	P4
Summer 1996	25	24	51	53	58
Winter 1997	-	-	-	54	*
Spring 1997	83	77	42	10	16

- Samples not collected due to weather conditions.

* Size-fractioned incubation samples showed greater respiration than the whole water samples.

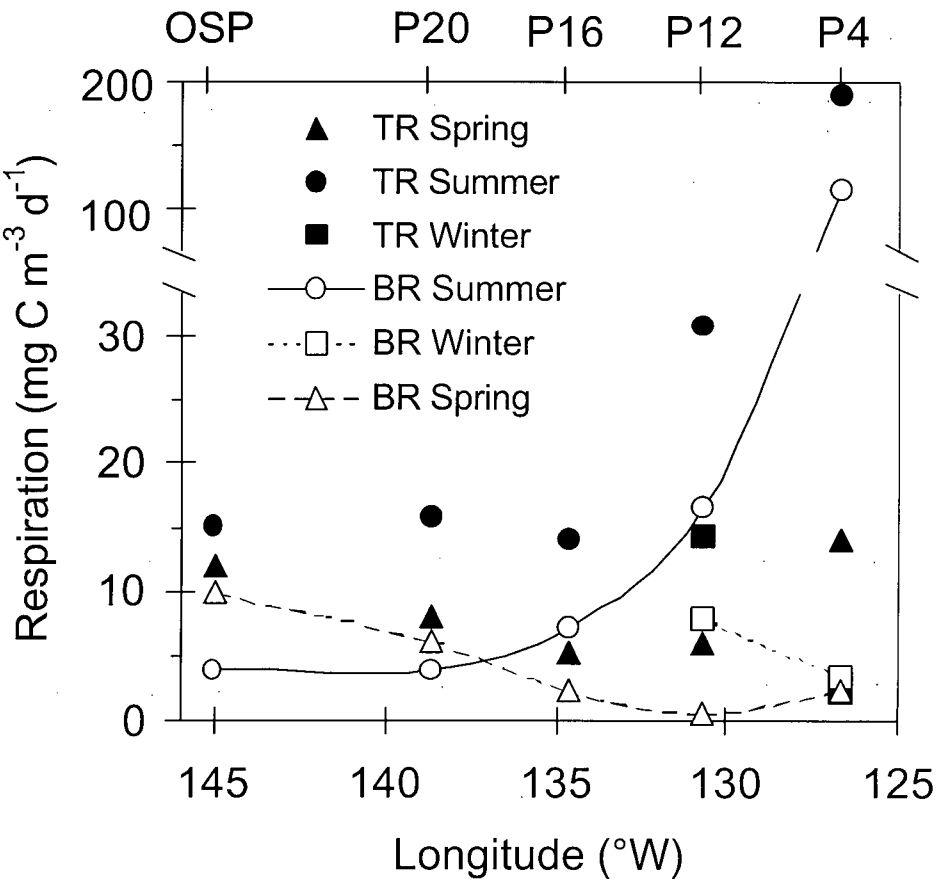

Figure 3.4. Total respiration (TR, filled symbols) and bacterial respiration (BR, open symbols) along line-P during winter, spring, and summer. Data points were calculated from a stepwise integration of euphotic zone measurements divided by the depth of the euphotic zone. The error associated with each data point is ± 50% at a 95% confidence (not shown).

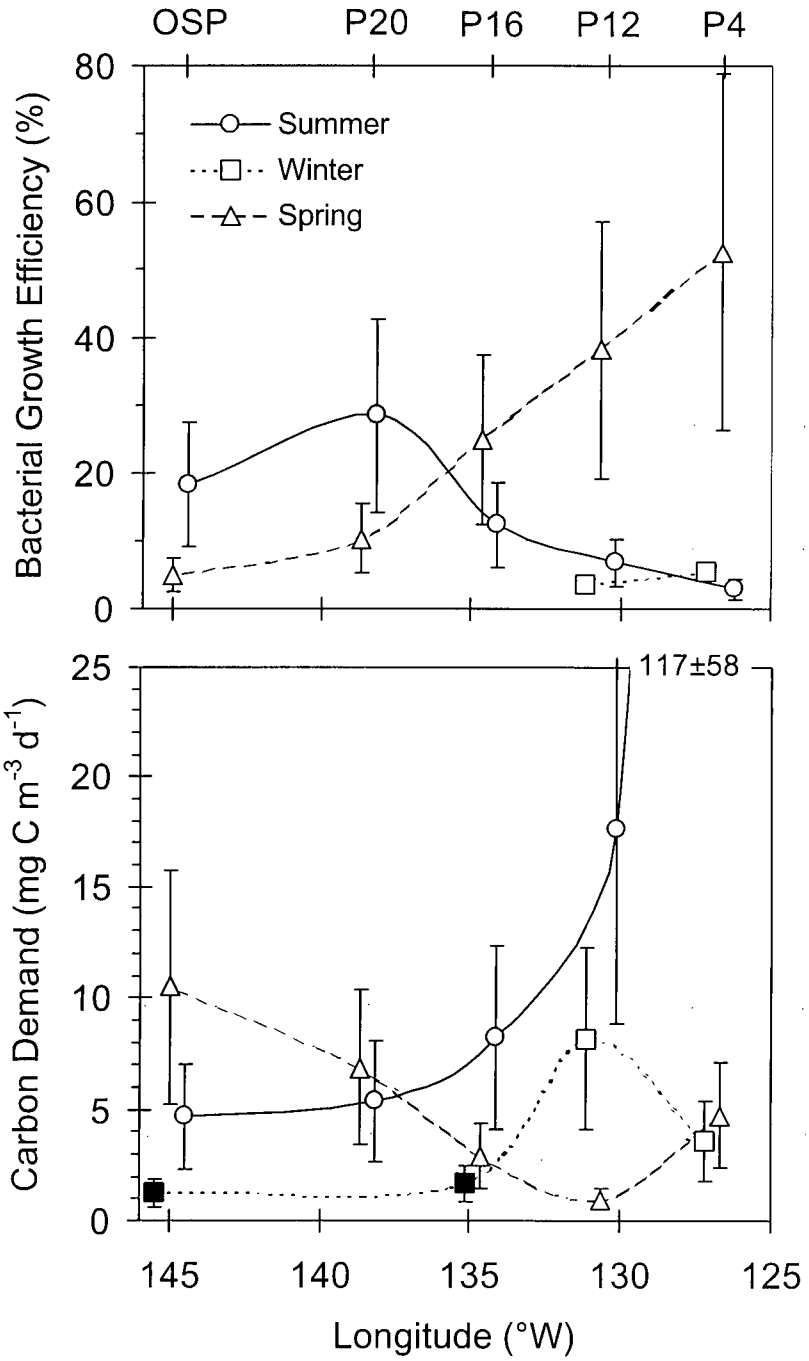

Figure 3.5. Bacterial growth efficiency and bacterial carbon demand along line-P during winter (···□··), spring (– -△- –), and summer (—○—). Data collected only over one year (summer 96, winter 97, and spring 97). Filled symbols were calculated from bacterial production assuming 10% growth efficiency based on P4 and P12 winter measurements. Error bars represent 95% confidence intervals (n = 6).

3.4.0 Discussion

3.4.1 Conversion Factors

The conversion factor (*F*) used to convert the label incorporation rates into BP is variable and probably the most uncertain factor associated with determining BP and Bμ. Conversion factors have been derived theoretically based on estimates of label dilution, precursor content within macromolecules and macromolecule content within cells, etc. for both TdR (Furman and Azam 1982, Moriarty 1986) and Leu (Simon and Azam 1989). However, since these various factors can vary depending on the community composition and environmental conditions, there is the potential for significant and unknown accumulated error (Kirchman *et al.* 1982, Kirchman 1992, Ducklow 2000). To account for the unknown variability as well as label incorporation into non-target macromolecules, the use of empirically determined conversion factors was introduced by Kirchman *et al.* (1982) and is now widely used. However, running carefully controlled replicate grow-out experiments consumes time and resources that might be better spent measuring other experimental parameters or *in situ* productivity. Unfortunately, this study further emphasizes the need for even more consistent empirical conversion factor determination in association with bacterial productivity estimates based on macromolecule precursor incorporation rates.

This study found a positive linear relationship between TdR and Leu conversion factors (Leu = 0.03 TdR, $R^2 = 0.75$) (Fig. 3.6). However, the correlation between TdR and Leu conversion factors did not lead to *in situ* TdR and Leu productivity estimates that always agreed (Fig. 3.2). These data show Leu based productivity estimates to be ≤ TdR based estimates during the spring and summer (Fig. 3.2).

Interestingly, the empirically derived conversion factors (*F*) calculated in this study were positively correlated with bacterial abundance (Fig. 3.7). If these regressions are included in the analysis of these data, the overall trends in BP are exaggerated by the associated changes in BB and suggest generally lower winter and higher summer BP, along with a greater overall decrease in BP between 1995 and 1998. This relationship between bacterial abundance and *F* also suggests a decrease of ~ 40% for the TdR conversion factor and 50 – 60% for the Leu conversion factor during summers

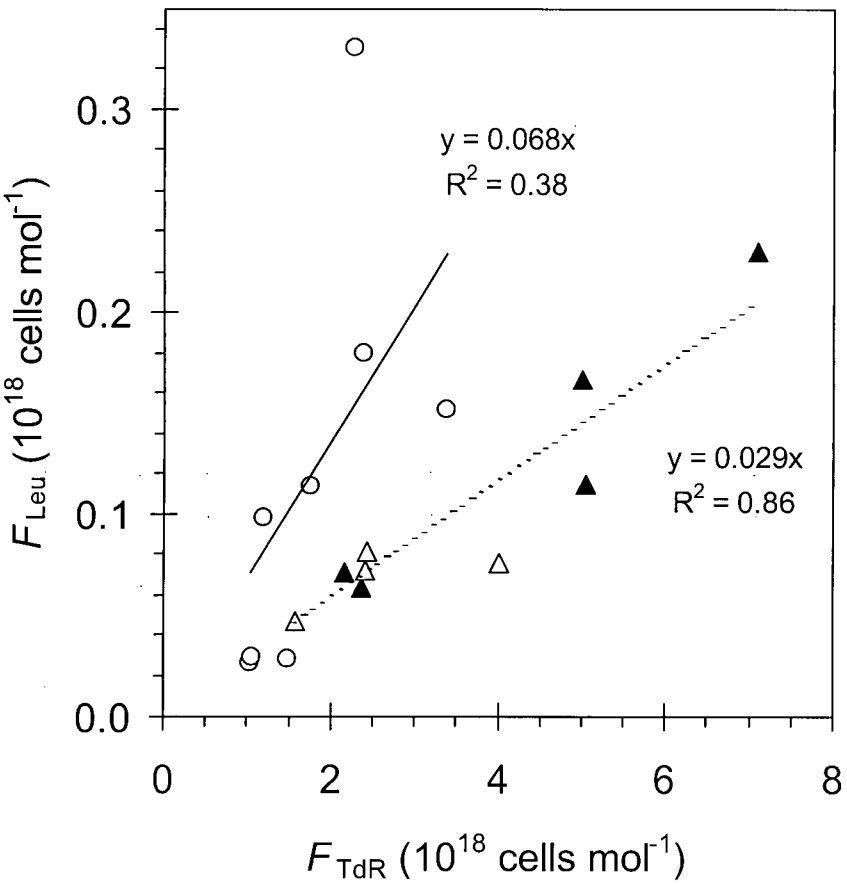

Figure 3.6. Comparison between TdR and Leu conversion factors (F_{TdR}, F_{Leu}) determined from dilution/incubation grow-out experiments using either duplicate or dual labeled samples from Kirchman et al. (1992) (circles and solid line) and this study (triangles and dashed line). Open symbols are values from Ocean Station Papa. Closed symbols are from other line-*P* stations (see Table 3.2).

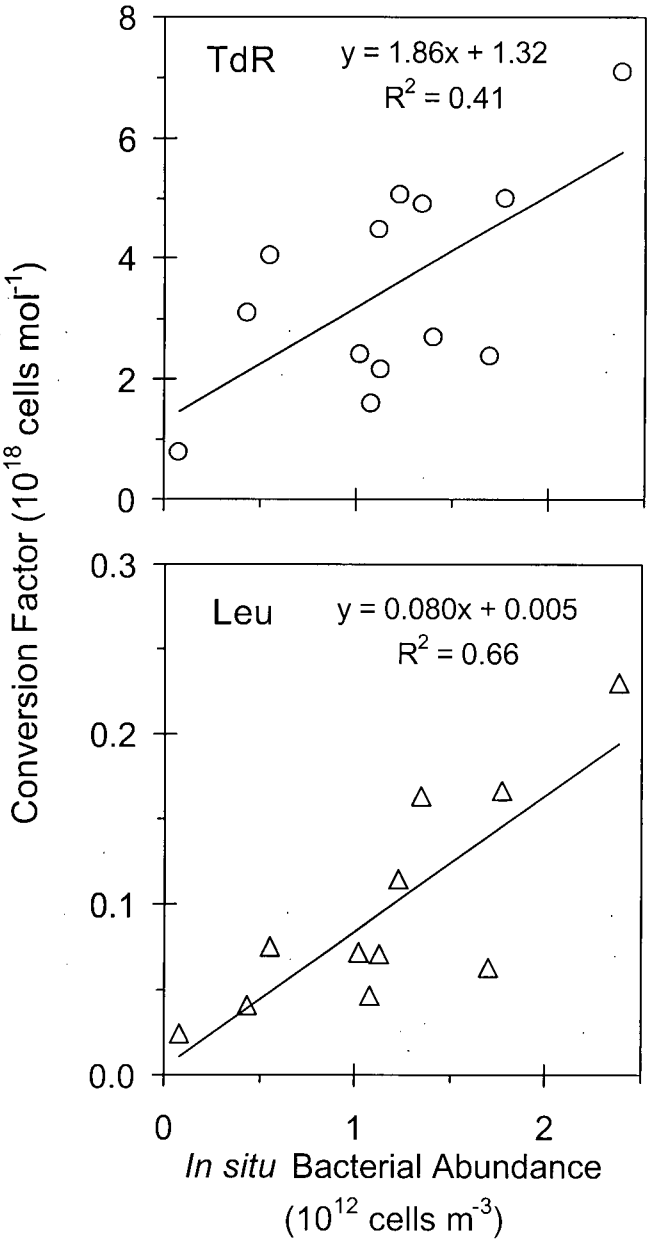

Figure 3.7. Calculated conversion factors relative to in-situ bacterial abundance.

from 1995 to 1997. The range of F, based on cell abundance, varied across the range of commonly reported conversion factors ($1.5 - 5 \times 10^{18}$ for TdR, $5 - 20 \times 10^{16}$ for Leu).

At least some of the correlation between F and cell abundance may be a handling artifact. The difference in label incorporation per cell between *in situ* measurements and the t_0 sample of the filtration/dilution incubations (differential label incorporation rate, t_0 – *in situ*) was negatively correlated with cell abundance (Fig. 3.8). This negative relationship was substantially stronger for Leu than for TdR. To explain these observations in terms of isotope dilution, handling must have reduced the incorporation of the label, and isotope dilution must have increased with biomass as might be expected if amount of cell damage increased in proportion to the number of cells being filtered. However, this does not explain the increase in label incorporation per cell observed at the lower end of the cell abundance range. To explain these observations in terms of enhanced growth rates following manipulation, there could be an assumed substrate enhancement due to contamination or filtration artifacts. The substrate enhancement would lead to enhanced growth, but a reduced level of enhancement when more cells were present and sharing the resource. However, a shared resource enhancement only explains the response in the low range of cell abundance, because on the higher end, the differential label incorporation rate becomes negative. Neither of these speculations adequately explain the data, although when considered together, they might explain the response.

Independent of handling artifacts, other mechanisms might also explain at least some of the relationship between F and bacterial abundance. Higher cell abundance may be correlated with smaller cells containing less DNA and protein (these measurements were not made in this study), or samples with greater cell abundance may be associated with higher rates of isotope dilution because of associated increases in *de novo* synthesis of the precursors under highly competitive conditions, or finally, more competitive or "efficient" cells may dominate under higher abundance conditions leading to greater growth associated with lower label incorporation. Determining the mechanism and extent of the relationship between F and BB will require further study.

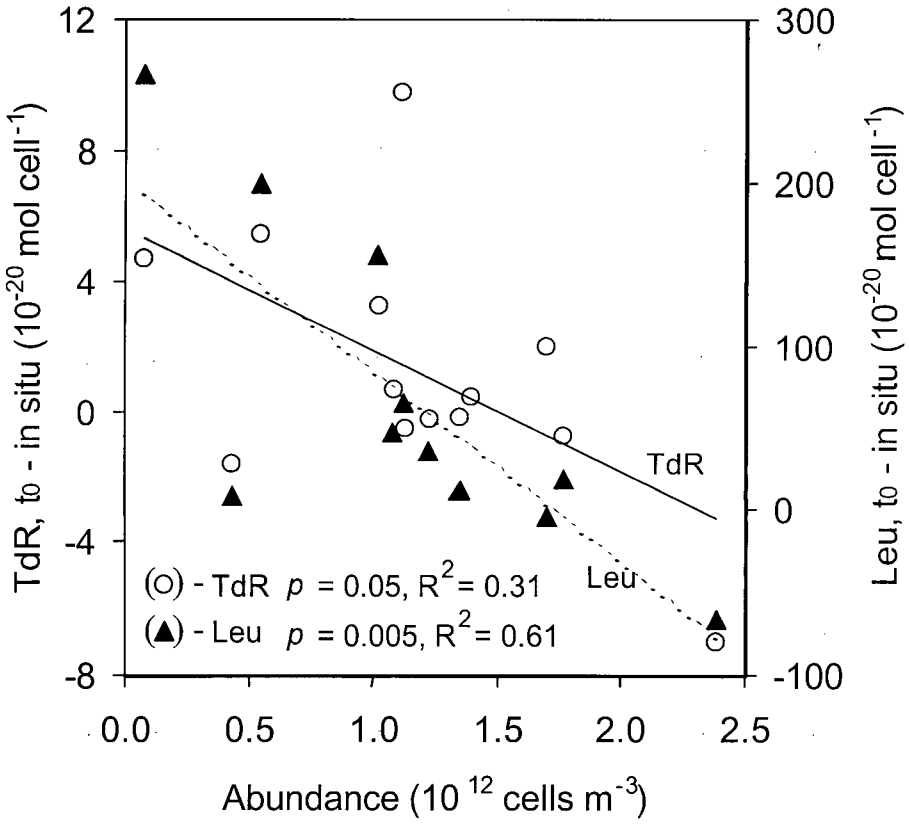

Figure 3.8. Perturbation induced anomalies relative to *in situ* bacterial abundance for TdR and Leu. Perturbation induced anomalies in the label uptake rate were calculated as the initial uptake rates in the dilution/incubation experiments minus the *in situ* label uptake rate.

3.4.2 Carbon biomass and respiration

Both BB and BP numbers in this study are based on an assumed cellular carbon content of 10 fg C $cell^{-1}$, not the more commonly used 20 fg C $cell^{-1}$ (Lee and Fuhrman 1987); cellular carbon content was not estimated in this study. Fukuda *et al.* (1998) suggest that the cellular carbon in open ocean bacteria averages ~12 fg C $cell^{-1}$, but is lower in the HNLC equatorial Pacific and the Southern Ocean (5.9 and 6.5 fg C $cell^{-1}$, respectively). Because the subarctic NE Pacific is an open ocean HNLC region, 10 fg C $cell^{-1}$ was chosen as a reasonable estimate. The uncertainties in cellular carbon content are inconsequential when comparing between BB, BP, and Bμ in this study because a consistent cellular carbon content was used throughout. However, if bacterial productivity was underestimated by 50% (e.g. 10 vs. 20 fg C $cell^{-1}$), then BGE would be underestimated by about a factor of 2 (since the respiration calculations were independent of cellular carbon conversion factors), and the BCD reported herein would be underestimated by 3 to 30% depending on whether BGE was low or high. Also, if carbon per cell was higher at the shelf break region (P4) than at the open ocean HNLC stations, then the trends toward increasing BB and BP closer to shore would be further exaggerated.

Since bacterial processes can be sensitive to handling and may be enhanced by filtration, it is possible that the BR derived from size-fractionated dark bottle O_2 consumption over 24 - 48 h are an overestimate of the actual BR. To minimize this bias, data from size-fractionated samples were carefully compared to both non-fractionated samples and killed controls (t_0) as discussed below. Since no coincident bacterial productivity measurements were made along with the dark-bottle incubations during this study, the most robust defense of the BR values reported herein is that both the bacterial growth efficiency (BGE) and the BR:TR ratios were within the range of other published oceanic studies and the percentage of the samples eliminated as having clearly anomalous O_2 consumption was minimal.

3.4.3 Slope Waters vs. the HNLC Open Ocean

Data from OSP and P4 are presented in the most detail since they were the end members of line-*P* and highlight the differences along the transect from the continental slope to the open ocean. Generally speaking, OSP was similar to the other two oceanic stations (P16 and P20), while P4 was unique and P12 showed either intermediate or anomalous characteristics compared to P4 and P16 on either side of it.

There is little difference in the magnitude of BB observed between the two end-members of line-*P* (P4 and OSP) during either summer or winter. Winter BP was similar at both P4 and OSP, but at P4, BP increased 10 to 15-fold from winter to summer. In contrast OSP showed a reduced BP seasonality (0 to 5-fold increase from winter to summer). Elevated BP at P4 may be indicative of the different annual phytoplankton cycles observed in these regions. P4 experiences spring bloom conditions (Boyd and Harrison 1999, Thibault *et al.* 1999), while OSP displays little seasonal variability in chlorophyll (Parslow 1981, Miller 1993).

At P4, the greatest increase in BP relative to BB was between winter and spring, suggesting a substantial increase in loss processes in the spring relative to the winter at P4. At OSP, the biggest increase in BP relative to BB (biggest increase in loss processes) was between spring and summer. Interestingly, both of these increases in apparent loss processes coincided with the disappearance of the copepod *Neocalanus plumchrus* from the surface waters (Goldblatt *et al.*, 1999) (discussed further below).

Spring levels of BB and BP were higher than winter over the entire water column at P4, whereas at OSP there was no clear seasonal response below 100 m, the approximate depth of the permanent pycnocline. If increases in BB and BP were associated with increased substrate supply derived from surface phytoplankton production, then increased bacterial activity at depth implies an increased input of surface material to depth. Conversely, a reduction in bacterial seasonality at depth may imply a reduction in the export of surface material to depth. Also export ratios, from thorium disequalibria, indicate more seasonality and higher rates of downward particulate flux over the annual cycle at P4 than at OSP (Charette *et al.*, 1999). These observations support the idea that spring primary productivity at P4 may consist of larger phytoplankton contributing to greater downward export flux, whereas at OSP and during

late summer at P4, primary productivity may be dominated by smaller phytoplankton that are primarily recycled in the mixed layer and contribute little to downward export flux.

Respiration rates were consistently low at both P4 and OSP during spring. However, during summer, P4 showed a > 10-fold increase in both BR and TR leading to a similar increase in BCD. BGE showed strikingly opposite spring and summer trends between P4 and OSP with BGE being lowest (< 5%) during the summer at P4 and during the spring at OSP. Conversely, BGE was highest in the spring at P4 (~ 50%) and in summer at OSP (~ 20%). The high summer BGE at OSP and the low summer BGE at P4 may be counter-intuitive since P4 and OSP are generally characterized by high and low dissolved iron levels, respectively (LaRoche *et al.*, 1996), and Tortell *et al.* (1996) suggest that low iron may reduce BGE. However, the low BGE in the slope water may be explained by nitrogen stress since nitrate depletion is a summer feature of the P4 region (Whitney and Freeland, 1999), and it has been suggested that nitrogen limitation can significantly reduce BGE (Goldman *et al.*, 1987).

3.4.4 Trends Along Line-P

In general, there was little difference in the magnitude of either BB or BP among any of the line-*P* stations during winter. Spring and summer BB along line-*P* was much more variable than in winter and averaged about twice the winter BB, a trend also noted for this transect in 1993/4 (based on a limited dataset) by Doherty (1995). BP was highest at P4 during the spring and summer with the three most oceanic stations showing lower values and little difference between them. BGE showed opposite spring and summer trends with spring BGE being high near the shelf break and decreasing further offshore, and compared to summer, BGE was low at the shelf break and increased further offshore.

One of the dominant characteristics of these data is the large (often 2 to 10-fold) interannual change in BB and/or BP that occurred at all stations and which generally decreased over the time of this study (Fig. 3.2). Though not as extreme, the Hawaiian Ocean Time-series data[1] show a ~30% decrease in bacterial abundance from 1996 to

[1] Data aquired from the Hawaii Ocean Time-series Data Organization & Graphical System. http://hahana.soest.hawaii.edu/hot/hot-dogs/interface.html

1998. In the subarctic NE Pacific, there was a 2 – 3°C mixed layer temperature increase during summer 97 in association with the 1997 El Niño (Brown 1998) but the El Niño temperature change does not directly explain the continued low BB and BP values in summer 98.

In the present study, increases in OSP BP from spring to summer were not matched in magnitude by BB, suggesting an increase in loss processes during the summer and thus suggesting that the increase in BB was limited by top-down control. The increased losses may have been induced by the increasing BB leading to increased contact rates with both viruses (Suttle and Chan 1994) and protist grazers (Boenigk *et al.* 2002). Grazing experiments done concurrently with the present study (Rivkin *et al.* 1999) showed a substantial increase in summer bacterivory rates relative to winter and spring, further supporting the idea that changes in loss processes limited increases in BB during the summer. Increased grazing efficiency could be due to changes in bacterial or grazer community structure, an increase in the abundance of bacteria and grazers (increased collision rates), or a temperature increase driving increased grazer activity. Although the actual mechanisms responsible for the increase in loss processes were not elucidated in this study, it is interesting to note that *Neocalanus plumchrus*, an abundant copepod which migrates out of OSP surface waters in late spring (Goldblatt *et al.* 1999), is capable of grazing on the protists which graze on heterotrophic bacteria. The departure of *N. plumchrus* may release bacterivorous protists from grazing pressure and thus allow protist numbers to increase. The increased protist numbers could then provide a mechanism for increased bacterial loss processes in the summer relative to winter and spring at OSP. Unfortunately, this hypothesis is neither conclusively supported or refuted by the observed seasonal changes in the total number of protists (Booth *et al.* 1993, Rivkin *et al.* 1999).

3.4.5 Bacterial Respiration, Carbon Demand, and Growth Efficiency

The contribution of BR to TR ranged from ~ 10 – 80% (Table 3.3). The changes in BGE between spring and summer, both in the slope waters and in the open ocean, were driven primarily by changes in BR rates, not changes in BP as del Giorgio and Cole (2000) suggest for the global ocean as a whole. This important role of respiration further supports the pleas by Janhke and Craven (1995) and Cole and Pace (1995) for more oceanic microbial respiration measurements.

The presence of flavodoxin, a molecular marker for algal iron stress, indicated that algal cells were not iron-stressed at P4 in summer when low BGE was observed, but they were iron-stressed at OSP in summer when a higher BGE was observed (LaRoche *et al.* 1996). Thus, it appears that BGE was not reduced as much under low levels of iron (sufficient to stress the algal community) as it was under the nitrate depleted conditions present over the slope during the summer. The highest BGE observed during spring at P4 was likely tied to the nutrient replete conditions and the high primary productivity of spring bloom conditions.

3.4.6 Comparison to Other Studies

Over the last decade that bacterial measurements have been made by four different investigators at OSP, bacterial abundance and productivity has generally ranged across similar values (Table 3.4, Fig. 3.2). During this study, the bacterial abundance and TdR incorporation rates over the spring and summer at OSP were similar to those found in 1987/88 by Kirchman *et al.* (1993) (Table 3.4). In May 1988, sampling at OSP was done prior to the spring thermocline formation (Kirchman *et al.* 1993), and showed relatively low BB and BP, similar to the winter measurements made during this study. In the present study, the average levels of BB and BP at OSP are comparable to those reported by Boyd *et al.* (1995a, b), Doherty (1995), and Kirchman *et al.* (1993) (Table 3.4, Fig. 3.2). As in the present study, the previous studies noted the homogeneous distributions of BB, and rates of BP in the surface mixed layer.

Bacterial abundance throughout the year at OSP is generally on the high side ($0.4 – 1.8 \times 10^{12}$ cells m^{-3}) compared to the subtropical gyres ($0.1 – 0.7 \times 10^{12}$ cells m^{-3}) or the

Table 3.4 Summary of literature values for euphotic zone and/or mixed layer measurements related to bacterial biomass, bacterial productivity, and bacterial respiration from various regions and seasons. Reported data include bacterial abundance (B#s, 10^{12} cells m^{-3}), biomass (BB, mg C m^{-3}), carbon per cell used for BB calculations (C/cell, fg C $cell^{-1}$), [^{3}H]-thymidine incorporation rate (TdR, nmol m^{-3} d^{-1}), TdR based bacterial production (BP_{TdR}, mg C m^{-3} d^{-1}), TdR conversion factor (F_{TdR}, 10^{18} cells mol^{-1}), [^{3}H]-leucine or [14C]-leucine incorporation rate (Leu, μmol m^{-3} d^{-1}), Leu based bacterial production (BP_{Leu}, mg C m^{-3} d^{-1}), Leu conversion factor (F_{Leu}, 10^{18} cells mol^{-1}),bacterial respiration (BR, mg C m^{-3} d^{-1}), bacterial growth efficiency (BGE = BP/(BP × BR)). All reported values were converted to standard units either directly or by using conversion factors listed in the table. Shaded values were not reported by the cited authors, but rather assumed or derived for this table from other values in the same row to provide more complete comparisons between the various works. Many values are extrapolated from published plots and should thus not be considered actual values, but rather reasonable approximations there of.

Notes on Table 3.4

The isotope-incorporation:bacterial-production conversion factor is denoted by F in the following notes. Doherty (1995) – BB and BP recalculated from the author's B#s and TdR incorporation based on cellular carbon and conversion factors used in this study. Cherrier et al. (1996) – BP was based on change in POC, not radiolabel incorporation rates. Ducklow et al. (1995) – TdR is taken from profile plots, BP is taken from time-series plots (mean of 120 m, 1% Lt). Cochlan (2001) – Leu provided by Author. Ducklow et al. (1999) – μ calculated from incubations experiments and associated cell yield. Only treatments at ambient temperature and without amendments are included. Ducklow et al. (1992/93) – the two entries are to show the difference in values depending on how F is calculated (either cumulative or modified derivative). Leu incorporation is back-calculated from the reported Leu BP assuming that the F used by the authors was the average of the values determined via the modified derivative method in the 1992 paper. The label incorporations associated with the cumulative method are assumed to be the same as those back-calculated from the modified derivative method above. Fasham et al. (1999) – TdR F is assumed to be the same as Kirchman 1993 (F = 1.74 and C/Cell = 20) since Kirchman 1993 was the methods reference. Zubkov et al. (2000) – the cellular Leu F was estimated from the reported carbon based Leu F and C/cell. The conversion reported by the authors is not correct because g C mol^{-1} should be divided, not multiplied by g C $cell^{-1}$. Carlson et al. (1996) – C/cell is based on reported cell volume and authors' choice of 120 fg C μm^{-3}. Lochet et al. (1997), Kähler et al. (1997) – BP values are TdR and Leu averaged. Cellular based Leu F was calculated from the reported carbon based Leu F using 18.7 fg/cell as reported by the authors. Kirchman et al. (1995) – BP is the average of both TdR and Leu values. Church et al. (2000) – Leu BP was not calculated because the authors consider absolute magnitude to be erroneous due to isotope dilution associated with the experimental protocol. Bjornsen & Kuparinen (1991) – the Leu F was converted from biovolume mol^{-1} to cells mol^{-1} using reported biovolume to C conversion and assuming 10 fg $cell^{-1}$. Jones et al. (1996) – the authors reported BB and μ based on the assumption that 15% of the cells were active. This table shows BB and μ values based on 100% of the DAPI positive cells. The authors' values are thus multiplied by 6.67 to be comparable with other cited works. BP was based on ^{3}H-adenine incorporation into DNA instead of TdR incorporation. Li et al., (1993) – values were measured under both early bloom and fully developed bloom conditions. The F derived using both cumulative and integrative methods agreed with each other, although cumulative is stated in the table. For the present study, the winter conversion factor was calculated based on a non-linear fit to cumulative data (see text).

other major HNLC regions ($0.2 - 1.2 \times 10^{12}$ cells m^{-3}) but lower than the N Atlantic spring bloom ($1.0 - 2.5 \times 10^{12}$ cells m^{-3}) (Table 3.4). In contrast, BP at OSP (based on unconverted label incorporation rates) is similar to other oceanic regions during summer and winter, while during the spring at OSP, BP is generally lower than the equatorial and temperate regions and more similar to the subtropical gyres and Southern Ocean (Table 3.4). These values suggest generally lower growth rates in the subarctic NE Pacific compared to other regions. The lower growth rates are due to greater than average cell abundance along with a typical or lower than average BP. These observations suggest generally slower (per cell) loss processes in the subarctic NE Pacific compared to most other oceanic regimes.

None of these regional comparisons address potential uncertainties and differences in cell volume/carbon, or conversion factors for BP from TdR or Leu incorporation rates. The lack of consistent empirical measurements of these parameters throughout all the various regions and seasons makes these comparisons untenable at this time.

3.5.0 Conclusions

The subarctic NE Pacific and the line-*P* transect offer a unique opportunity to study bacterial processes over a range of changing environments from slope waters which are seasonally nitrogen depleted and influenced by coastal processes, to open ocean HNLC waters where macronutrients are plentiful and primary productivity appears to be limited by iron. Winter BB and BP were surprisingly invariant all along line-*P*. BB was typically 2-fold higher in spring and summer than in winter. BP showed stronger and more variable spatial and temporal patterns than BB. Distinct seasonal changes in BP and BB were observed in the mixed layer. With the exception of P4, seasonal changes below 100 m did not mirror mixed layer changes suggesting that seasonal changes in the downward export of organic material may have been buffered by more recycling within the mixed layer at OSP. There was also a general trend of decreasing spring and summer

BB and BP at both OSP and P4 from 1996 through 1998. BR and the associated BGE, changed dramatically both seasonally and spatially confirming the need for regular respiration measurements as an integral part of any study attempting to quantify the microbial carbon budget. The enhanced seasonality of bacterial processes in the slope waters relative to the open ocean probably reflects the more dynamic physical environment associated with the continental slope including eddies, jets, upwelling, and nutrient variability. Compared to the other oceanic regions discussed, the subarctic NE Pacific appears to have generally greater bacterial abundance while supporting similar BP. This study represents the first comprehensive dataset on bacterial processes from the subarctic NE Pacific region.

Chapter 4

Factors Controlling Change in Bacterial Abundance, Productivity, and Growth Rate in the Subarctic NE Pacific Ocean

4.1.0 Introduction

Central to understanding the roles of microbial processes in the ocean is understanding when, where, why, and by how much microbial processes change in response to changes in the physical, chemical, and biological environment. Chapter 3 addressed when, where, and by how much microbial processes changed both seasonally and regionally over multiple years in the subarctic NE Pacific. However, in order to predict (or hindcast) the ecosystem's response to biological or physical perturbations, such as plankton blooms, weather events, or climate change, an understanding of the mechanisms driving the changes observed in bacterial properties is vital.

To determine the mechanisms responsible for changes in bacterial abundance and productivity, manipulation experiments and statistical comparisons have been used. In general, in most marine environments, bacterial productivity has been shown to increase with the addition of dissolved organic carbon (DOC) (Kirchman *et al.* 1993, Carlson and Ducklow 1996, Cherrier *et al.* 1996, Kahler *et al.* 1997, Kirchman *et al.* 2000, Appendix I). A few studies have shown bacterial production to be limited by mineral nutrients alone including nitrogen and phosphorus (Elser *et al.* 1995, Shiah *et al.* 1998), or iron (Pakulski 1996). Bacteria have also been shown to be co-limited by both mineral nutrients and DOC (Elser *et al.* 1995, Caron *et al.* 2000, Church *et al.* 2000, Appendix I). Bacterial abundance, productivity, and/or growth rates have also been statistically compared to chlorophyll, primary productivity, and temperature, all with mixed results. In a broad review of both marine and freshwater studies, Cole *et al.* (1988) found bacterial abundance to be positively correlated with chlorophyll, and bacterial productivity positively correlated to primary productivity. Ducklow *et al.* (1992) showed a 5-fold increase in bacteria in the N Atlantic in response to the spring bloom, and Cochlan (2001) showed a large increase in bacterial abundance and productivity in

association with the bloom generated in the IronEx II experiment. Yet, Ducklow *et al.* (1995) discussed a weak or decoupled relationship between bacterial productivity and primary productivity in the equatorial Pacific, and Carlson and Ducklow (1996) found little bacterial response to changes in primary productivity in the Sargasso Sea. Kirchman *et al.* (1995) showed a plot with bacterial productivity laying almost directly on top of primary productivity along an eastern equatorial Pacific transect from 12°S to 2°N, after which the two variables diverge completely from each other along 2 – 9°N. Sherry *et al.* (1999) suggested that bacterial productivity was positively correlated with temperature in the subarctic NE Pacific, while Rivkin *et al.* (1996) found no significant difference between bacterial growth rates measured in warm vs. cold oceans.

This chapter attempts to elucidate the mechanisms that were responsible for driving the observed spatial and seasonal changes in bacterial abundance, productivity, and growth rates (for brevity, referred to herein as bacterial properties) in the subarctic NE Pacific. Mixed layer bacterial abundance and productivity data were collected in conjunction with physical, chemical, and other biological variables during winter, spring, and late summer between 1993 and 1999. Groups of correlations between the above variables showed consistent patterns that suggested specific mechanisms were responsible for the observed changes. Identifying these mechanisms offers the potential for improving the predictability of changes in microbial processes in the ocean. Also, included in Appendix I are the results of a number of substrate addition experiments that further support the conclusions drawn from the comparative analysis. To my knowledge, there have been no other studies that have attempted to integrate this quantity of field measurements across multiple years and regions in order to elucidate the likely mechanisms driving changes in bacterial processes over these temporal and spatial scales.

4.2.0 Materials and Methods

4.2.1 Sampling and Data Collection

Data and samples were collected between February 1994 and February 1999 as part of the Canadian JGOFS and the line-P programs, primarily from P4, P12, P16, P20, or OSP (Fig. 1.1). Data collected at intermediate stations were included in the analysis

where appropriate. Biological measurements were drawn from acid-cleaned 10 L GOFLO bottles on a Kevlar line. Salinity, temperature, and nutrient data were taken primarily from CTD/rosette casts from the same sampling station just prior to, or shortly after the GOFLO bottle casts for the biological process measurements. Salinity and temperature measurements were made with either a Guildline WOCE CTD prior to 1997 or a SeaBird 911+ CTD from 1997 onward. Nutrient measurements (NO_3, PO_4, SiO_4) were done on unfiltered seawater with a Technicon Autoanalyser using the methods of Barwell-Clarke and Whitney (1996). These data are available as archived CTD data files, or bottle data files from either the Institute of Ocean Sciences (IOS), or the Marine Environmental Data Service (MEDS), Fisheries and Oceans, Canada (http://www.meds-sdmm.dfo-mpo.gc.ca/meds/Home_e.htm). Primary productivity and chlorophyll values were from Boyd *et al.* (1996), Boyd and Harrison (1999), or Whitney (pers. comm.). Mixed-layer and euphotic zone depths were obtained from either Varela and Harrison (1999) or Chapter 3. The data used for bacterial abundance, productivity, and growth rates were the same as those used in Chapter 3, except in this chapter, comparisons were based on the average mixed-layer values instead of the average euphotic zone values. Mixed-layer values instead of euphotic zone values were chosen to remove the added complexity of biological change associated with depth below the mixed layer.

Heterotrophic flagellate abundance was determined by epifluorescence microscope counts. Duplicate flagellate samples were preserved by diluting 100 mL of sample with 100 mL of a 4% formaldehyde/filtered seawater solution. Samples were preserved immediately (less than 1 h) following collection. Preserved samples were filtered through 0.8 μm pore-size polycarbonate track-etched filters (Poretics PN 11021) to a volume of 5 ml for staining. One duplicate was stained with acridine orange while the other was stained with DAPI (see staining details in Sherr *et al.* 1997). After staining, filtration was completed and filters were mounted on slides with immersion oil as described in Chapter 3 for bacteria.

Six sampling depths for biological measurements were chosen between the surface and 1% light level (see Chapter 3). The values used in this chapter were the mean of all the measurements made within the mixed-layer at each station during each cruise. Therefore, winter values were typically the mean of six measurements (the euphotic zone

was all within the mixed layer), while summer values were typically the mean of two or three depths (the mixed layer was shallower than the euphotic zone). The variability measured within the mixed layer at any given station during a given cruise was negligible compared to the differences between stations, seasons, and years.

The mixed-layer depth was determined subjectively by plotting temperature and salinity profiles and selecting the depth just above the point where the first sign of a consistent temperature decrease or salinity increase occurred. This method of determining mixed-layer depth describes a mixed-layer with homogeneous water properties and is significantly shallower than methods that define the bottom of the mixed-layer as either the middle of the pycnocline, or the point after which a certain rate of change in density has been observed. This conservative method was chosen for this study to avoid adding depth as a complicating factor.

4.2.2 Data Analysis

All statistical analysis was done using JMPin® v 4.0.2 (Academic) (SAS Institute Inc., Cary, NC, U.S.A.). Correlations were calculated using Spearman's Rho correlation since the distributions of many variables did not meet the assumptions of normality and constant variance for parametric tests. Determination of the difference in average bacterial properties between regions was done on log transformed data with Student's *t*-test. Determination of a difference in average bacterial properties between seasons was done on log transformed data with the Tukey HSD. All regression analysis was done on log transformed data using standard least squares, type one, linear regression methods. Data from stations P4 and P12 were pooled together as the "slope" region, and data from stations P20 and OSP were pooled together as the "oceanic" region. At the risk of obscuring potential patterns, these regional data were pooled to provide a larger sample size for the analyses. Aside from the difference in the quantity of outliers, data from P4 and P12 appeared (subjectively) to show the same general relationships between bacterial properties and the other measured variables.

4.3.0 Results

4.3.1 Bacterial Property Distributions

The data distributions for bacterial abundance, productivity, and growth rate values were all highly skewed toward lower values with a few extremely high values (Fig. 4.1). There were eight bacterial productivity values in two groups of four that were substantially higher than all other values. The most extreme group of four data points had a median bacterial productivity ~ 7-fold higher than the remaining data with the eight extreme values removed (4.4 vs. 0.61 mg C m^{-3} d^{-1}). The four highest values accounted for 63% of the variance in bacterial productivity. These highest four bacterial productivity values were associated with the four highest primary productivity values and three of the four highest bacterial abundance and chlorophyll values (see Appendix II). These four most extreme productivity values were also associated with low or depleted macro-nutrients, high levels of primary productivity in the smallest size fraction (0.2 – 5 μm), and mixed-layer depths < 10 m. They appeared to occur primarily near the apices of fingers or jets of water being swirled into water of another temperature (Fig. 4.2). These four most extreme bacterial productivity values all occurred during the spring and summer, three of them at P4 and one at P20.

The second group of four extreme bacterial productivity values (see Fig 4.1), included three from the summer of 1995 that appeared to be associated with eddies in a dramatic 1995 eddy field, or with other physical fronts (Fig. 4.2). They had a median bacterial productivity ~ 4-fold higher than the data with the eight most extreme values removed (2.6 vs. 0.61 mg C m^{-3} d^{-1}) and accounted for 53% of the variance in bacterial productivity after the four most extreme values was removed. These extreme values appeared to lie on the edge of linear fronts instead of the apices of filaments or jets. Unlike the most extreme outliers, this second group was not associated with unusually high primary productivity and only the 1995 summer samples were associated with high bacterial abundance. These outliers occurred in regions with mixed-layer depths between 14 and 22 m.

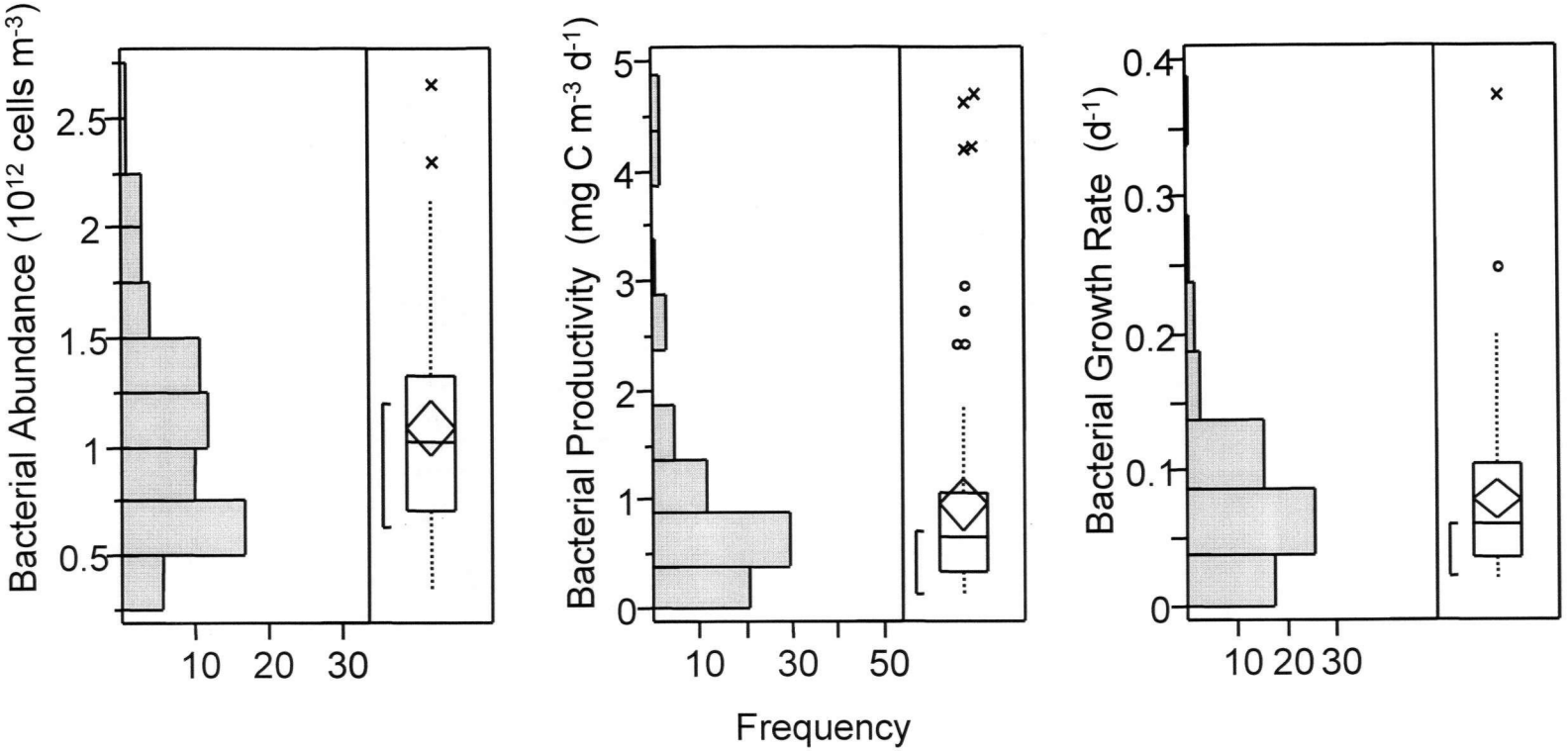

Figure 4.1 Frequency distribution of measured bacterial properties: bacterial abundance, bacterial productivity, and bacterial growth rate. Points marked by an "x" are the four most extreme bacterial productivity outliers. Points marked by an "o" are the second set of extreme bacterial productivity outliers (see text). The box signifies the median ± the quartiles. The whiskers signify 1.5 times the interquartile range. The diamond represents the mean. The bracket marks the middle 50% of the data.

Figure 4.2 Plots showing the position of selected outlier sampling stations overlaid on an AVHRR sea surface temperature map (colored contours), and TOPEX/ERS sea surface height anomaly map from the same time frame. TOPEX/ERS contours represent sea-surface height anomalies derived from 14 day averages centered on the sampling time and suggest eddy scale surface currents (see http://www-ccar.colorado.edu/~realtime/global-real-time_ssh/). Currents flow clockwise around positive anomalies (solid contours) and counter clockwise around negative anomalies (dashed contours). AVHRR colors were selected to maximize contrasts in the temperatures within the regions of interest and do not represent specific temperature values. AVHRR images were selected from the best available image within two days of the sampling time. An exception was Jun 97 when the nearest clear image was from one week after sampling. Due to a strong NW to SE temperature gradient, the east and west sides of the Aug 95 AVHRR image were processed separately to improve contrast in the regions of interest.

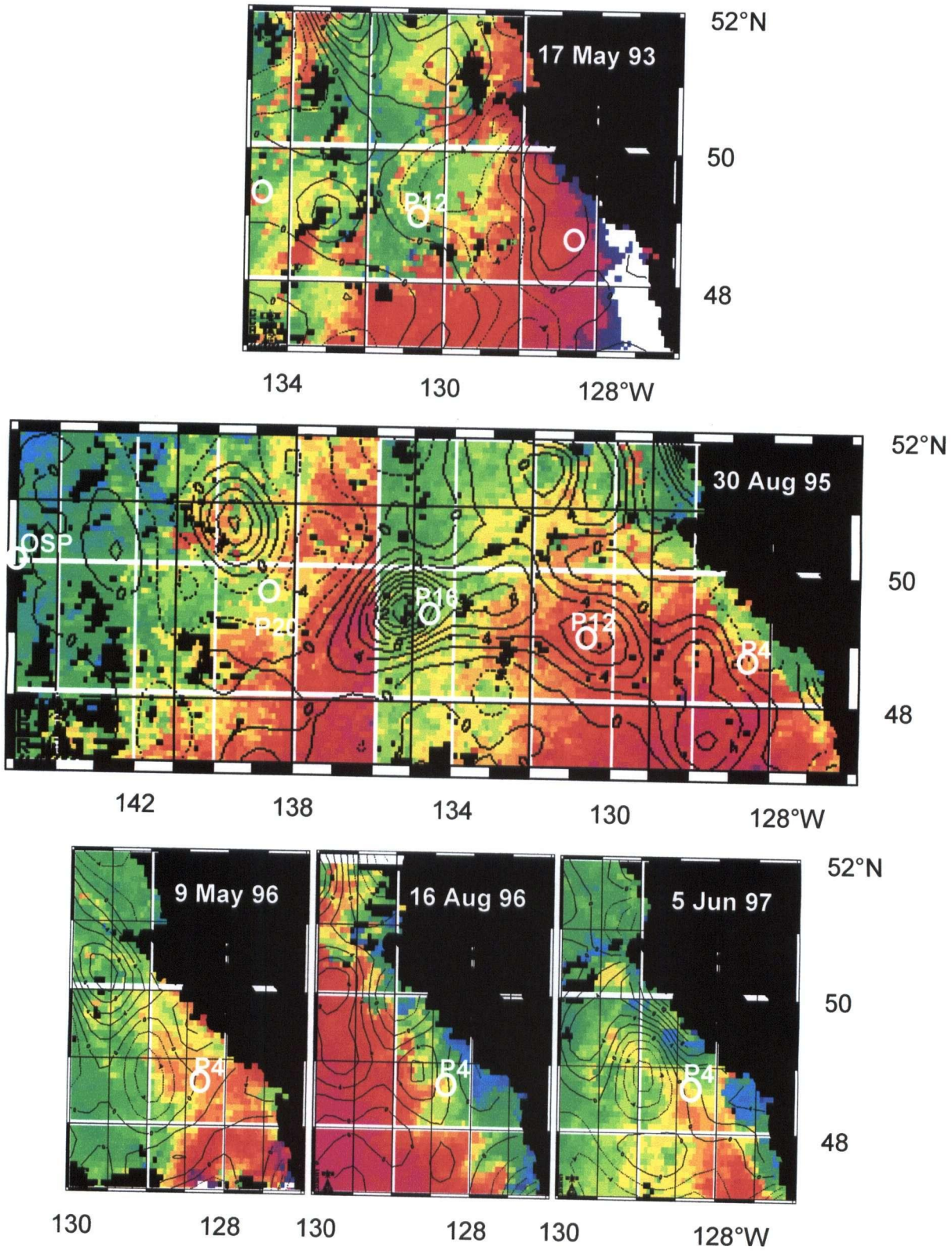
17 May 93
52°N
50
48
P12
134
130
128°W
30 Aug 95
OSP
P20
P16
P12
P4
52°N
50
48
142
138
134
130
128°W
9 May 96
16 Aug 96
5 Jun 97
P4
52°N
50
48
130
128
130
128
130
128°W

Of the 78 mixed-layer bacterial productivity measurements included in this analysis, the greatest changes in magnitude were not associated with seasonal or regional differences, but with just eight data points which appeared to be associated with physical features visible as temperature fronts and/or sea-surface height anomalies (Figs. 4.1 and 4.2).

In addition to the eight extreme bacterial productivity values described above, there were five mixed-layer bacterial productivity values measured in the winter of 1994 that were exceptionally high relative to all other winter values. Although these values may be real, they were not associated with anomalous values in any of the other measured variables and were collected by previous investigators. The 1994 winter bacterial productivity values were > 4-fold higher than those collected during the other four years of this study.

4.3.2 Averages and Variability

After removing the data associated with the eight most extreme bacterial productivity values and the winter 1994 values, the magnitude of the remaining bacterial, productivity, and growth rates across seasons, could be described as having two modes, the winter mode and the spring/summer mode (see Table 4.1). The winter mode showed significantly lower values than the spring/summer mode ($p < 0.05$). While bacterial abundance in slope waters shared the two mode pattern of productivity and growth rates, the average bacterial abundance in oceanic waters was different in all three seasons, with the highest values in the summer, the lowest values in the winter, and intermediate values in the spring. Interestingly, with the extreme values removed from the analysis, there was not a statistically significant difference in magnitude between the oceanic and slope values during any season for any of the three bacterial properties ($p >> 0.05$). This observation suggests that the differences in the magnitude of bacterial properties between oceanic and slope waters previously observed (Sherry *et al.* 1999 and Chapter 3), was driven primarily by a few extreme data points and was not an intrinsic difference in the regional background water properties. These extreme values (the dominant variability)

Table 4.1

Table 4.1 Summary statistics including the median, mean, standard deviation (σ), and number of samples (n) for bacterial abundance (B#), bacterial productivity (BP), and bacterial growth rates (Bμ) for each of the data groupings – all the data and data split into both seasonal (winter, spring, and summer) and regional (oceanic and slope stations) groupings. Values presented include data from all 78 mixed layer records. Values in parentheses are from the data groupings after removing the records associated with the eight spring and summer, extreme bacterial productivity values, and the five extreme winter values from 1994 (see text for details).

		All data			Oceanic waters			Slope waters		
		B#s	BP	Bμ	B#s	BP	Bμ	B#s	BP	Bμ
All	median	1.02 (0.95)	0.67 (0.56)	0.060 (0.045)	0.95 (0.95)	0.70 (0.63)	0.066 (0.043)	1.11 (1.05)	0.72 (0.52)	0.060 (0.046)
	mean	1.08 (1.01)	0.95 (0.64)	0.079 (0.058)	1.08 (1.00)	0.85 (0.65)	0.069 (0.059)	1.15 (1.05)	1.26 (0.67)	0.098 (0.056)
	σ	0.50 (0.42)	1.02 (0.44)	0.061 (0.031)	0.55 (0.45)	0.84 (0.44)	0.039 (0.033)	0.50 (0.39)	1.38 (0.51)	0.087 (0.033)
	n	68 (55)	76 (63)	67 (54)	27 (23)	28 (24)	26 (22)	24 (17)	27 (20)	24 (17)
Winter	median	0.66 (0.64)	0.18 (0.16)	0.034 (0.031)	0.63 (0.52)	0.16 (0.15)	0.033 (0.031)	0.69 (0.69)	0.24 (0.17)	0.033 (0.027)
	mean	0.63 (0.61)	0.31 (0.18)	0.049 (0.031)	0.62 (0.58)	0.33 (0.16)	0.050 (0.030)	0.67 (0.67)	0.32 (0.21)	0.050 (0.030)
	σ	0.15 (0.16)	0.26 (0.06)	0.035 (0.007)	0.19 (0.20)	0.34 (0.05)	0.038 (0.005)	0.09 (0.08)	0.22 (0.07)	0.037 (0.009)
	n	22 (17)	22 (17)	21 (16)	9 (7)	8 (6)	8 (6)	8 (6)	9 (7)	8 (6)
Spring	median	1.67 (1.15)	0.75 (0.72)	0.075 (0.067)	0.97 (0.97)	0.77 (0.77)	0.077 (0.077)	1.30 (1.28)	1.29 (0.79)	0.131 (0.054)
	mean	1.15 (1.06)	1.02 (0.75)	0.086 (0.069)	1.00 (1.00)	0.72 (0.72)	0.070 (0.070)	1.44 (1.20)	1.83 (0.96)	0.131 (0.079)
	σ	0.43 (0.32)	0.98 (0.34)	0.056 (0.030)	0.30 (0.30)	0.24 (0.24)	0.027 (0.027)	0.50 (0.24)	1.53 (0.51)	0.082 (0.048)
	n	26 (23)	34 (31)	26 (23)	10 (10)	12 (12)	10 (10)	8 (5)	10 (7)	8 (5)
Summer	median	1.35 (1.28)	1.10 (0.84)	0.083 (0.060)	1.620 (1.43)	1.240 (0.96)	0.101 (0.067)	1.290 (1.22)	0.920 (0.67)	0.071 (0.060)
	mean	1.49 (1.37)	1.53 (0.93)	0.100 (0.069)	1.700 (1.49)	1.580 (1.00)	0.088 (0.070)	1.350 (1.30)	1.600 (0.86)	0.115 (0.063)
	σ	0.46 (0.39)	1.24 (0.48)	0.078 (0.031)	0.520 (0.36)	1.260 (0.56)	0.049 (0.041)	0.370 (0.40)	1.500 (0.48)	0.111 (0.016)
	n	20 (15)	20 (15)	20 (15)	8 (6)	8 (6)	8 (6)	8 (6)	8 (6)	8 (6)

are more common in the slope waters, and at least partially explained by stochastic physical features (fronts, jets, eddies) or events (i.e., dust deposition).

4.3.3 Comparative Analysis

In order to identify the factors that most likely influenced and/or controlled bacterial abundance, productivity, and growth rates, this study examined the correlations between these three bacterial properties and a range of other variables measured concurrently (see Table 4.2). When all the data were pooled together for analysis over all seasons and both regions, both bacterial abundance and bacterial productivity were significantly correlated ($p < 0.05$) to each other and to all the measured variables, except chlorophyll. Although it was surprising not to find a correlation with chlorophyll, it was not surprising to find that most water properties were correlated in some manner when they were grouped across seasons, because most water properties change relative to each other in a fairly consistent manner over the annual cycle (Whitney and Freeland 1999). But, the question remains as to what the dominant physical or biological mechanisms were that drove the observed differences in bacterial properties over the annual cycle, during different seasons, and in different regions in the subarctic NE Pacific.

An initial multiple correlation analysis suggested that 14 of the 78 data points needed to be removed as outliers. For data to be considered outliers, they needed to stand out substantially from the cloud of background data in multiple correlation relationships, and do so in a manner that disproportionately biased the correlation away from the background trend or provided the only trend present. The removal of these 14 outliers was supported by their distance from the multivariate mean, the Mahalanobis distance. These 14 outliers included the four most extreme bacterial productivity data points (Fig. 4.3), the five winter 1994 data points, and five other data points from both spring and summer at stations P4, P12, and P20 (Appendix II). If the outliers were included in the following multivariate analysis, stronger correlations were found between more variables; however, these stronger correlations provided little insight into the mechanisms driving the more continuous change in the majority (90%) of the data.

For the reasons mentioned above, the outliers were removed from the following correlation analysis. The analysis of the remaining background data addresses the

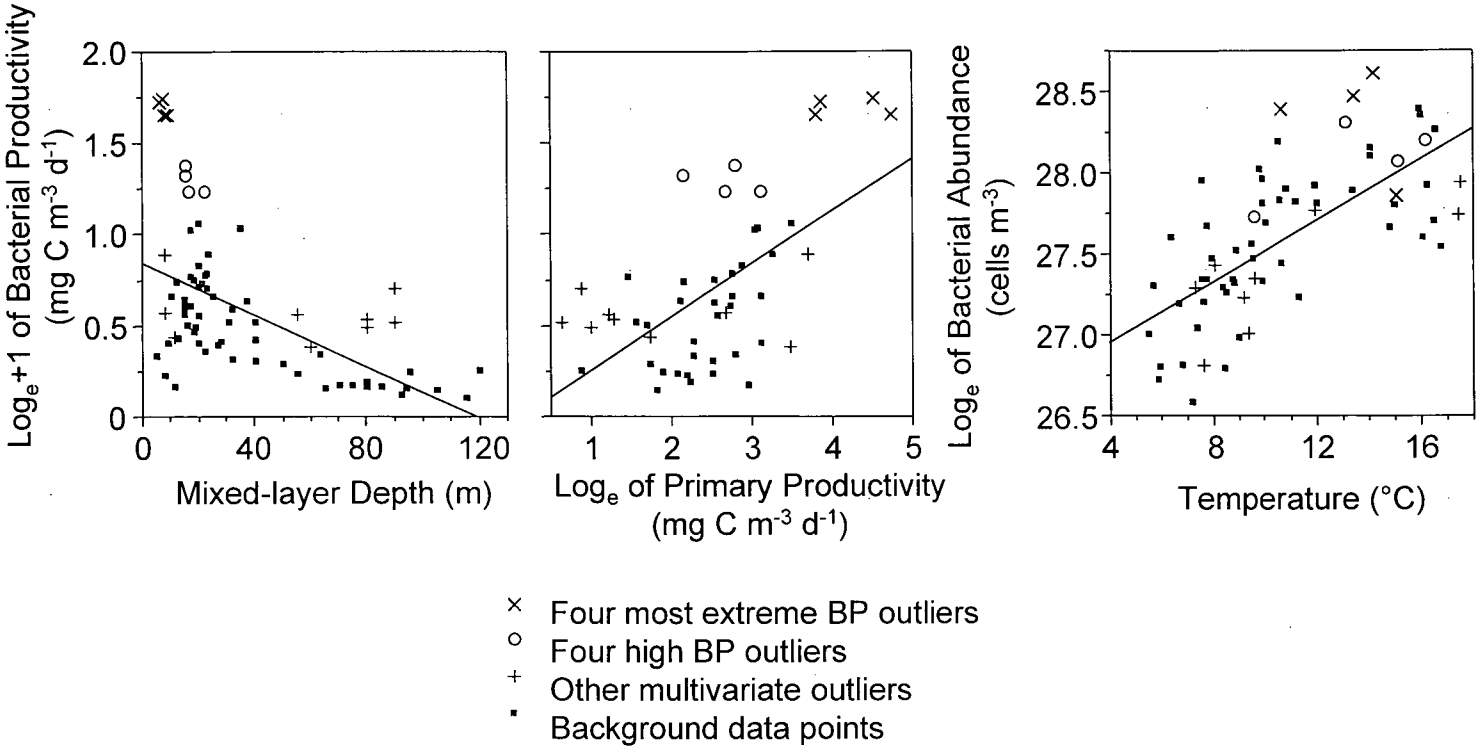

Figure 4.3 Bacterial productivity regressed against mixed-layer depth and primary productivity, and bacterial abundance regressed against temperature for all mixed-layer samples. The "x" and "o" symbols indicate the two sets of extreme bacterial productivity values referred to in the text. The "+" symbols represent other data removed as outliers in the comparative analysis. Bacterial abundance, bacterial productivity, and primary productivity values were log-transformed to meet parametric assumptions of normality.

Table 4.2 Correlations of bacterial abundance (B#), bacterial productivity (BP), and bacterial growth rate (Bμ) with physical variables (salinity, temperature, mixed-layer depth), mineral nutrients (NO3, PO4, and SiO4), size-fractionated primary productivity, size-fractionated chlorophyll, and heterotrophic flagellate abundance. Data were pooled for analysis into "background" (all data after removing the outliers, see text), "oceanic" across seasons (stations P20 and OSP), "slope" across seasons (stations P4 and P12), and each season (winter, spring, and summer) across regions. Brackets indicate negative correlations. Grayed values are "not significant" ($p > 0.05$). Values were left blank if there were insufficient data to provide valid calculations.

	Background			Oceanic			Slope			Winter			Spring			Summer		
	B#	BP	Bμ	B#	BP	Bμ	B#	BP	Bμ	B#	BP	Bμ	B#	BP	Bμ	B#	BP	Bμ
Salinity	(0.39)	(0.40)	(0.44)	(0.61)	(0.64)	(0.62)	(0.50)	(0.66)	(0.61)	(0.53)	(0.67)	(0.13)	0.20	0.11	(0.08)	0.11	(0.17)	(0.27)
Temperature	0.72	0.68	0.52	0.82	0.72	0.53	0.58	0.63	0.53	0.30	0.27	(0.19)	0.37	0.29	(0.09)	(0.15)	(0.20)	(0.14)
Mixed-layer depth	(0.57)	(0.56)	(0.47)	(0.57)	(0.49)	(0.45)	(0.40)	(0.47)	(0.53)	(0.31)	(0.32)	(0.14)	(0.01)	0.12	0.30	(0.35)	(0.37)	(0.29)
SiO_4	(0.29)	(0.23)	(0.15)	(0.73)	(0.48)	(0.36)	(0.54)	(0.48)	(0.29)	(0.63)	(0.44)	0.01	0.05	(0.02)	0.14	0.37	0.37	0.20
NO_3	(0.53)	(0.48)	(0.38)	(0.83)	(0.68)	(0.49)	(0.62)	(0.67)	(0.62)	(0.68)	(0.52)	0.00	(0.03)	(0.20)	0.02	0.26	0.11	(0.05)
PO_4	(0.53)	(0.47)	(0.34)	(0.78)	(0.64)	(0.45)	(0.58)	(0.65)	(0.59)	(0.64)	(0.45)	0.03	(0.15)	(0.30)	(0.09)	0.21	0.13	(0.01)
Total primary productivity	0.43	0.53	0.49	0.64	0.65	0.58	0.31	0.37	0.45	0.24	(0.10)	(0.11)	0.35	0.37	0.33	0.01	0.59	0.46
PP 0.2-5 μm	0.54	0.48	0.36	0.62	0.48	0.38	0.55	0.13	0.22	0.49	(0.43)	(0.43)	0.38	0.23	0.01	(0.14)	(0.07)	(0.02)
PP 5-20 μm	0.51	0.54	0.56	0.76	0.73	0.76	0.18	0.31	0.43	0.49	(0.43)	(0.43)	0.21	0.39	0.49	0.29	0.50	0.14
PP > 20 μm	0.39	0.36	0.36	0.78	0.76	0.68	0.15	0.13	0.15	0.49	(0.43)	(0.43)	0.14	0.26	0.28	0.55	0.29	(0.14)
Total Chlorophyll	(0.31)	(0.38)	(0.30)	0.08	0.26	0.20	(0.82)	(0.77)	0.58	0.79	0.45	0.18	(0.15)	(0.18)	(0.32)	0.10	0.09	(0.05)
Chl 0.2-5 μm	0.11	(0.29)	(0.34)	0.23	0.25	0.16	(0.82)	(0.81)	(0.60)	0.89	0.11	(0.49)	0.18	0.08	(0.25)	0.00	0.10	(0.05)
Chl 5-20 μm	(0.33)	(0.33)	(0.19)	0.16	0.29	0.45	(0.82)	(0.77)	(0.58)	0.66	0.00	(0.31)	(0.46)	0.00	0.23	0.12	(0.10)	(0.43)
Chl > 20 μm	(0.51)	(0.54)	(0.40)	(0.20)	(0.13)	(0.05)	(0.45)	(0.71)	(0.65)	(0.20)	0.43	0.54	(0.60)	(0.64)	(0.27)	0.45	0.43	(0.02)
Heterotrophic flagellates	0.32	0.46	0.35	0.18	0.22	0.36		(0.50)					0.65	0.72	0.44	(0.30)	0.90	0.90
Bacterial abundance	-	0.82	-	-	0.69	-	-	0.91	-	-	0.75	-	-	0.38	-	-	0.45	-
Bacterial growth rate	0.51	0.89	-	0.46	0.92	-	0.74	0.93	-	(0.09)	0.52	-	(0.23)	0.70	-	0.04	0.89	-

relationships among the more continuous changes across seasons and regions, not the abrupt changes associated with stochastic features (which do have both a seasonal and regional component). Except where noted, the following analysis was done with the outliers excluded (done only on the background data).

4.3.4 Correlation Analysis

In general, bacterial productivity was highly correlated to both bacterial abundance and growth rate (Table 4.2), although in some groupings of the data, bacterial abundance and growth rate were not significantly correlated (see further discussion below). In most comparisons, bacterial abundance and productivity shared similar relationships with the other variables. Unless otherwise noted, the correlations discussed compare bacterial properties to the other measured variables, and do not compare non-bacterial variables among themselves.

Across the background data, bacterial properties were positively correlated with each other, with temperature, and with primary productivity. Bacterial properties were negatively correlated with salinity, mixed-layer depth, macro-nutrients, and chlorophyll (primarily the largest size fraction, > 20 μm) (Table 4.2). The primary change seen in the background data relative to the complete data set (including the outliers) was the appearance of a significant negative correlation with chlorophyll due to the removal of the high chlorophyll associated with the four most extreme bacterial productivity outliers.

After dividing the background data into oceanic and slope regions, it appears that the oceanic waters were responsible for the positive correlation between bacterial properties and primary productivity, while the slope waters were responsible for the negative relationship between bacterial properties and chlorophyll (Table 4.2). These correlations suggest that the strong seasonal relationship between phytoplankton and bacteria found in both oceanic and slope regions is brought about by fundamentally different mechanisms. However, the above relationships do not hold when addressing the interannual variability of a given season in a given region (regression data not shown). Except during the spring, in slope waters, when primary productivity was highly correlated with bacterial productivity and growth rates ($R^2 > 0.9$, $p < 0.03$, $n = 4$), neither

primary productivity nor chlorophyll were statistically significant predictors of the bacterial productivity from year to year for a given season in a given region.

When divided into seasonal groupings, the only relationships that were different from the background and statistically significant were, a positive relationship between bacterial numbers and chlorophyll in the winter, and a positive relationship between bacterial properties and heterotrophic flagellate abundance in the spring and summer (Table 4.2). The significant correlations of bacterial properties with both nutrients and physical properties were no longer present during the spring and summer. Also lost were the positive correlations between bacterial abundance and growth rate in all the seasonal groupings across regions.

Temperature, which showed strong significant positive correlations in all groupings across seasons, showed weak correlations that were not significant within any of the three seasonal groupings. The only statistically significant relationship between bacterial properties and temperature, within any season was a strong negative correlation between bacterial abundance and temperature during the summer in slope waters (R^2 = 0.93, $p < 0.005$, n = 5).

There were not enough data to statistically elucidate many of the relationships that may be important in driving bacterial variability during a particular season in a given region. However, a few observations offered some insight. The median bacterial productivity for summer slope samples with no measurable nitrate was 0.67 mg C m^{-3} d^{-1}, while the two samples that contained measurable levels of nitrate, showed ~ 4 – 6-fold higher bacterial productivity (both were extreme bacterial productivity values from summer at P4, 3.0 and 4.7 mg C m^{-3} d^{-1}). In contrast, summer oceanic samples showed a negative correlation between bacterial abundance and nitrate (Rho = -0.50, $p < 0.05$, n = 7).

4.4.0 Discussion

Throughout the world's oceans, bacterial productivity has been shown to be frequently limited by the availability of labile dissolved organic carbon (LDOC) (Kirchman *et al.* 1993, Carlson and Ducklow 1996, Cherrier *et al.* 1996, Kahler *et al.* 1997, Kirchman *et al.* 2000), at times limited by the availability of mineral nutrients (N, P, Fe) (Elser *et al.* 1995, Shiah *et al.* 1998, Pakulski 1996), and occasionally co-limited by both LDOC and mineral nutrients (Elser *et al.* 1995, Caron *et al.* 2000, Church *et al.* 2000). The manipulation experiments presented in Appendix I support this view with a persistent positive response to LDOC additions along with intermittent responses to the additions of ammonium and/or iron.

In general, bacterial productivity is limited by the supply rate of a limiting substrate. As such, bacterial productivity should be directly proportional to the substrate supply rate. Assuming substrate limited growth, bacterial productivity is independent of both bacterial abundance and growth rate. Further, under substrate limited growth conditions, the bacterial growth rate depends on the biomass of the bacteria which are responsible for the given productivity (in essence, $B\mu = BP/BB$).

4.4.1 Conceptual Model

To provide a theoretical structure (a framework of relationships) within which to fit the correlation analysis presented in this study, a conceptual model was developed. This model defines the flow of control – which parameters cause or control change in which other parameters (Fig. 4.4). This model does not infer a flow of energy or mass. This model framework was used to define expected interaction patterns – sets of particular correlations between measured variables that are indicative of a particular process (i.e., nutrient stress, see below). From the observed dominance or absence of each expected interaction pattern, inferences were made about the which mechanisms controlled change in bacterial properties during different seasons and in different regions.

The model consists of seven physical variables near the top (rectangular boxes), two chemical variables in the middle (rounded rectangles), and six biological variables in the lower part of the diagram (ellipses) (Fig. 4.4). Shaded variables were not measured

Figure 4.4 Model schematic showing the assumed flow of control between variables measured in the subarctic NE Pacific. Signs (+ and -) indicate positive or negative control of the upstream variable over the downstream variable. Signs in brackets indicate controls that only act when mineral nutrients are below a critical threshold. The dashed arrow indicates the ability of low nutrients to increase the rate of phytoplankton excretion of DOM under nutrient stress. Rectangles, rectangles with rounded corners, and ellipses represent physical parameters, potentially limiting nutrients/substrates, and biological parameters respectively. Shaded compartments are parameters that are only inferred, not directly measured.

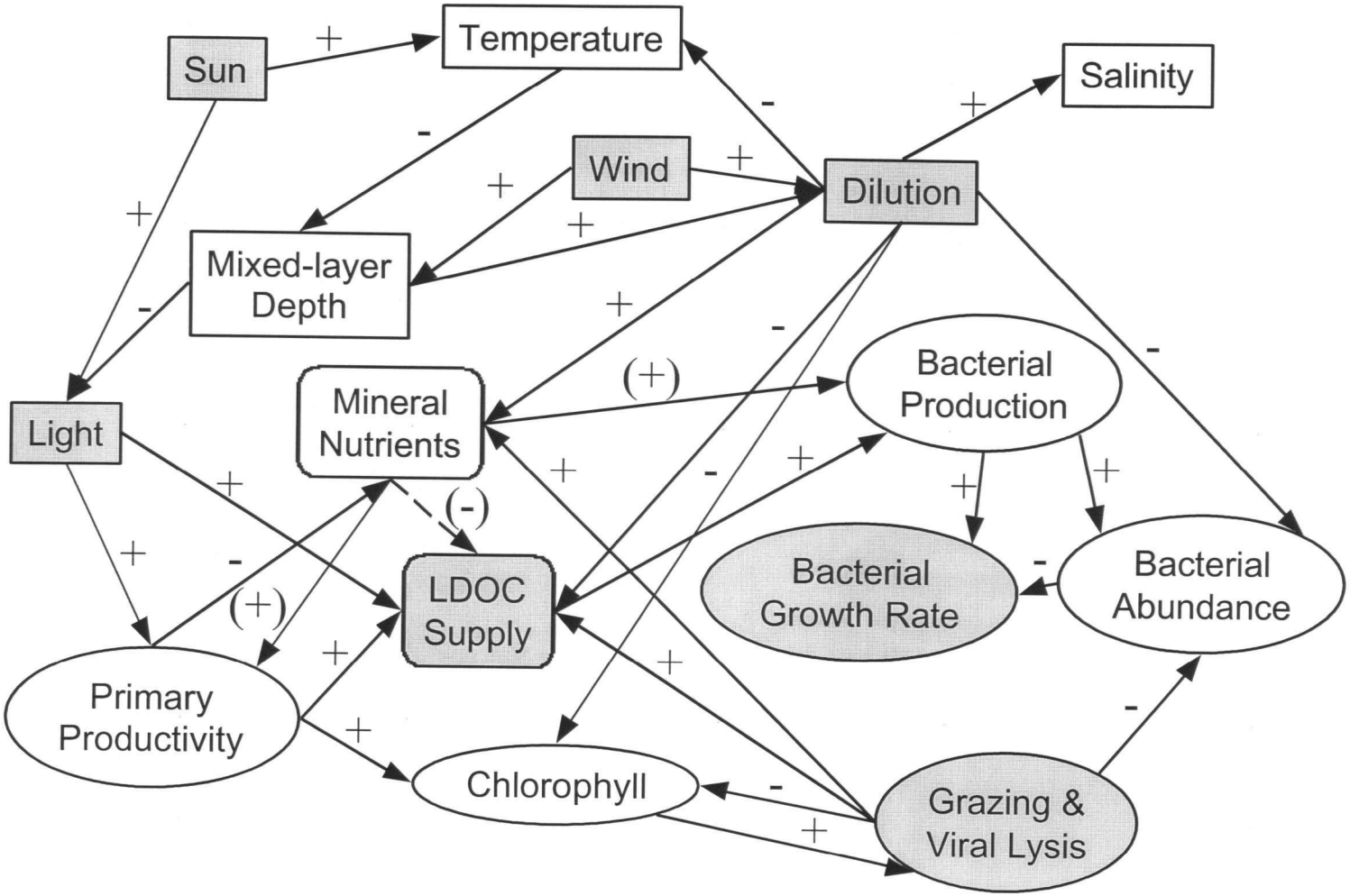
Sun
Temperature
Salinity
Wind
Dilution
Mixed-layer Depth
Light
Mineral Nutrients
Bacterial Production
LDOC Supply
Bacterial Growth Rate
Bacterial Abundance
Primary Productivity
Chlorophyll
Grazing & Viral Lysis

during this study and can only be inferred. Arrows define the proposed direction of influence, either positive (+) or negative (-), exerted by the upstream variable over the downstream variable. These boxes and arrows denote the direction of influence or control; they do not necessarily indicate a flow of material or biomass. It is assumed that a strong positive control results in a positive correlation between the variables and a strong negative control results in a negative correlation. Signs in brackets denote pathways that only express control when the limiting nutrient is below some threshold. The dashed arrow represents increased phytoplankton exudation when the phytoplankton are stressed by low mineral nutrients.

Since correlations do not prove a direct relationship, this model is not tested by these data, but rather, it offers a consistent mechanistic explanation of the patterns and relationships seen in these data. The assumptions and relationships described below may not necessarily transfer to other microbial systems in other regions.

Expected Interaction Patterns – There are four major control factors used in describing the observations made during this study: 1) dilution processes, 2) phytoplankton production of LDOC via both exudation and sloppy feeding, 3) mineral nutrient limitation, and 4) biological loss processes and recycling (grazing and viral lysis of bacterial cells). All of these control factors can alter the supply rate of LDOC (and thus bacterial productivity) either directly or indirectly. Dilution and biological loss processes both alter bacterial abundance directly.

Dilution – was not directly measured in this study, however, it is inferred from the interaction patterns of the measured properties both upstream and downstream of dilution in the model (Fig. 4.4). This view characterizes dilution as the upward mixing of deeper water into the surface mixed layer. There are two processes considered to dilute the surface mixed layer with deeper water, deepening of the mixed layer and upwelling. Since mixed-layer depth was measured, it was used as one indicator of dilution. Also, dilution drives other variables closer to the values measured in the deeper water (below the mixed-layer). Since salinity and mineral nutrient concentrations increase with depth, dilution is associated with increased salinity and mineral nutrient concentrations. Since,

temperature, chlorophyll, bacterial abundance, and bacterial productivity (a proxy for LDOC supply rate) all decrease with depth (Sherry *et al.* 1999, Nagata *et al.* 2000), dilution is associated with a decrease in these properties.

When dilution processes are the dominant control of the system, salinity and mineral nutrients are positively correlated with each other and negatively correlated with temperature, chlorophyll, bacterial abundance, and bacterial productivity. As the influence of dilution processes decreases (the seasonal thermocline develops) and/or LDOC production increases (through increased primary productivity and/or grazing) the correlations between the physical properties and the chemical/biological properties should change. Dilution directly decreases bacterial abundance, but, it acts less directly on bacterial productivity by altering the resource availability (lower LDOC and higher mineral nutrients) (see below).

Primary Productivity – Phytoplankton productivity was measured over the course of this study. However, different levels of phytoplankton biomass production may not always be linked to similar changes in the production of LDOC. Teira *et al.* (2001) present data from a range of eutrophic (upwelling) and oligotrophic locations in the Atlantic Ocean showing that there was not a significant difference between ecosystem types in the production rates of dissolved organic carbon (DOC) because, the proportion of primary production lost to the DOC pool was greater in the low productivity oligotrophic areas dominated by small (< 2 μm) phytoplankton. The proportional increase of DOC production in oligotrophic waters may be attributable to either or both increased exudation from smaller (leakier) phytoplankton and/or more rapid grazing turnover of the fast growing small cells (Teira *et al.* 2001 and references within). Aota and Nakajima (2001) suggest that phytoplankton excrete greater quantities of DOC under higher light and increased nutrient stress, because they are fixing carbon at a higher rate than their nutrient supply rate allows them to grow. Increased DOC excretion with higher light and lower nutrients could provide a poor, or even negative correlation between changes in measured primary productivity and changes in bacterial productivity because of the proportional increase in LDOC production associated with nutrient-limited phytoplankton growth. Changes in primary production and bacterial production may also be decoupled

because of a time lag between increased primary productivity and the associated increase in phytoplankton loss processes that release LDOC (grazing, viral lysis, and/or late bloom nutrient stress) or because available DOC was semi-labile and required time for bacterial breakdown and consumption (Carlson *et al.* 1996, Ducklow *et al.* 1999).

Within this model, phytoplankton production of LDOC is not only inferred by increased primary productivity, but also by increased light (decreased mixed-layer depth), decreased mineral nutrient concentrations, and increased grazing of phytoplankton biomass (reduced chlorophyll). Thus when changes in bacterial production are driven by changes in phytoplankton LDOC production, bacterial productivity and primary productivity can be positively correlated with each other and negatively correlated with mixed-layer depth, mineral nutrient concentrations, and chlorophyll. Also, bacterial abundance, productivity, and growth rates will all be positively correlated with each other whenever changes in the LDOC supply rate are a dominant influence on changes in bacterial properties.

Decreases in mineral nutrients can also be indicative of past primary production which may have increased not only LDOC in the past, but semi-labile DOC that provided a time-lagged LDOC supply.

Nutrient Limitation – Mineral nutrient limitation plays two independent roles in this model. Low mineral nutrient concentrations are assumed to stress phytoplankton and increase the excretion of photosynthetically fixed carbon (represented by the dashed arrow between mineral nutrients and LDOC, see above discussion) and thus increase bacterial productivity (Aota and Nakajima 2001 and references within). However, bacterial productivity can also be directly limited by the supply rate of mineral nutrients (Elser *et al.* 1995, Shiah *et al.* 1998, Pakulski 1996, Appendix I). It is believed that bacteria outcompete phytoplankton for mineral nutrients at low concentrations (Thingstad and Rassoulzadegan 1995), while they are also dependent on primary production for LDOC. Accordingly, these dynamics between bacteria and phytoplankton should produce two distinct interaction patterns.

The first interaction pattern due to mineral nutrient limitation occurs when phytoplankton become nutrient stressed under high light and they excrete more LDOC

which the bacteria consume, subsequently increasing bacterial productivity (since the bacteria are not yet nutrient stressed). Thus, the interaction pattern is an increase in bacterial productivity with a decrease in mineral nutrients and a shallower mixed-layer depth (more light). In this case, bacterial productivity may be decoupled from measurements of phytoplankton production – the particulate primary productivity typically measured (see above).

However, as the growing season progresses and mineral nutrients in the surface mixed layer continue to decline, the second interaction pattern, that is also due to mineral nutrient limitation, develops as bacterial productivity becomes directly limited by the low mineral nutrient availability. Under these conditions, the interaction pattern shows increased bacterial productivity when mineral nutrients increase (supplied by dilution in the case of nitrate or aerosols in the case of iron), along with increased primary productivity (depending on the magnitude of nutrient injection). It should also be noted that under competitive nutrient limitation, when bacteria and small phytoplankton are competing for the same limiting recycled nutrient(s), preferential grazing on one group of organisms can shift biomass from that more heavily grazed group to the less heavily grazed group. Thus a shift in grazing preference from bacteria to phytoplankton (or visa versa) would lead to a negative correlation between bacterial abundance and chlorophyll.

Biological Loss Processes and Recycling – Bacterial abundance is controlled by the balance between bacterial production and loss processes over time. Loss processes can be either biological (grazing, viral lysis) or physical (dilution). Biological loss processes feed back into bacterial production through recycling via sloppy feeding, zooplankton waste, or viral lysates. In resource limited systems, biological loss processes should thus increase bacterial productivity at the expense of biomass, whereas physical loss processes should cause a decrease in both bacterial abundance and productivity (unless bacterial productivity is limited by the availability of mineral nutrients).

In resource limited systems, if there is a change (e.g., a decrease) in bacterial abundance due to a change (e.g., an increase) in grazing (without a change in bacterial productivity), there should be an associated and opposite change in the bacterial growth rate (e.g., fewer cells competing for the same resource supply). An extreme case would

be when there is an inverse relationship between bacterial productivity and bacterial abundance suggesting that changes in recycling within the bacterial community are dominant over changes in the external resource supply (e.g., phytoplankton derived LDOC). This is because loss processes, not only reduce bacterial abundance, but also make more recycled resources available to increase bacterial productivity. If bacterial abundance, productivity and growth rate are all positively correlated, the change must be dominated by a change in bacterial productivity (assumed to be brought about by a change in the supply rate of the limiting resource).

In a system that has not yet achieved steady-state, a change in bacterial productivity should be directly associated with a proportional change in growth rate until sufficient time has passed for an associated change in bacterial biomass to occur. Therefore, in a resource limited system, bacterial productivity and growth rate should be more tightly coupled to each other than to bacterial biomass. If bacterial productivity was negatively correlated to bacterial growth rate, the system would no longer be resource limited; productivity would then be limited by biomass (i.e., loss processes). There was no evidence of loss processes controlling bacterial productivity during this study. This model does not attempt to address potential changes in bacterial growth efficiency.

In summary, the mechanisms dominating control of the changes in bacterial properties are recognized according to the following patterns:

1) Dilution processes dominate when bacterial properties are negatively correlated with salinity, mixed-layer depth and mineral-nutrient concentrations, but positively correlated with temperature.

2) Changes in phytoplankton produced LDOC concentrations dominate when bacterial properties are all positively correlated with each other, and positively correlated with primary productivity and/or negatively correlated with chlorophyll.

3) Limiting concentrations of a mineral nutrient dominate when bacterial properties are positively correlated with mineral-nutrient concentrations.

4) Biologically driven bacterial loss and recycling processes dominate when bacterial abundance and growth rate are negatively correlated with each other, when bacterial productivity and bacterial abundance are more weakly correlated, and when

bacterial productivity has a more positive correlation with heterotrophic flagellate abundance than does bacterial abundance.

Needless to say, changes in bacterial properties are probably driven, most of the time, by multiple mechanisms operating concurrently. The following discussion attempts to highlight the dominant mechanisms driving the changes observed during this study.

4.4.2 Fitting Correlation Data to the Conceptual Model

All data – The apparent mechanisms responsible for driving changes in bacterial properties can vary dramatically depending on how the data are pooled or grouped for correlation analysis. The first of three issues is the problem of outliers. If extreme values extend and/or reinforce the relationships evident between the more abundant and moderate data points, they can provide greater statistical rigor and analytical confidence to generalizations based on the observed correlations. However, many of the outliers in these data did not extend or reinforce the relationships observed in the more abundant and moderate data (the background data), suggesting that the mechanisms causing the extreme values were intrinsically different than those causing the change in the more typical background conditions (see outliers below).

The second issue is that of correlations based primarily on a change in variability instead of a change in magnitude. An example of this is the change in bacterial productivity relative to the change in mixed-layer depth (Fig. 4.3). Deep mixed layers always have relatively low bacterial productivity, while shallow mixed layers show both low and high productivity. Thus a shallow mixed-layer depth cannot be considered the driving force for high bacterial productivity (i.e., shallow mixed layers show some of the lowest productivity also), but a shallow mixed-layer depth was either a prerequisite for high productivity or directly associated with some other variable that was a prerequisite. This type of relationship may provide a strong correlation, but it does not provide support for a direct cause and effect relationship.

The third issue is that of mode-switching vs. linear trends. A good example of mode switching is the relationship between bacterial abundance and temperature (Fig. 4.3). A simple linear regression of all the data suggests that bacterial abundance increases with increasing temperature. A different assessment of the same data can

describe the relationship between bacterial abundance and temperature as bimodal, where below 12°C bacterial abundance was positively correlated with temperature, and above 12°C, although bacterial abundance was relatively high, there was not a temperature response. Interestingly, when the mixed-layer temperature was > 12°C, the mixed-layer depth was always < 40 m, and slope waters were always depleted in nitrate. In fact, the trend for data points greater 12°C suggests a possible decrease in bacterial abundance with increasing temperature. Conversely, when the mixed-layer temperature was < 12°C, there was greater variability in the mixed-layer depth and nitrate concentrations increased linearly as temperature decreased. This alternative interpretation of these data does not support a simple direct positive relationship between temperature and bacterial abundance. In this interpretation, temperature appears to be primarily a co-variant of general seasonal changes and is possibly tied to nutrient dynamics and/or mixed-layer stability (see Li 1998). When the data were divided into seasonal groupings, there was no longer a significant relationship between bacterial productivity and temperature during any season (Table 4.2).

While it is risky to use individual pairwise comparisons (i.e., bacterial abundance vs. temperature) to infer cause and effect relationships, the following discussion uses patterns in multiple pairwise comparisons within the context of the conceptual model presented above ("expected interaction patterns") to infer cause and effect relationships.

4.4.3 Tying mechanisms to Observations

Over a year, the mixed layer depth at OSP typically ranges from < 20 to > 80 m (Sherry *et al.*, 1999) providing > 4-fold dilution of the mixed layer between summer and winter. This seasonal dilution can account for much of the decrease in bacterial abundance and productivity between summer and winter reported in Chapter 3. This strong seasonal dilution signal is apparent in the strong interaction patterns indicative of dilution processes and present in all the data pooled across seasons (background, oceanic, and slope).

During the winter, weather systems drive increased oceanic upwelling in the central NE subarctic gyre (Crawford, pers. comm.) as well as increased mixed layer depths. Greater winter dilution along with lower winter bacterial production explain the

significant relationships between bacterial properties and the interaction patterns indicative of dilution processes during the winter.

Over a year, mixed layer primary productivity ranges from < 5 in the winter to ~ 35 mg C m^{-3} d^{-1} in the spring and/or summer at OSP, and from ~ 20 in the winter to ~ 100 mg C m^{3} d^{-1} in the spring and/or summer at P4 (Boyd and Harrison 1999). This strong seasonality in primary productivity likely explains the significant positive correlations between all three bacterial properties, and thus the interaction patterns indicative of increased phytoplankton LDOC production observed in all the data pooled across seasons. The lack of significant correlation between bacterial properties and primary productivity in the slope region suggests a decoupling between LDOC production and phytoplankton productivity. Since slope waters have the strongest negative correlation between bacterial properties and chlorophyll, particularly in the smaller size-fractions, LDOC production in this region may be strongly influenced by increased grazing pressure on smaller phytoplankton experiencing nutrient stress from the seasonal post-bloom nitrate depletion typical of this region (Whitney and Freeland 1999).

The remaining two interaction patterns discussed above, mineral nutrient limitation and loss/recycling, did not show statistically significant relationships in these data. This lack of significance may be attributed to two factors. First, both nutrient limitation and loss/recycling are expressed as correlations that are counter to the prevailing trends produced by dilution and LDOC production. Thus the trends produced by nutrient limitation and/or recycling may be expressed as little more than reduced negative correlations between bacterial properties and nutrients, or reduced positive correlations between the bacterial properties themselves. Second, both of these patterns, and especially mineral nutrient limitation can be transient and local in nature so they would play a dominant role only during certain seasons in certain regions, the resolution for which, there are too few data points in this study to provide a robust analysis.

Intermittent mineral nutrient limitation might explain why the significant negative correlations between bacterial properties and mineral nutrients were lost in both the spring and summer data groups. The amendment experiments presented in Appendix I show increased bacterial productivity in response to the addition of ammonium in slope waters during both the spring and summer, while there was also a positive response to the

addition iron and LDOC during one summer in oceanic waters (see Table A1). All but samples in slope waters during the summer were depleted in nitrate and showed a low median bacterial productivity (0.67 mg C m^{-3} d^{-1}) while the two data points with measurable nitrate levels showed much higher bacterial productivity (3.0 and 4.7 g C m^{-3} d^{-1}). Only the highest of these bacterial productivity values (one treated as an outlier in the correlation analyses) was also associated with high chlorophyll and primary productivity values (Appendix II). These patterns all suggest that bacterial properties were limited by the availability of mineral nutrients, especially in the summer and in slope waters.

Bacterial abundance and growth rate always showed weaker correlations with each other than either property did with bacterial productivity. As suggested above, this pattern is indicative of either non-steady-state conditions and/or changes in biological loss processes. The spring and summer groupings also lose their significant correlation between bacterial abundance and productivity which suggests the possibility of increased biological loss and recycling of bacterial biomass. Reinforcing the idea that recycling played an increased role during late summer is also the strong positive correlation between heterotrophic flagellates and both bacterial productivity and growth rates, correlations not shared with bacterial abundance.

Outliers – Being typically associated with physical fronts, shallower than average mixed layer depths, low or depleted nutrients, and high primary productivity in the smallest phytoplankton size fraction, it is likely that occasions of extreme bacterial abundance and productivity were tied to late bloom conditions initiated by the convergence of water masses. These observations suggest abundant nutrient stressed phytoplankton growing in high light with abundant heterotrophic flagellate grazers driving increased LDOC production and thus increased bacterial abundance, productivity, and growth rates. Confirming this hypothesis will require further studies focusing on the biological processes in these frontal systems.

Background – The background data (i.e., with the outliers removed, see Appendix 2) suggest that the dominant control of changes in bacterial properties across all seasons and

regions was related to previous phytoplankton production and/or nutrient stress under high light providing increased LDOC supply. Differences in dilution also played a significant role, while changes in grazing and recycling processes, or direct nutrient limitation of bacterial production were either not important, or masked by the overwhelming influence of the first two mechanisms.

Oceanic – The relationships within the oceanic grouping were indicative of processes driving changes in the oceanic region across the different seasons. The oceanic relationships, although similar to the background data, showed stronger correlations associated with dilution processes and primary productivity while no longer showing a significant negative correlation with chlorophyll. Accordingly, increased bacterial abundance and production were associated with decreased dilution, a shallower mixed layer, lower mineral nutrients and greater primary productivity.

Slope – In slope waters across seasons, the strong positive correlations among all three measured bacterial properties suggests that change in LDOC was a predominant factor controlling seasonality in this system along with (or as part of) dilution. However, unlike the oceanic region, bacterial properties appear to be decoupled from phytoplankton productivity in all size fractions and are highly negatively correlated to chlorophyll especially in the smaller size fractions. Although these observations may seem counter-intuitive, they may be explained by one or more of the following scenarios: 1) Nutrient stressed low biomass phytoplankton communities in the spring and summer support proportionately higher bacterial productivity due to increased leakiness of cells and higher turnover due to grazing (Teira *et al.* 2001). 2) There was a time-lag between phytoplankton derived DOC production and bacterial utilization, because high phytoplankton DOC produced prior to sampling (during an earlier bloom) was broken down over time into LDOC and utilized during the time of sampling when post-bloom conditions with lower primary productivity and chlorophyll are present (Carlson *et al.* 1996, Ducklow *et al.* 1999). Finally, 3) if bacteria were competing with phytoplankton for limited mineral nutrients (see above), then allochthonous input of LDOC could have released the bacteria from their dependence on phytoplankton production for LDOC, and

thus, the bacteria may have been able to use more mineral nutrients to the detriment of the phytoplankton biomass. Determining the mechanism(s) driving change in LDOC production in slope waters will require more work focused on identifying the source(s) of LDOC and following the community response to changing DOC/LDOC over time.

If phytoplankton production, and thus LDOC supply, in the oceanic HNLC region is limited primarily by the availability of iron which can act to reduce the carbon fixation of phytoplankton through inhibition of the electron transport system (Geider and LaRoche 1994), it is reasonable to suggest that changes in iron availability, which drive changes in phytoplankton production, would likely lead to increased LDOC supply to the bacteria. In contrast, primary production in the slope region is primarily limited by nitrate availability following the spring bloom. If the highest LDOC concentrations occur as the bloom crashes (as chlorophyll drops) (see discussion in Carlson *et al.* 1996, Ducklow *et al.* 1999) and/or when the system is nitrogen stressed and thus fixing carbon faster than the phytoplankton can grow (Aota and Nakamima 2001), it is reasonable to suggest that bacterial productivity could be decoupled from particulate primary production, and negatively correlated with chlorophyll.

Winter – Winter appears to have been dominated by dilution processes as suggested by the negative relationships of bacterial properties with salinity and macro-nutrients, while there was no clear relationship between bacterial properties and primary productivity. The positive relationship between bacterial abundance and chlorophyll (independent of primary productivity) further supports a strong dilution influence assuming that dilution was greater and phytoplankton growth rates were lower in the winter, leading to both bacteria and phytoplankton experiencing similar dilution driven losses. The lack of correlation between bacterial abundance and growth rate may also be indicative of dilution, since dilution should decrease bacterial abundance and LDOC independent of growth (fewer cells exploiting decreased LDOC) and thus lead to a weakening of the correlation between growth rate and bacterial productivity.

Spring and Summer – With the establishment of the seasonal thermocline, dilution no longer played a significant role in the changes observed in bacterial processes. Without

the input of mineral nutrients associated with dilution processes, spring and summer bacterial properties were not negatively correlated with macronutrients as they were during the winter and across seasons. Manipulation experiments have shown that low concentrations of mineral nutrients can directly limit bacterial production in both the oceanic and slope regions during the summer (see Appendix I). Also, during both spring and summer, bacterial loss processes and recycling appeared to play a larger role since bacterial abundance was no longer strongly correlated with both bacterial productivity and growth rate. Recycling as a controlling influence was further supported in the summer by the strong positive relationship between bacterial productivity and heterotrophic flagellate abundance. It appears that bactivory is proportionately greater during the spring and summer than during the winter.

Dominant controlling influences for each of the various data groupings are summarized in Table 4.3.

4.5.0 Conclusions

Positive correlations between bacterial properties and both chlorophyll and primary productivity were dominated by only a few data points (outliers) associated with identifiable physical fronts. Aside from the outliers, bacterial properties were typically negatively correlated with chlorophyll and either not, or only weakly positively correlated with primary productivity. Bacterial properties increased in association with indicators of past algal production and/or current algal nutrient stress in conjunction with high light (low macro-nutrients, low chlorophyll, and shallow mixed-layer). Bacterial properties decreased with increased dilution processes (increased salinity and mixed-layer depth, and decreased temperature). Dilution processes were prominent in the winter when growth rates were low, and over the annual cycle in association with the fall deepening of the mixed-layer from ~ 20 to 100 m. Past algal production and/or current algal nutrient stress appeared to drive seasonal increases in bacterial abundance and productivity. However, at times, direct mineral nutrient stress also limited bacteria in the spring and

Table 4.3 Dominant control mechanisms influencing the changes observed in bacterial abundance, productivity, and growth rates in each of the various data groupings. See text for definitions and the details of the mechanisms listed.

	Background	Oceanic	Slope
All	LDOC Production Dilution	Dilution LDOC Production (Primary Productivity)	Dilution LDOC Production (Nutrient stress / phyto grazing)
Winter	Dilution	Dilution	Dilution
Spring	LDOC Production (Nutrient stress / phyto grazing) Loss/recycling	Past LDOC Prod Loss/recycling	LDOC Production (Primary Production)
Summer	Nutrient Stress Loss/recycling	Dilution LDOC Production (Phyto growth & Loss) Iron stress	Nutrient stress

Season and Location	Reference	B#s 10^{12} cells m^{-3}	BB mg C m^{-3}	C/cell fg C $cell^{-1}$	TdR nmol m^{-3} d^{-1}	BP_{TdR} mg C m^{-3} d^{-1}	$F_{TdR\ (used)}$ 10^{18} cells mol^{-1}	$F_{TdR\ (measured)}$ 10^{18} cells mol^{-1}	Leu µmol m^{-3} d^{-1}	BP_{Leu} mg C m^{-3} d^{-1}	$F_{Leu\ (used)}$ 10^{18} cells mol^{-1}	$F_{Leu\ (measured)}$ 10^{18} cells mol^{-1}	F Method	μ d^{-1}
Spring														
Subarctic NE Pac.	Kirchman (1992), Kirchman et al. (1993)	0.4-1.3	7-25	20	2.9-37	0.1-1.3	1.74	1.5-3.4	-	-	0.108	0.027	Integrative	0.03-0.1
Subarctic NE Pac.	Doherty (1995)	0.6-1.2	6-12	10	11-16	0.4-0.6	3.50	-	-	-	-	-	-	0.04-0.08
Subarctic NE Pac.	This study	1-1.3	10-13	10	15-27	0.5-0.9	3.50	2.0	0.3-0.8	0.3-0.8	0.106	0.060	Cumulative	0.03-0.6
California Current	Cherrier et al. (1996)	0.1	2	19.6	-	0.6[a]	-	-	-	-	-	-	-	0.3
California Upwelling[b]	Kirchman et al. (2000)	0.6-1	12-20	20	-	-	-	-	2.5-3.9	5.8-9.0	0.115	-	-	0.4
California Upwelling[c]	Kirchman et al. (2000)	0.9	18	20	-	-	-	-	0.6-14.6	1.4-33.6	0.115	-	-	0.07-1.1
Eastern Equatorial Pac.	Ducklow et al. (1995)	0.3-0.8	8-11	20	36-84	2	2.17	-	0.72-1.32	1.7-3.0	0.115	-	-	0.2
Eastern Equatorial Pac.	Cochlan (2001)	0.2-0.9	1.4-5.2	5.9	-	-	-	-	1.0-1.3	0.7-0.9	0.115	-	-	0.2
Ross Sea	Ducklow et al. (1999)	0.1-0.3	2-6	20	16	0.19	0.6	0.4-0.9	0.14	0.11	0.04	0.03-0.05	Cumulative	0.06-0.5
NW Atlantic	Li et al. (1993)	1.5-2	30-40	20	96-170	2-7	1 & 2.3	1 & 2.3	2.7-5.0	3-17	0.055 & 0.17	0.055 & 0.17	Cumulative	0.08 & 0.25
N. Atl. Drift	Ducklow et al. (1992 & 1993)	1-2.5	20-50	20	75-189	4-10	2.65	2.03-3.69	1.6	6	0.183	0.14-0.22	Mod Der	0.1-0.3
N. Atl. Drift	Ducklow et al. (1992 & 1993)	1-2.5	20-50	20	75-189	1.8-4.5	1.2	0.67-1.5	1.6	3	0.095	0.04-0.13	Cumulative	0.05-0.12
N. Atl. Drift	Fasham et al. (1999)	0.1-0.15	2-3	20	57-201	2-7	1.74	-	-	-	-	-	-	~1.0
N. Atl. Drift	Zubkov et al. 2000	0.6-1.4	4-10	7	71-161	0.4-0.9	0.80	0.80	0.84-3.4	0.2-0.8	0.034	0.034	Cumulative	~0.08
N. Atl. Subtropical Gyre	Zubkov et al. 2000	~0.3	~2	7	18-107	0.1-0.2	0.80	0.80	0.63-1.3	0.15-0.3	0.034	0.034	Cumulative	~0.09
Sargasso Sea (BATS)	Carlson et al. (1996)	0.3-0.6	2.0-2.4	6.6	12-36	0.1-0.4	1.63	0.4-0.6	0.24-0.84	0.1-0.4	0.078	0.030	Cumulative	0.10
Equatorial Atl.	Zubkov et al. 2000	0.3-0.7	2-5	7	107-143	0.2-0.8	0.80	0.80	0.84-2.5	0.2-0.6	0.034	0.034	Cumulative	~0.13
S. Atl. Subtropical Gyre	Zubkov et al. 2000	~0.1	~1	7	5-18	0.03-0.1	0.80	0.80	0.42-0.84	0.1-0.2	0.034	0.034	Cumulative	0.03-0.14
Atl. Subantarctic	Zubkov et al. 2000	0.1-0.6	1-4	7	36-107	0.2-0.6	0.80	0.80	0.42-2.1	0.1-0.5	0.034	0.034	Cumulative	~0.13
Atl. Antarctic Circumpolar Current	Lochte et al. (1997), Kahler et al. (1997)	0.3-0.5	2-6	18.7	11-16	0.2-0.3	1.00	-	0.07-0.1	0.2-0.3	0.16	-	Cumulative	~0.06
Summer														
Arctic Ocean	Rich et al. (1997)	0.4-1.4	8-28	20	6-7	0.5-2	2.15	-	0.36-4.2	0.8-4	0.115	-	-	0.03-0.45
Subarctic NE Pac.	Kirchman (1992), Kirchman et al. (1993)	0.6-1.3	12-25	20	17-66	0.6-2.3	1.74	1.1-2.4	-	-	0.108	0.03-0.3	Integrative	0.04-0.1
Subarctic NE Pac.	This study	0.9-1.8	9-18	10	10-70	0.4-2.5	3.50	4.5	0.83	0.88	0.106	-	-	0.04-0.12
Eastern Equatorial Pac.	Kirchman et al. (1995)	0.5-0.8	9-15	20	16-47	0.7-2	2.15	-	0.30-0.87	0.7-2	0.115	-	-	~0.1
Antarctic Circumpolar Current	Church et al. (2000)	0.8	3.5	~4	40	0.34	2	-	0.075	-	-	-	-	0.09
Ross Sea	Ducklow et al. (1999)	0.2-1.2	4-24	20	39	2	2.5	2.5	0.66	3.4	0.26	0.26	Cumulative	0.3-0.4
Ross Sea	Ducklow et al. (2000)	1.5	10	6.7	-	-	-	-	1.0	1.5	0.224	-	-	0.15
Sargasso Sea (BATS)	Carlson et al. (1996), Carlson & Ducklow (1996)	0.3-0.7	~3	6	12-60	0.1-0.6	1.63	0.8	0.24-0.72	0.1-0.3	0.078	0.03	Cumulative	0.08
Scotia Sea	Bjornsen & Kuparinen (1991)	1	10	10	24	0.3	1.23	1.23	0.13	0.4	0.3	0.3	Cumulative	0.04
Winter														
Subarctic NE Pac.	Boyd et al. (1995a, 1995b)	0.70	7.0	10	13-19	0.5-0.7	3.50	-	-	-	-	-	-	0.09
Subarctic NE Pac.	This study	0.4-0.7	4-7	10	2-8	0.1-0.3	3.50	4.0	0.1-0.4	0.1-0.4	0.106	0.075	Cumulative	0.02-0.05
Eastern Equatorial Pac.	Kirchman et al. (1995)	0.4-0.7	8-13	20	19-35	0.8-1.5	2.15	-	0.34-65	0.8-1.5	0.115	-	-	~0.1
W. Equatorial Pac	Shiah et al. (1998)	0.2-0.5	5-9	20	40-130	1-3	1.18	-	-	-	-	-	-	0.2-0.4
Sargasso Sea (BATS)	Carlson et al. (1996), Carlson & Ducklow (1996)	0.3-0.5	1.6-1.8	4.8	12-24	0.1-0.2	1.63	0.2-3.7	0.19-0.48	0.1-0.2	0.078	0.02-0.3	Cumulative	0.07
Autumn														
Subarctic NE Pac.	Kirchman (1992), Kirchman et al. (1993)	0.5-0.7	10-14	20	23-32	0.8-1.1	1.74	3.4	-	-	0.108	0.15	Integrative	0.07
Eastern Equatorial Pac.	Ducklow et al. (1995)	0.5-1.2	9-18	20	48-84	1-2	2.17	-	0.48-0.84	1.1-1.9	0.115	-	-	0.1
N. Atl. Drift	Zubkov et al. 2000	0.3-0.6	2-4	7	36-161	0.2-0.9	0.80	0.80	0.84-4.2	0.2-1	0.034	0.034	Cumulative	~0.18
N. Atl. Subtropical Gyre	Zubkov et al. 2000	~0.1	~1	7	9-36	0.05-0.2	0.80	0.80	~0.63	~0.15	0.034	0.034	Cumulative	~0.12
Sargasso Sea (BATS)	Carlson et al. (1996), Carlson & Ducklow (1996)	0.4-0.6	2.4	5.4	12-36	0.1-0.3	1.63	1.1-4.1	0.24-0.6	0.1-0.3	0.078	0.100	Cumulative	0.06
Equatorial Atl.	Zubkov et al. 2000	0.1-0.7	1-5	7	9-143	0.05-0.8	0.80	0.80	0.42-3.4	0.1-0.8	0.034	0.034	Cumulative	~0.13
S. Atl. Subtropical Gyre	Zubkov et al. 2000	0.1-0.3	1-2	7	~18	~0.1	0.80	0.80	~84	~0.2	0.034	0.034	Cumulative	~0.10
Atl. Subantarctic	Zubkov et al. 2000	0.6-1.0	4-7	7	107-161	0.2-0.9	0.80	0.80	0.42-2.1	0.1-0.5	0.034	0.034	Cumulative	~0.09
Spring & Autumn Combined														
N. Pac. Subtropical Gyre	Jones et al. (1996)	0.4	7	20	-	~1[e]	-	-	-	-	-	-	-	0.13

[a] BP derived from change in particulate organic carbon, not TdR uptake rates.

[b] Data from regions considered by authors to be low Fe.

[c] Data from regions considered by authors to be Fe replete.

[d] BGE derived from glucose and amino acid amended incubations.

[e] BP derived from ^{3}H-adenine uptake instead of TdR.

summer. These data suggest that bacterial abundance and productivity were often decoupled from phytoplankton productivity either because of physical processes (dilution) acting differently on bacteria (LDOC limited) and phytoplankton (mineral nutrient limited), or due to increased algal DOM excretion associated with high light and nutrient stress (i.e., primary production did not contribute to phytoplankton biomass production). These data also suggest that statistically significant regressions between bacterial properties and phytoplankton properties over a large range of values may offer little insight into the causes of change over the typical ranges of values encountered.

This comparative analysis of bacterial properties in the ocean, supported by manipulation experiments, proposed a specific set of mechanisms as the factors that control change in bacterial abundance, productivity, and growth rates, both in slope and oceanic regions, as well as during different seasons of the year. This theoretical framework, supported by both observational and experimental evidence, may now be incorporated into improved modeling efforts to predict changes in bacterial properties in response the changes in the environment.

Chapter 5

Conclusions

Prior to this study, the bacterial properties and processes in the subarctic NE Pacific were described primarily from spring and summer occupations of Ocean Station Papa (OSP) during the SuPER program in 1987-98 (Kirchman 1990, Kirchman *et al.* 1993), and the winter and spring preliminary survey work associated with phase I of the Canadian JGOFS program presented in Boyd *et al.* (1995a, b) and Doherty (1995). High bacterial abundance tended to be associated with low bacterial productivity, and bacterial abundance and productivity increased with the addition of DOM and with increased temperature (Kirchman 1990, Kirchman *et al.* 1993). Good correlations were observed between bacterial productivity and primary productivity, with bacterial productivity being ~ 10% of primary productivity, while bacterial biomass varied over depth from slightly less to roughly equal to phytoplankton biomass in the upper 100 m (Kirchman *et al.* 1993). Winter bacterial abundance and productivity were lower than those typical of the spring and summer during the SuPER program (Boyd *et al.* 1995a, 1995b, Doherty 1995). Bacterial abundance and productivity were relatively constant all along line-P during the winter while bacterial productivity was higher at P4 than at OSP during the spring (Doherty 1995).

The results of this study agreed well with the previous studies, but along with the addition of respiration measurements, included more than two years of data that allowed comparisons to be made which addressed interannual variability. This thesis also addressed the potential for bacterial productivity to be limited by the availability of iron as well as well as DOM. Also, measurements of physical, chemical, and biological properties were tied together into a conceptual model that was used to explain potential cause and effect relationships associated with correlations between these various properties.

This thesis found winter bacterial abundance and biomass to be surprisingly constant from year-to-year along line-P (Chapter 3). Winter biomass was typically 30 to 50% of spring and summer values, while bacterial productivity was typically < 30% of

spring and summer values. Also, the summers of 1997 and 1998 showed dramatically lower than average bacterial abundance and productivity values, possibly associated with the 1997 El Niño and the 1998 La Nina.

Measurements of bacterial respiration suggested that, unlike the assumption of a constant bacterial growth efficiency often used in simple models, bacterial growth efficiency in the subarctic NE Pacific varied dramatically, from < 5% to > 50%, depending on the season and location of the measurements.

Manipulation experiments (Appendix I) not only supported the conclusion that bacteria in the subarctic NE Pacific HNLC region are limited by the availability of DOM, as found by Kirchman (1990), but also that during certain times (found during summer 1997) bacterial productivity can be co-limited by the availability of both iron and DOM. Co-limitation by both DOM and mineral nutrients was also found in slope waters where nitrogen was co-limiting along with DOM during the summer.

Kirchman *et al.* (1982) developed the idea of empirically determining the conversion factor for converting thymidine incorporation rates into bacterial productivity. Kirchman (1992) calculated a wide range of conversion factors for both thymidine and leucine at OSP. Chapter 2 presented model output that helped identify and explain the discrepancies often observed during grow-out experiments used for the empirical determination of conversion factors. Chapter 2 reviewed the different published methods for calculating empirical conversion factors and developed a model to test the effectiveness of these different methods when the assumptions about constant growth rate and linear incorporation rates are not met in real-world experiments. A non-linear cumulative method for calculating conversion factors was proposed as the most robust compromise when grow-out experiments do not meet the assumptions built into the other calculation methods. After determining conversion factors for measurements done during this study (Chapter 3), another previously unobserved pattern emerged suggesting that when conversion factors are determined empirically with grow-out experiments, there is a biomass dependent trend of decreased conversion factor values with increased biomass..

Chapter 4 brought all the measurements and manipulation experiments together into a conceptual model to identify the forces most likely to be responsible for driving the

changes observed in bacterial variables. The idea of "expected interaction patterns" was developed as a tool to provide strength and context to inferences based on property correlations. This study found physical forcing (i.e., the dilution of surface waters with deeper waters) to be a dominant control mechanism of both bacterial abundance and productivity over the seasonal cycle. Changes in phytoplankton derived DOM were also strongly associated with changes in bacterial variables, although bacterial productivity and particulate primary productivity were not always correlated. This decoupling of bacterial productivity from particulate primary productivity suggests that particulate primary productivity is not a good direct measure of phytoplankton derived DOM. Mechanisms to explain this discrepancy were also discussed in Chapter 4. Limitation of bacterial productivity was also tied to mineral nutrient stress along with DOM limitation in late summer.

The results of this thesis highlight three significant directions for futures study: 1) The success of the multiple correlation analysis in Chapter 4 provides a strong impetus for continuing a similar suite of measurements and analyses, both in the subarctic NE Pacific region and elsewhere. Larger, longer data sets will provide for further identification of the mechanisms eliciting the changes we observe in ocean biological processes over time, most importantly those that elicit interannual change in any given season within a single region (a scale for which this study did not have sufficient data density). 2) The outlier analysis in Chapter 4 highlighted the importance of physical fronts in driving the vast majority of variability in the bacterial properties measured. Specifically targeting these fronts in future studies would provide a quantitative assessment of their impact on ocean biology both seasonally and spatially. 3) The range and variability in respiration estimates presented in Chapter 3 suggests that the variability in bacterial growth efficiency plays a significant role, not only in bacterial carbon utilization, but also in the recycling and/or consumption of other associated nutrients at concentrations that may limit biological production processes. Our understanding of ocean biological processes will be greatly enhanced if methods can be developed that improve not only the accuracy and precision of respiration measurements, but also reduce the logistical time and expense of doing these analyses. There is need for the

development of new and improved analytical techniques as well as , future field studies that include or even focus on respiration measurements.

This thesis has clarified some of the ambiguities associated with converting radiolabel incorporation rates into bacterial productivity, it has extended in both time and space our knowledge of bacterial abundance and productivity in the subarctic NE Pacific region, it has provided the first measurements for this region of bacterial respiration, bacterial growth efficiency, and bacterial carbon demand, and it has developed a conceptual framework onto which observational data was tied to provide insights into the factors responsible for eliciting changes in bacterial abundance, productivity and growth rate.

References

Aota Y, Nakajima H (2001). Mutualistic relationships between phytoplankton and bacteria caused by carbon excretion from phytoplankton. *Ecological Research*, 16:289-299.

Azam F, Fenchel T, Field JG, Gray JS, Myer-Reil LA, Thingstad F (1983). The ecological role of water-column microbes in the sea. *Marine Ecology Progress Series*, 10:257-263.

Barwell-Clarke J, Whitney FA (1996). Institute of Ocean Sciences nutrient methods and analysis. Canadian Technnical Report of Hydrography and Ocean Sciences, 182:vi + 43 p.

Bell RT (1993). Estimating production of heterotrophic bacterioplankton via incorporation of tritiated thymidine. In: *Handbook of Methods in Aquatic Microbial Ecology*, P. F. Kemp, B. F. Sherr, E. V. Sherr and J. J. Cole, editors, Lewis Publishers, Boca Raton, Florida, pp. 495-503.

Berman T, Nawrocki M, Taylor GT, Karl DM (1987). Nutrient flux between bacteria, bacterivorous nanoplanktonic protists and algae. *Marine Microbial Food Webs,* 2:69-82.

Bird DF, Kalff J (1984). Empirical relationships between bacterial abundance and chlorophyll concentration in fresh and marine waters. *Canadian Journal Fisheries Aquatic Science,* 41:1015-1023.

Bjørnsen PK, Kuparinen J (1991). Determination of bacterioplankton biomass, net production and growth efficiency in the Southern Ocean. *Marine Ecology Progress Series*, 71:185-194.

Boenigk J, Matz C, Jurgens K, Arndt H (2002). Food concentration-dependent regulation of food selectivity of interception-feeding bacterivorous nanoflagellates. *Aquatic Microbial Ecolocy*, 27:195-202.

Bograd SJ, Thomson RE, Rabinovich AB, LeBlond PH (1999). Near-surface circulation of the northeast Pacific Ocean derived fromWOCE-SVP satellite-tracked drifters. *Deep-Sea Research II*, 46:2371-2403.

Booth BC, Lewin J, Postel JR (1993). Temporal variation in the structure of autotrophic and heterotrophic communities in the subarctic Pacific. *Progress in Oceanography*, 32:57-99.

Boyd PW, Harrison PJ (1999). Phytoplankton dynamics in the NE subarctic Pacific. *Deep-Sea Research II*, 46:2405-2432.

Boyd PW, Strom S, Whitney FA, Doherty S, Wen ME, Harrison PJ, Wong CS, Varela DE (1995a). The NE subarctic Pacific in winter: I. Biological standing stocks. *Marine Ecology Progress Series*, 128:11-24.

Boyd PW, Whitney FA, Harrison PJ, Wong CS, (1995b). The NE subarctic Pacific in winter: II. Biological rate processes. *Marine Ecology Progress Series*, 128:25-34.

Boyd PW, Muggli DL, Varela DE, Goldblatt RH, Chretien R, Orians KJ, Harrison PJ (1996). In vitro iron enrichment experiments in the NE subarctic Pacific. *Marine Ecology Progress Series*, 136:179-193.

Boyd PW, Berges JA, Harrison PJ (1998). In vitro iron enrichment experiments at iron-rich and -poor sites in the NE subarctic Pacific. *Journal of Experimental Marine Biology and Ecology*, 227:133-151.

Brown R (1998). Line P data. Fisheries and Oceans Canada, Pacific Region, Science Branch, http://www.pac.dfo-mpo.gc.ca/sci/Pages/linep.htm#RecentTempData.

Carlson CA, Ducklow HW (1996). Growth of bacterioplankton and consumption of dissolved organic carbon in the Sargasso Sea. *Aquatic Microbial Ecology*, 10:69-85.

Carlson CA, Ducklow HW, Sleeter TD (1996). Stocks and dynamics of bacterioplankton in the northwest Sargasso Sea. *Deep-Sea Research*, 43:491-515.

Caron DA, Lim EL, Sanders RW, Dennett MR, Berninger UG (2000). Responses of bacterioplankton and phytoplankton to organic carbon and inorganic nutrient additions in contrasting oceanic ecosystems. *Aquatic Microbial Ecology*, 22:175-184.

Charette M, Bishop J, Moran B (1999). Estimates of export production from Thorium disequilibria in the NE subarctic Pacific. *Deep-Sea Research II*, 46:2833-2861.

Cherrier J, Bauer JE, Druffel ERM (1996). Utilization and turnover of labile dissolved organic matter by bacterial heterotrophs in eastern North Pacific surface waters. *Marine Ecology Progress Series*, 139:267-279.

Chin-Leo G, Kirchman DL (1988). Estimating bacterial production in marine waters from the simultaneous incorporation of thymidine and leucine. *Applied and Environmental Microbiology*, 54:1934-1939.

Cho BC, Azam F (1988). Major role of bacteria in biogeochemical fluxes in the ocean's interior. *Nature*, 332:441-443.

Church, MJ, Hutchins DA, Ducklow HW (2000). Limitation of bacterial growth by dissolved organic matter and iron in the Southern Ocean. *Applied and Environmental Microbiology*, 66:455-466.

Coale KH, Johnson KS, Fitzwater SE, Gordon RM, Tanner S, Chavez FP, Ferioli L, Sakamoto C, Rogers P, Millero F, Steinberg P, Nightingale P, Cooper D, Cochlan WP, Landry MR, Constantinou J, Rollwagen W, Trasvina A, Kudela R (1996). A massive phytoplankton bloom induced by an ecosystem-scale iron fertilization experiment in the equatorial Pacific Ocean. *Nature*, 383:495-501.

Cochlan WP (2001). The heterotrophic bacterial response during a mesoscale iron enrichment experiment (IronEx II) in the eastern equatorial Pacific Ocean. *Limnology and Oceanography*, 46:428-435.

Cole JJ, Pace ML (1995). Quantifying the role of heterotrophic bacteria in the carbon cycle: A need for respiration rate measurements. *Limnology and Oceanography*, 40:441-444.

Cole JJ, Findlay S, Pace ML (1988). Bacterial production in fresh and saltwater ecosystems: a cross-system overview. *Marine Ecology Progress Series*, 43:1-10.

del Giorgio PA, Cole JJ (1998) Bacterial growth efficiency in natural aquatic systems. *Annual Review of Ecological Systems*, 29:503-541.

del Giorgio PA, Cole JJ (2000). Bacterial energetics and growth efficiency. In: Kirchman, D. L. (Ed), *Microbial ecology of the oceans*. Wiley-Liss. New York, pp. 289-325.

del Giorgio PA, Cole JJ ,Cimbleris, A (1997). Respiration rates in bacteria exceed phytoplankton production in unproductive aquatic systems. *Nature*, 385:148-151.

Dodimead AJ, Favorite F, Hirano T (1963). Salmon of the North Pacific Ocean. II Review of oceanography of the subarctic Pacific region. *International North Pacific Fisheries Commission Bulletin*, 13, 195 pp.

Doherty S (1995). The abundance and distribution of heterotrophic and autotrophic nanoflagellates in the NE subarctic Pacific. M.Sc. thesis, Dept. of Zoology, University of British Columbia, Vancouver, B.C., Canada, 198 pp.

Ducklow HW (1994). Modeling the microbial food web. *Microbial Ecology*, 28:303-319.

Ducklow HW (1999). The bacterial component of the oceanic euphotic zone. *FEMS Microbial Ecology*, 30:1-10.

Ducklow HW (2000). Bacterial production and biomass in the ocean. In: Kirchman, D. L. (Ed), *Microbial ecology of the oceans*. Wiley-Liss. New York, pp. 85-120.

Ducklow HW, Hill SM (1985). Tritiated thymidine incorporation and growth of heterotrophic bacteria in warm core rings. *Limnology and Oceanography*, 30:260-272.

Ducklow HW, Kirchman DL, Quinby HL (1992). Bacterioplankton cell growth and macromolecular synthesis in seawater cultures during the north Atlantic spring phytoplankton bloom, May, 1989. *Microbial Ecology*, 24:125-144.

Ducklow HW, Kirchman DL, Quinby HL, Carlson CA, Dam HG (1993). Stocks and dynamics of bacterioplankton carbon during the spring bloom in the eastern North Atlantic Ocean. *Deep-Sea Research*, 40:245-263.

Ducklow HW, Quinby HL, Carlson CA (1995). Bacterioplankton dynamics in the Equatorial Pacific during the 1992 El Niño. *Deep-Sea Research*, 42:621-638.

Ducklow HW, Carlson C, Smith W (1999). Bacterial growth in experimental plankton assemblages and seawater cultures from the *Phaeocystis antarctica* bloom in the Ross Sea, Antarctic. *Aquatic Microbial Ecology*, 19:215-227.

Ducklow HW, Dickson M, Kirchman DL, Steward G, Orchardo J, Marra J, Azam F (2000). Constraining bacterial production, conversion efficiency and respiration in the Ross Sea, Antarctica, January-February, 1997. *Deep-Sea Research II*, 47:3227-3247.

Elser JJ, Stabler, LB, Hassett RP (1995). Nutrient limitation of bacterial growth and rates of bacterivory in lakes and oceans: a comparative study. *Aquatic Microbial Ecology*, 9:105-110.

Fasham MJR, Boyd PW, Savidge G (1999). Modeling the relative contributions of autotrophs and heterotrophs to carbon flow at a Lagrangian JGOFS station in the northeast Atlantic: The importance of DOC. *Limnology and Oceanography*, 44:80-94.

Fukuda R., H. Ogawa, T. Nagata and I Koike (1998) Direct determination of carbon and nitrogen contents of natural bacterial assemblages in marine environments. *Applied and Environmental Microbiology*, 64, 3352-3358.

Fuhrman JA, Azam F (1980). Bacterioplankton secondary production estimates for coastal waters of British Columbia, Antarctica, and California. *Applied and Environmental Microbiology*, 39:1085-1095.

Fuhrman JA, Azam F (1982). Thymidine incorporation as a measure of heterotrophic bacterioplankton production in marine surface waters: evaluation and field results. *Marine Biology*, 66:109-120.

Furuya K, Harada K (1995). An automated precise Winkler titration for determining dissolved oxygen on board ship. *Journal of Oceanography*, 51:375-383.

Gargett AE (1991). Physical processes and the maintenance of nutrient-rich euphotic zones. Limnology and Oceanography, 36:1527-1545.

Geider RJ, Laroche J (1994). The role of iron in phytoplankton photosynthesis, and the potential for iron-limitation of primary productivity in the sea. *Photosynthesis Research*, 39:275-301.

Goldblatt RH, Mackas DL, Lewis AG (1999). Mesozooplankton community characteristics in the NE subarctic Pacific. *Deep-Sea Research II*, 46:2619-2644.

Goldman JC, Caron DA, Dennett MR (1987). Regulation of gross growth efficiency and ammonium regeneration in bacteria by substrate C:N ratio. *Limnology and Oceanography*, 32:1239-1252.

Jahnke RA, Craven DB (1995). Quantifying the role of heterotrophic bacteria in the carbon cycle: A need for respiration rate measurements. *Limnology and Oceanography*, 40:436-441.

Johnson KS, Burney CM, Sieburth J (1981). Enigmatic marine ecosystem metabolism measured by direct diel TCO_2 and O_2 flux in conjunction with DOC release and incorporation. *Marine Biology*, 65:49-60.

Jones DR, Karl DM, Laws EA (1996). Growth rates and production of heterotrophic bacteria and phytoplankton in the north Pacific subtropical gyre. *Deep-Sea Research I*, 43:1561-1580.

Kaehler P, Bjornsen PK, Lochte K, Antia A (1997). Dissolved organic matter and its utilization by bacteria during spring in the Southern Ocean. *Deep-Sea Research*, 44:341-353.

Kirchman DL (1990). Limitation of bacterial growth by dissolved organic matter in the subarctic Pacific. *Marine Ecology Progress Series*, 62:47-54.

Kirchman DL (1992). Incorporation of thymidine and leucine in the subarctic Pacific: application to estimating bacterial production. *Marine Ecology Progress Series*, 82:301-309.

Kirchman DL (1994). The incorporation of inorganic nutrients by heterotrophic bacteria. *Microbial Ecology*, 28:255-271.

Kirchman DL, Ducklow HW (1993). Estimating conversion factors for the thymidine and leucine methods for measuring bacterial production. In: *Handbook of Methods in Aquatic Microbial Ecology*, P. F. Kemp, B. F. Sherr, E. V. Sherr and J. J. Cole, editors, Lewis Publishers, Boca Raton, Florida, pp. 513-518.

Kirchman DL, Ducklow HW (1997) Estimating conversion factors for the thymidine and leucine methods for measuring bacterial production. In: Kemp PF, Sherr BF, Sherr EB, Cole JJ (Eds), *Handbook of Methods in Aquatic Microbial Ecology*. Lewis Publishers. Boca Raton, pp. 513-517.

Kirchman DL, Hoch MP (1988). Bacterial production in the Deaware Bay estuary estimated from thymidine and leucine incorporation rates. *Marine Ecology Progress Series*, 45:169-178.

Kirchman DL, Ducklow H, Mitchell R (1982). Estimates of bacterial growth from changes in incorporation rates and biomass. *Applied and Environmental Microbiology*, 44:1296-1307.

Kirchman DL, K'nees E, Hodson R (1985). Leucine incorporation and its potential as a measure of protein synthesis by bacteria in natural waters. *Applied and Environmental Microbiology*, 49:599-607.

Kirchman DL, Newell SY, Hodson R (1986). Incorporation versus biosynthesis of leucine: implications for measuring rates of protein synthesis and biomass production by bacteria in marine systems. *Marine Ecology Progress Series*, 32:47-59.

Kirchman DL, Keil RG, Simon M, Welschmeyer NA (1993). Biomass and production of heterotrophic bacterioplankton in the oceanic subarctic Pacific. *Deep-Sea Research*, 40:967-988.

Kirchman DL, Rich JH and Barber RT (1995). Biomass and biomass production of heterotrophic bacteria along 140 degree W in the Equatorial Pacific: Effect of temperature on the microbial loop. *Deep-Sea Research*, 42:603-619.

Kirchman DL, Meon B, Cottrell MT, Hutchins DA, Weeks D, Bruland K (2000). Carbon versus iron limitation of bacterial growth in the California upwelling regime. *Limnology and Oceanography*, 45:1681-1688.

Landry MR, Hassett RP (1982). Estimating the grazing impact of marine micro-zooplankton. *Marine Biology*, 67:283-288.

LaRoche J, Boyd PW, McKay RML, Geider RJ (1996). Flavodoxin as an in situ marker for iron stress in phytoplankton. *Nature*, 382:802-805.

Lee S, Fuhrman JA (1987). Relationships between biovolume and biomass of naturally derived marine bacterioplankton. *Applied and Environmental Microbiology*, 53:1298-1303.

Li WK (1998). Annual average abundance of heterotrophic bacteria and *Synechococcus* in surface waters. *Limnlology and Oceanography*, 43(7):1746-1753.

Li WK, Dickie PM, Harrison WG, Irwin BD (1993). Biomass and production of bacteria and phytoplankton during the spring bloom in the western North Atlantic Ocean. *Deep-Sea Research II*, 40:307-327.

Lochte K, Bjørnsen PK, Giesenhagen H, Weber A (1997). Bacterial standing stock and production and their relation to phytoplankton in the Southern Ocean. *Deep-Sea Research*, 44:321-340.

Maldonado MT, Boyd PW, Harrison PJ, Price NM (1999). Co-limitation of phytoplankton growth by light and Fe during winter in the NE subarctic Pacific Ocean. *Deap Sea Research II*, 46:2475-2485.

Martin JH, Gordon RM, Fitzwater S, Broenkow, WW (1989). VERTEX: phytoplankton/iron studies in the Gulf of Alaska. *Deep-Sea Research*, 36:649-680.

Miller CB (1993). Pelagic production processes in the subarctic Pacific. *Progress in Oceanography*, 32:1-15.

Moriarty DJW (1985). Measurements of bacterial growth rates in aquatic systems from rates of nucleic acid synthesis. *Advances in Microbial Ecology*, 9:245-292.

Nagata T (2000). Production mechanisms of dissolved organic matter. In: Kirchman, D. L. (Ed), *Microbial ecology of the oceans*. Wiley-Liss. New York, pp. 121-152.

Pakulski JD, Coffin RB, Kelley CA, Holder SL, Downer R, Aas P, Lyons MM, Jeffrey WH (1996). Iron stimulation of Antarctic bacteria. Nature, 383:133-134.

Parslow JS (1981). Phytoplankton-zooplankton interactions: data analysis and modeling (with particular reference to Ocean Station Papa [50N 145W] and controlled ecosystem experiments). Ph.D. Thesis, University of British Columbia, Canada.

Pomeroy LR (1974). The ocean's food web, a changing paradigm. *BioScience*, 24:499-504.

Riemann B, Bjørnsen PK, Newell S, Fallon R (1987). Calculation of cell production of coastal marine bacteria based on measured incorporation of [3H]thymidine. *Limnology and Oceanography*, 32:471-476.

Rivkin RB, Anderson MR, Lajzerowicz C (1996). Microbial processes in cold oceans. I. Relationship between temperature and bacterial growth rate. *Aquatic Microbial Ecology*, 10:243-254.

Rivkin RB, Putland JN, Anderson MR, Deibel D (1999). Microzooplankton bactivory and herbivory in the eastern subarctic Pacific. *Deep-Sea Research II*, 46:2579-2618.

Sherr EB, Sherr BF (2000). Marine microbes: An overview. In: Kirchman, D. L. (Ed), *Microbial ecology of the oceans*. Wiley-Liss. New York, pp. 13-46.

Sherr EB, Caron DA, Sherr BF (1993). Staining of heterotrophic protists for visualization via epifluorescence microscopy. In: *Handbook of Methods in Aquatic Microbial Ecology*, P. F. Kemp, B. F. Sherr, E. V. Sherr and J. J. Cole, editors, Lewis Publishers, Boca Raton, Florida, pp. 213-227.

Sherry ND, Boyd PW, Sugimoto K, Harrison PJ (1999). Seasonal and spatial patterns of heterotrophic bacterial production, respiration, and biomass in the subarctic NE Pacific. *Deep-Sea Research II*, 46:2557-2578.

Shiah FK, Kao SJ, Liu KK (1998). Bacterial production in the western equatorial Pacific: Implications of inorganic nutrient effects on dissolved organic carbon accumulations and consumption. *Bulletin of Marine Science*, 62(3):795-808.

Suttle CA, Chan AM (1994). Dynamics and distribution of cyanophages and their effect on marine *Synechococcus* spp. *Applied and Environmental Microbiology*, 60:3167-3174.

Simon M, Azam F (1989). Protein content and protein synthesis rates of planktonic marine bacteria. *Marine Ecology Progress Series*, 51:201-213.

Tabata S, Peart JL (1985). Statistics of Oceanographic Data Based on Hydrographic/STD casts made at Ocean Station P During August 1956 through June 1981. *Canadian Data Report of Hydrography and Ocean Science* 31.

Teira E, Pazo MJ, Serret P, Fernandez E (2001). Dissolved organic carbon production by microbial populations in the Atlantic Ocean. *Limnology and Oceanography*, 46:1370-1377.

Thibault D, Roy S, Wong CS (1999). Phytoplankton pigment budgets in the NE subarctic Pacific. *Deep-Sea Research II*, 46:2669-2697.

Thingstad TF, Rassoulzadegan F (1995) Nutrient limitations, microbial food webs, and biological C-pumps – suggested interactions in a P-limited Mediterranean. *Marine Ecology Progress Series*, 117:299-306.

Tortell PD, Maldonado MT, Price NM (1996). The role of heterotrophic bacteria in iron-limited ocean ecosystems. *Nature*, 383:330-332.

Turley C.M. (1993). Direct estimates of bacterial numbers in seawater samples without incurring cell loss due to sample storage. In: *Handbook of Methods in Aquatic*

Microbial Ecology, P. F. Kemp, B. F. Sherr, E. V. Sherr and J. J. Cole, editors, Lewis Publishers, Boca Raton, Florida, pp. 143-148.

Varela DE, Harrison PJ (1999). Seasonal variability in the nitrogenous nutrition of phytoplankton in the NE subarctic Pacific Ocean. *Deep-Sea Research II*, 46:2505-2538.

Vézina AF, Savenkoff C (1999). Inverse modeling of carbon and nitrogen flows in the pelagic food web of the Northeast subarctic Pacific. *Deep-Sea Research II*, 46:2909-2940.

Whitney FA, Freeland H (1999). Variability in the upper-ocean water properties in the NW Pacific Ocean. *Deep-Sea Research II*, 46:2351-2370.

Whitney FA, Wong CS, Boyd PW (1998). Interannual variability in nitrate supply to surface waters of the Northeast Pacific Ocean. *Marine Ecology Progress Series*, 170:15-23.

Wilhelm SW, Suttle CA (1999). Viruses and nutrient cycles in the sea. *BioScience*, 49:781-788.

Williams PJ le B (1981a). Microbial contribution to overall marine plankton metabolism: direct measurements of respiration. *Oceanologica Acta*, 4:359-364.

Williams PJ le B (1981b). Microbial contribution to overall plankton community respiration - studies in CEE's In: *Marine mesocosms: biological research in experimental ecosystems*, G.D. Grice and H.R. Reeve, editors. Springer, Berlin, pp. 305-321.

Williams PJ le B (1998). The balance of plankton respiration and photosynthesis in the open-oceans. *Nature*, 394:55-57.

Williams PJ le B (2000). Heterotrophic bacteria and the dynamics of dissolved organic material. In: Kirchman, D. L. (Ed), *Microbial ecology of the oceans*. Wiley-Liss. New York, pp. 153-200.

Wong CS, Whitney FA, Crawford DW, Iseki K, Matear RJ, Johnson WK, Page JS, Timothy D (1999). Seasonal and interannual variability in particle fluxes of carbon, nitrogen, and silicon from time series of sediment traps at Ocean Station P, 1982:1993: Relationship to changes in subarctic primary productivity. *Deap Sea Research II*, 46:2735-2760.

Zubkav MV, Sleigh MA, Burkill PH, Leakey RJG (2000). Bacterial growth and grazing loss in contrasting areas of north and south Atlantic. *Journal of Plankton Research*, 22:685-711.

Appendix I

Manipulation Experiments

A1.1 Introduction

Controlled manipulation experiments show the response of a system to a particular and known manipulation (e.g., the addition of a specific mineral nutrient) while all other variables are held constant. Controlled manipulations can directly infer cause and effect relationships . But, in a system where there are many possible interacting influences, it is often more manageable to measure several properties in the natural environment and compare them to infer relationships. On the other hand, correlations can only suggest potential cause and effect, since any correlation between two variables may be the result of the influence of other unmeasured variable. However, correlations can narrow down the likely interacting variables to help focus manipulation experiments on the relationships most likely to provide interesting and positive results. While this thesis focused primarily on patterns of correlations between various properties measured in the natural environment, this appendix presents the results of manipulation experiments that support the conclusions drawn from the correlations presented as the main focus of this work.

A1.2 Materials and Methods

Four different multi-factor amendment experiments were conducted over the course of this study (Table A1). All experiments used whole water samples collected from within the surface mixed layer with trace metal clean acid-washed 30 L GOFLO bottles, handled in a clean-room setting. Incubations were done at ambient sea surface temperature in deckboard incubators at 50% of ambient light. In 1996 incubations were done in 1 L Nalgene (PN 2015-1000) polycarbonate bottles, while in 1997 4 L low-density polyethylene collapsible cubitainers were used and subsamples were drawn at t = 0, 12, 36, 60, 84, and 108 h. Prior to use, all incubation containers were washed with Sparkleen detergent followed by sequential soaking in 5% reagent grade HCl for > 24 h

Table A1 Changes in bacterial productivity observed during manipulation experiments performed at stations P4, OSP, and MS05 between February 1996 and September 1997 showing final concentrations of amendments, bacterial productivity (BP) ± the standard error of the mean, the number of replicates in parenthesis, and the statistical probability (*p*) that the amended treatment was not different than the control. Also shown is the length of the incubation (h) used in determining the response. See text for further details.

Season	Date	Property	Q_{10}	Glu ±SE (n)	DOM ±SE (n)	Fe/Glu	NH_4/Glu	Fe	NH4	Fe/NH_4	Control	h
Winter												
	Feb-96	Amendment	2.0		1 drop extract*						-	
		BP (mg C m^{-3} d^{-1})			1.3 ±0.01 (3)**						0.95 ±0.01 (3)	4
		p			< 0.01						-	
Spring												
	May-96	Amendment	-		42% enrichment***						42% filtered	
		BP (mg C m^{-3} d^{-1})			2.5 ±0.2 (2)						1.8 ±0.1 (2)	24
		p			< 0.01						-	
		Amendment	-					2 nM	0.3 µM	2 nM/0.3 µM	-	
		BP (mg C m^{-3} d^{-1})						1.00 ±0.06 (3)	1.15 ±0.05 (3)	1.3 ±0.2 (3)	0.90 ±0.06 (3)	24
		p						NS	NS	< 0.02	-	
Summer			-									
OSP	Sep-96	Amendment	-	5 µM		1 nM/5 µM	5 µM/5 µM	1 nM	5 µM	1 nM/5 µM	-	
		BP (mg C m^{-3} d^{-1})	-	36.7 ±3.5 (2)		34.0 ±6.4 (2)	24.0 ±2.7 (2)	1.8 ±0.3 (2)	2.4 ±0.4 (2)	3.0 ±0.5 (2)	2.4 ±0.4 (2)	40
		p		< 0.001		< 0.001	< 0.001	NS	NS	NS	-	
P4	Sep-96	Amendment	-	5 µM		1 nM/5 µM	5 µM/5 µM	1 nM	5 µM	1 nM/5 µM	-	
		BP (mg C m^{-3} d^{-1})	-	9.5 ±0.1 (2)		9.7 ±1.0 (2)	18.1 ±2.2 (2)	6.9 ±0.4 (2)	10.7 ±0.8 (2)	9.2 ±1.3 (2)	8.8 ±0.7 (2)	12
		p		NS		NS	< 0.001	NS	NS	NS	-	
MS05[a]	Sep-97	Amendment	-			1 nM/5 µM	5 µM/5 µM	1 nM				
		BP (mg C m^{-3} d^{-1})				10.1 ±1.7 (9)	4.9 ±0.7 (8)	4.0 ±0.4 (8)			4.0 ±0.5 (7)	60-108
		p				0.025	NS	NS			-	
P4	Sep-97	Amendment				1 nM/5 µM	5 µM/5 µM	1 nM				
		BP (mg C m^{-3} d^{-1})				24.7 ±4.7 (9)	20.1 ±1.7 (9)	3.5 ±0.2 (9)			2.8 ±0.3 (9)	36-80
		p				< 0.001	< 0.001	NS			-	

* Yeast extract, see text.

** TdR only because Leu uptake dropped in nutrient addition probably because of leucine dilution in yeast extract

*** Phytoplankton DOM enrichment, see text.

[a] MS05 was a station south of OSP. See text for details.

NS signifies $p > 0.05$

then stored containing 0.1% ultra-pure HCl until use. With the exception of the DOM amendment in the winter and spring of 1996, all amendments except iron were run through a chelex column to remove metals and then stored under trace metal clean conditions. Bacterial abundance was determined from microscope counts of DAPI-stained slides (see Sherry *et al.* 1999). Bacterial productivity was determined using the same methods as for *in situ* measurements (rates of either [^{3}H]-thymidine incorporation or combined [^{3}H]-thymidine and [^{14}C]-leucine incorporation) (see Chapter 3).

The yeast extract used in Feb 96 was made from baker's yeast dissolved in warm tap water and allowed to sit for 2 h before being filtered through a 0.2 μm pore size Gelman Acrodisc® filter (PN 4187). The phytoplankton DOM enrichment was done by gravity filtering 10 L of seawater down to 1 L through a 142 mm diameter, 5 μm pore size PCTE membrane filter, and then exposing the seawater concentrate to high light for 5 h. During the enrichment experiments, 550 mL of sample water was enriched with 400 ml of the phytoplankton concentrate for 24 h.

Due to weather conditions during Sep 97, experiments were done south of OSP at station MS05 (47°30'N, 144°00'W). Station MS05 was determined to still be within the High Nitrate, Low Chlorophyll (HNLC) region of the Subarctic NE Pacific (mixed-layer NO_3 = 3.6 μM, Chl = 0.34 mg m^{-3}, Fe < 0.15 nM) (Nishioko *et al.* 2001)

A1.3 Results

Between Feb 1996 and Sep 1997 a variety of manipulation experiments were carried out both at OSP and at P4 to explore the bacterial response to various nutrient and substrate amendments. Unfortunately, this was not a coherent set of experiments, with a single end goal, but rather a series of separate experiments addressing a range of questions. However, some interesting conclusions can be drawn from these results (Table A1).

Dissolved organic carbon (DOC), either alone (glucose) or in combination with other nutrients (see Table A1), always elicited an increase in bacterial productivity. In very few experiments was there a measurable change in bacterial abundance relative to the controls. The lack of change in bacterial abundance may be explained by suggesting

that the increased bacterial production was removed by increased grazing rates, or increased rates of viral lysis.

May 1996 stands out as the only time when bacterial productivity increased measurably at OSP (in HNLC waters) with the addition of inorganic nutrients alone. There was a positive response (42% increase) to the addition of both iron and ammonium together while neither iron nor ammonium elicited a statistically significant response on their own. It appeared that the iron/ammonium response was not actually co-limitation, but rather an additive response where the response of either nutrient alone was insufficient to meet statistical standards with only three replicates (see Table A1). If the additive response is correct, it suggests that the limitation of bacterial productivity by iron and ammonium was not co-limitation of a single metabolic pathway, but was limitation of two separate pathways (possibly in two separate species or groups of bacteria). During similar concurrent incubations with phytoplankton DOM extract (see methods), bacterial productivity increased > 2.5-fold during the same time interval. Clearly, limitation due to iron and nitrogen availability, though interesting, was small compared to the dramatic response elicited with the substrate potpourri of the phytoplankton extract.

Co-limitation of bacterial productivity by both DOC and an inorganic nutrient was observed in both slope (P4) and oceanic (MS05) waters during Sep 96 and Sep 97 respectively (both in late summer). In this study, bacterial productivity was considered to be co-limited when there was an increase in bacterial productivity associated with the simultaneous addition of two different substances, while there was no measurable response to the addition of either of those substances alone.

In the nitrate-depleted summer slope waters, bacterial productivity increased ~ 2-fold (over 12 h) in response to both glucose and ammonium together, while the bacteria did not respond to either addition alone. This suggests that under these conditions, bacteria were likely to be competing with phytoplankton for a limited supply of reduced nitrogen while being dependent on the phytoplankton for organic substrate.

The second case of co-limitation, occurred in the iron-limited HNLC waters of MS05 in Sep 97. Here, bacterial productivity increased 2.5-fold (over 60+ h) over the control with the addition of both iron and glucose, while the response was not different from the control for either amendment alone. Unlike Sep 97 at MS05, OSP in Sep 96 did

not show co-limitation with iron and glucose, but rather exhibited a consistently positive (≥ 10-fold) response to glucose, whether it was added alone or in combination with iron or ammonium.

These results suggest that bacterial productivity in the subarctic NE Pacific was almost always limited by the availability of LDOC. However, mineral nutrient availability also played a significant role in co-limiting productivity along with LDOC limitation. P4 appeared to be co-limited by both nitrogen and LDOC during both the summers of 1996 and 1997, times when surface waters were depleted of nitrate. Conversely, the high nitrate, low chlorophyll region near OSP was limited by only LDOC availability during 1996, while it was co-limited by both iron and LDOC availability in 1997, during the time of strongest El Niño warming (see Chapter 3).

Kirchman (1990) found bacterial productivity at OSP increased in response to the addition of LDOC (glucose), yet productivity increased even more in response to the addition of dissolved free amino acids or glucose and ammonium combined, suggesting that even in regions where excess nitrate was available, the availability of more reduced forms of nitrogen enhanced the LDOC limited bacterial productivity.

Although it appears as though bacterial productivity in the subarctic NE Pacific is generally limited by LDOC availability, and we can predict nitrogen/LDOC co-limitation in regions where nitrate is seasonally depleted, we do not yet have a long enough and high enough resolution time-series of manipulation experiments in the subarctic NE Pacific to be able to predict when co-limitation or even if mineral nutrient limitation alone may be important in the HNLC open ocean region around OSP.

Appendix II

Parameters Measured in the Mixed Layer

Appendix II

Table of all mixed-layer data used for the Chapter 4 correlation analysis. The outliers include the most extreme four bacterial productivity values (A), the four less extreme bacterial productivity values (B), and the values excluded from the comparitive analysis as bivariate outliers (C).

Cruise	Station ID	Season	Year	Outliers	Sal	Temp	Mixed Z	SiO2	NO3	PO4	PP	Chl	HF	B#s	BP	Bμ	PP 0.2-5	PP 5-20	PP > 20	Chl 0.2-5	Chl 5-20	Chl > 20
9309	P04	Spr	1993		32.305	10.8	35	8.2	1.7	0.56	21.5	0.29		1.28	1.76	0.14	3.0	12.9	5.8	0.19	0.08	0.02
9309	P12	Spr	1993	BC	32.377	9.5	15	11.0	4.5	0.73	8.4	0.33	8.2E+09	1.10	2.74	0.25	6.9	1.3	0.3	0.20	0.10	0.02
9309	P16	Spr	1993		32.470	9.5	16	10.6	4.9	1.31	5.4	0.19	7.4E+09	0.84	0.62	0.07	4.1	1.2	0.1	0.13	0.04	0.01
9309	P20	Spr	1993		32.493	8.8	10	13.5	7.1	0.86	22.2	0.21	1.3E+10	0.88	0.90	0.10	15.1	5.6	1.6	0.14	0.05	0.02
9309	P26	Spr	1993		32.565	7.7	37	14.7	8.5	0.86	8.2	0.25	5.8E+09	1.02	0.86	0.08	2.9	3.0	2.4	0.09	0.12	0.04
9402	P04	Spr	1994	C	31.364	11.9	8	5.8	0.0	0.33	40.1	1.07	5.9E+08	1.15	1.44	0.13	23.7	10.4	9.6	0.77	0.26	0.43
9402	P12	Spr	1994		32.445	10.6	5				9.7	0.55	2.5E+08	0.82	0.37	0.05	5.3	2.1	2.1	0.29	0.09	0.16
9402	P16	Spr	1994		32.536	9.9	50	5.2	2.2	0.60	5.7	0.44	2.0E+08	0.73	0.31	0.04	2.0	1.6	2.0	0.21	0.07	0.17
9402	P20	Spr	1994		32.544	8.7	8				9.0	0.45	3.9E+08	0.73	0.24	0.03	4.2	2.3	2.4	0.23	0.12	0.10
9402	P26	Spr	1994		32.753	7.9	31	14.9	11.0	1.14	4.7	0.30	3.9E+08	0.84	0.65	0.08	3.2	1.1	0.4	0.22	0.05	0.03
9609	P04	Spr	1996	AC	30.653	10.6	8	6.3	0.2	0.36	113.9	1.34	5.4E+09	2.12	4.21	0.20	34.2	34.2	45.5	0.63	0.27	0.44
9609	P12	Spr	1996		32.521	9.7	28	7.1	4.0	0.72	9.7	0.22		1.46	0.48	0.03	5.3	2.0	2.3	0.15	0.04	0.04
9609	P16	Spr	1996		32.570	8.4	63	9.5	7.2	0.92	16.4	0.26	3.8E+09	0.43	0.39	0.09	7.2	3.8	5.4	0.15	0.04	0.07
9609	P20	Spr	1996	C	32.598	7.6	60	10.9	9.2	1.03	32.2	0.41		0.44	0.47	0.11	14.8	6.1	11.6	0.19	0.08	0.14
9609	P26	Spr	1996		32.681	7.5	9	18.0	12.1	1.20	22.5	0.26	1.1E+10	1.35	0.47	0.04	16.4	3.8	2.0	0.21	0.03	0.02
9711	P04	Spr	1997	AC	31.454	13.4	6	5.7	0.0	0.32	47.1	1.11		2.29	4.60	0.20	27.3	8.9	11.3	0.80	0.13	0.17
9711	P12	Spr	1997		32.470	11.9	20	7.2	3.3	0.67	13.1	0.37		1.31	0.72	0.05	7.4	2.2	3.5	0.28	0.04	0.05
9711	P13-15	Spr	1997		32.526	11.2	27							1.19	0.47	0.04						
9711	P16	Spr	1997		32.594	10.5	23	12.4	7.1	0.90	15.6	0.45		1.72	1.16	0.07	10.7	2.5	2.3	0.39	0.04	0.01
9711	P17-19	Spr	1997		32.617		32							1.27	0.77	0.06						
9711	P20	Spr	1997		32.546	9.9	25	14.1	8.0	0.97	15.7	0.44		1.18	0.90	0.08	10.8	2.2	2.7	0.36	0.05	0.03
9711	P21-23	Spr	1997		32.657	9.9	19							1.36	0.60	0.04						
9711	P24-25	Spr	1997		32.645		15							1.30	0.73	0.06						
9711	P26	Spr	1997		32.638	9.4	17	16.3	10.5	1.12	15.3	0.43	6.1E+09	0.92	0.81	0.09	8.9	3.5	2.9	0.28	0.10	0.04
9711	Z1-4	Spr	1997		32.641	10.0	15	24.5	12.9	1.27				1.04	0.87	0.08						
9711	Z5-9	Spr	1997		32.663	10.5	12	22.9	11.1	1.15				1.20	0.52	0.04						
9815	P04	Spr	1998		31.944	12.5	22	2.5	0.0	0.32					1.14							
9815	P12	Spr	1998		32.307	12.2	15	0.3	0.1	0.39					0.79							
9815	P16	Spr	1998		32.671	10.9	23	7.7	4.1	0.66					1.00							
9815	P20	Spr	1998		32.703	9.8	21	10.4	6.9	0.81					1.04							
9815	P26	Spr	1998		32.667	9.1	20	16.4	9.9	1.03					1.01							
9815	Z04	Spr	1998		32.206	8.7	40								0.66							
9815	Z09	Spr	1998		32.040	9.2									0.39							
9815	Z14	Spr	1998		31.939	10.0									0.71							
9512	P04	Sum	1995	B	31.978	16.1	15	5.4	0.1	0.30	15.8	0.10		1.76	2.96	0.17	10.3	3.5	2.1	0.07	0.01	0.01
9512	P12	Sum	1995		32.118	16.2	12	5.3	0.0	0.31	8.5	0.05		1.32	1.06	0.08	5.6	2.2	0.7	0.04	0.02	0.00
9512	P16	Sum	1995	B	32.163	15.1	16	10.2	0.0	0.35	14.1	0.07		1.55	2.43	0.16	7.6	5.3	1.1	0.05	0.02	0.00
9512	P20	Sum	1995	AC	32.537	14.2	9				44.2	0.38		2.65	4.18	0.16	15.0	1.8	11.5	0.12	0.14	0.01
9512	P26	Sum	1995	B	32.472	13.1	22	13.1	5.7	0.81	21.8	0.44		1.96	2.43	0.12	8.5	7.6	5.9	0.19	0.15	0.10

Appendix II (continued)

Cruise	Station ID	Season			Sal	Temp	Mixed Z	SiO2	NO3	PO4	PP	Chl	HF	B#s	BP	Bμ	PP 0.2-5	PP 5-20	PP > 20	Chl 0.2-5	Chl 5-20	Chl > 20
9618	P04	Sum	1996	AC	31.961	15.0	7	3.1	0.1	0.38	90.2	0.69	5.2E+09	1.26	4.68	0.37	52.3	18.0	19.8	0.48	0.10	0.10
9618	P12	Sum	1996		32.128	16.0	17	3.7	0.0	0.34	20.5	0.20		2.03	1.73	0.09	11.1	3.7	5.7	0.16	0.02	0.03
9618	P16	Sum	1996		32.375	14.8	20	1.4	0.0	0.39	17.8	0.20	3.9E+09	1.01	1.26	0.12	12.3	2.9	2.7	0.17	0.02	0.01
9618	P20	Sum	1996		32.455	14.0	20	11.1	4.4	0.69	32.7	0.53	4.3E+09	1.57	1.84	0.12	22.6	4.6	5.6	0.42	0.06	0.05
9618	P26	Sum	1996		32.586	13.4	24	14.0	6.6	0.86	25.9	0.36	3.4E+09	1.28	1.41	0.11	15.3	6.5	3.9	0.23	0.08	0.03
9715	MS05	Sum	1997		32.625	15.3	25	9.5	3.6	0.65		337.33										
9715	P04	Sum	1997	C	31.701	17.4	8	3.2	0.0	0.29	14.3	0.17	3.1E+08	1.37	0.78	0.06						
9715	P12	Sum	1997	C	31.865	17.4	11	2.8	0.0	0.31	5.7	0.17	1.3E+09	1.12	0.56	0.05						
9715	P16	Sum	1997		32.491	16.5	17	9.4	1.9	0.56	4.3	0.17		1.85	1.11	0.06						
9715	P20	Sum	1997		32.343	15.9	15	10.2	2.7	0.50	12.6	0.25	1.2E+09	2.10	0.84	0.04						
9715	P26	Sum	1997		32.527	15.0	18	17.2	7.7	0.81	12.4	0.40	1.6E+09	1.16	1.08	0.09						
9829	P04	Sum	1998		32.042	16.5	20	3.8	0.0	0.26				1.05	0.48	0.05						
9829	P12	Sum	1998		32.116	16.7	18	4.5	0.0	0.32				0.90	0.56	0.06						
9829	P16	Sum	1998		32.335	16.0	22	0.7	0.0	0.32				0.95	0.41	0.04						
9829	P20	Sum	1998		32.646	14.1	32	9.3	5.1	0.75				1.66	0.34	0.02						
9829	P26	Sum	1998		32.630	12.0	40	9.1	5.7	0.79				1.18	0.50	0.04						
9401	P04	Win	1994	C	32.349	9.5	55	8.0	3.5	0.59	3.4		2.4E+08	0.76	0.75	0.10	1.6	0.9	0.8			
9401	P12	Win	1994	C	32.319	9.3	80	11.4	5.6	0.79	2.7	0.21	4.3E+08	0.54	0.63	0.12	1.3	0.7	0.7	0.14	0.04	0.04
9401	P16	Win	1994	C	32.520	9.1	80	9.4	4.6	0.76	3.6	0.27	3.1E+08	0.67	0.71	0.11	1.2	0.9	1.5	0.13	0.10	0.05
9401	P20	Win	1994	C	32.546	8.0	90	13.0	7.6	0.94	2.4	0.26	1.9E+08	0.83	1.02	0.12	1.4	0.6	0.4	0.13	0.11	0.02
9401	P23	Win	1994	C	32.520	7.3	90	15.1	9.4	1.08	1.9	0.30	6.0E+08	0.71	0.67	0.09	0.7	0.8	0.4	0.15	0.11	0.04
9601	P04	Win	1996		32.354	8.7	70	8.0	3.7	0.69	19.2	0.54		0.74	0.17	0.02	9.8	6.5	2.7	0.37	0.14	0.04
9601	P12	Win	1996		32.567	7.7	40	8.9	6.0	0.84	12.4	0.68		0.74	0.34	0.05						
9601	P16	Win	1996		32.534	7.6	120	8.1	6.0	0.85	2.4	0.32		0.64	0.27	0.04	1.3	0.5	0.6	0.19	0.06	0.07
9601	P20	Win	1996		32.584	6.3	95				4.0	0.36		0.95								
9601	P26	Win	1996		32.708	5.6	95	19.5	12.9	1.27	6.6	0.36		0.71	0.25	0.04	4.1	1.3	1.2	0.23	0.07	0.06
9702	P04	Win	1997		32.460	8.4	55	11.8	8.5	0.96	7.9	0.42	2.4E+09	0.70	0.25	0.04	4.8	1.6	1.6	0.34	0.05	0.03
9702	P12	Win	1997		32.571	8.4	55	8.9	6.2	0.82	12.2	0.64	1.4E+09		0.24		6.1	3.4	2.7	0.44	0.13	0.07
9702	P16	Win	1997		32.540	7.4	80	12.7	8.5	0.96	9.3	0.30		0.54	0.19	0.04	5.4	2.0	1.9	0.18	0.06	0.06
9702	P26	Win	1997		32.725	5.9	105	18.8	13.3	1.25	6.2	0.28		0.43	0.14	0.03	3.9	1.2	1.1	0.19	0.05	0.05
9803	P04	Win	1998		32.699	11.3	65	5.3	3.5	0.63				0.66	0.15	0.02						
9803	P12	Win	1998		32.580	8.4	75							0.68	0.16	0.02						
9803	P16	Win	1998		32.616	7.5	80	11.6	8.4	0.93				0.74	0.16	0.02						
9803	P20	Win	1998		32.661	6.6	80	14.2	10.4	1.03				0.63	0.15	0.02						
9803	P26	Win	1998		32.665	5.4	85	20.3	13.0	1.2				0.52	0.16	0.03						
9901	P04	Win	1999		32.200	8.9	11	14.3	8.7	0.97				0.51	0.15	0.03						
9901	P16	Win	1999		32.820	7.2	92	13.7	9.4	0.99				0.34	0.11	0.03						
9901	P20	Win	1999		32.740	6.8	94	15.8	10.9	1.07				0.43	0.15	0.03						
9901	P26	Win	1999		32.790	5.8	115	20.6	14.4	1.30				0.39	0.09	0.02						